Weather forecasting and measurement for renewable energy predictability

Marion Schroedter-Homscheidt, M. Kosmale, Jose Luis Casado Rubio, Carlos M. Fernández-Peruchena, Martín Gastón, Luis Guerreiro

Weather forecasting and measurement for renewable energy predictability

Technical Report · July 2016

DOI: 10.13140/RG.2.2.24381.72162

6 authors, including:

Marion Schroedter-Homscheidt
German Aerospace Center (DLR)
234 PUBLICATIONS **1,760** CITATIONS
SEE PROFILE

Miriam Kosmale
Finnish Meteorological Institute
19 PUBLICATIONS **211** CITATIONS
SEE PROFILE

Carlos M Fernández-Peruchena
Centro Nacional de Energías Renovables
98 PUBLICATIONS **380** CITATIONS
SEE PROFILE

Martín Gastón
Centro Nacional de Energías Renovables
64 PUBLICATIONS **521** CITATIONS
SEE PROFILE

Deliverable D4.2

Validation sites

Grant Agreement	654984	
Date of Annex I	01 June 2015	
Dissemination Level	Public	
Nature	Report	
Work package	WP4- Weather forecasting and measurement for renewable energy predictability	
Due delivery date	31 May 2016	
Actual delivery date	30 July 2016	
Lead beneficiary	DLR	M. Schroedter-Homscheidt

Dissemination level[1]	PU
Nature[2]	R

Document Identifier	PREFLEXMS_DEL_D4.2_20160531_v3
Status	Version 3

Lead beneficiaries	DLR, M. Schroedter-Homscheidt, M. Kosmale AEMET, Jose Luis Casado Rubio CENER, Carlos M. Fernández Peruchena, Martin Gaston Romero Univ. Évora, Luis Guerreiro

[1] Dissemination level: **PU** = Public, **PP** = Restricted to other programme participants (including the JU), **RE** = Restricted to a group specified by the consortium (including the JU), **CO** = Confidential, only for members of the consortium (including the JU)

[2] Nature of the deliverable: **R** = Report, **P** = Prototype, **D** = Demonstrator, **O** = Other

Executive summary

This report has been prepared by DLR in collaboration with CENER within WP4 'Weather forecasting and measurement for renewable energy predictability'.

It describes meteorological conditions in Évora as the test site of PreFlexMS. Évora characteristics are compared to other stations in Portugal/Spain and in other regions being of interest als potential Concentrating Solar Power (CSP) markets. We want to avoid a development which would be too much driven by the Évora test site as such plant optimizations may not be applicable in other locations. Especially as other locations may not have the same wealth of numerical weather prediction available as on the Iberian Peninsula.

Chapter 1 provide a site assessment of Évora, Badajoz and Plataforma Solar de Almeria with respect to direct normal irradiation (DNI) as observed from ground and satellite-based platforms. Additionally, satellite-based cloud physical parameters and DNI variability classes are taken into account. Aerosols have been assessed with the help of AERONET ground observations of aerosol optical depth (AOD).

In Chapter 2 we review the ground-based DNI observation availability in South Africa, India, Morocco, Chile, and Saudi Arabia. The observations were quality controlled and frequency histograms with annual and monthly resolution are given. The same is done for a 10 year satellite-based time series. By that we can compare the conditions at the available ground stations to the reference locations Upington in South Africa and Noor in Morocco, which have no own publicly available ground observations. This helps to identify the most relevant ground observation station.

In chapter 3 the rationale of defining the optimum ground stations acting as 'virtual demo sites' in PreFlexMS is summarized. We focus on South Africa, Morocco, and Chile.

Research questions to be further addressed by both the dispatch optimizer developers and the meteorological forecast assessment team are named. The available numerical weather prediction (NWP) models for each of the research questions are named. Answering these research questions will quantify the value of aerosol forecasts, of storage, of higher temporal and spatial resolution, of higher forecast update frequencies, of post-processing efforts, and the use of probabilistic forecasts. This will serve as input to the business development task within WP4.

Finally, we suggest using station VAN (Vanrhynsdorp) in South Africa, Erfoud in Morocco, and either San Pedro de Atacama or Crucero in Chile as virtual demo sites for further work in PreFlexMS.

The decision for the station in Chile will be done in the upcoming weeks, when the recently found ground observations have been made available by the Chile government.

Table of Contents

Acronyms

3D-Var	Three-Dimensional Variational data assimilation
4D-Var	Four-Dimensional Variational data assimilation
AEMET	Agencia Estatal de Meteorología
AEMET-SREPS	AEMET Short Range Ensemble Prediction System
AERONET	Aerosol Robotic Network
AIREP	Air Report
ALADIN	Aire Limitée Adaptation Dynamique Initialisation
AMSU	Advanced microwave sounding unit
AOD	Aerosol optical depth
APOLLO	AVHRR Processing scheme Over cLouds, Land and Ocean
AROME	Applications of Research to Operations at Mesoscale
AROME/HARMONIE	Hirlam Aladin Regional/Meso-scale Operational NWP in Europe
ARPEGE	Model from Météo-France
ATOVS	Advanced TIROS-N Operational Vertical Sounder
BC	boundary condition
BMA	Bayesian Model Averaging
BSRN	Baseline Surface Radiation Network
BS	Brier Score
BSS	Brier Skill Score
CAMA	Pampa Camarones (Station in Chile)
CAMS	Copernicus Atmosphere Monitoring Service
CDF	cumulative distribution function
CENER	Centro Nacional de Energías Renovables
CMC-GDPS	Global Deterministic Prediction System from the Canadian Meteorological Centre
CNRM/GMME	Centre National de Recherches Météorologiques
CPI	Combined Performance Index
CRPS	Continous Ranked Probability Score
CSP	Concentration Solar Power
DCH	direction changes in DNI
DHI	diffuse hemispherical irradiation
DLR	German Aerospace Center
DMO	Direct Model Output
DNI	direct normal irradiation
DNIcast	Project acronym www.dnicast-project.net
DRIBU	buoys observations
DRIFTER	observations from drifting buoys
ECMWF	European Centre for Medium-Range Weather Forecast
ECMWF/EPS	ECMWF/Ensemble Prediction System
ECMWF/IFS	ECMWF/Integrated Forecast System
EDA	Ensemble Data Assimilation
ELR	extended logistic regression

em	ensemble mean
EMPS	Evora Molten Salt Platform
EnerMENA	project acronym
EPS	ensemble prediction system
ETKF	Ensemble Transform Kalman Filter
FONDEF	El Fondo de Fomento al Desarrollo Científico y Tecnológico, Chile)
GHI	global horizontal irradiation
GIZ	Deutsche Gesellschaft für Internationale Zusammenarbeit
GRT	Graaff-Reinet (SAURAN station)
gSREPS	AEMET New Mesoscale Short Range Ensemble Prediction System
Heliosat-4	surface downwelling solar irradiance model by MINES/DLR
HIRLAM	HIgh Resolution Limited Area Model
HITRAN	High Resolution Transmission Molecular Absorption Database
HRES	high-resolution forecast
IC	initial condition
IDEO	Inca de Oro (Station in Chile)
IR	infrared
JMA-GSM	Global Spectral Model from the Japan Meteorological Agency
JNNSM	Jawaharlal Nehru National Solar Mission
kcB	clear sky beam index
KSI	Kolgorov-Smirnov test integral
KZH	University of KwaZulu-Natal Howard College (SAURAN station)
KZW	University of KwaZulu-Natal Westville (SAURAN station)
LAF	lagged average forecast
LAM	limited-area models
LBC	lateral boundary conditions
LR	logistic regression
LTEKF	Local Transform Ensemble Kalman Filter
LW	long wave
MAD	mean absolute difference
MAE	mean absolute error
McRad	radiative transfer model used in ECMWF/IFS
MENA	Mediterranean Europe and Northern Africa regions
Met Office	United Kingdom Meteorological Office
MSG	Meteosat Second Generation
NCEP	National Center for Environmental Prediction
NCEP-GFS	the Global Forecast Model from NCEP
NEMS	NOAA Enviromental Modeling System
NMMB	Non-hydrostatic Multi-Scale Model
NMU	Nelson Mandela Metropolitan University (SAURAN station)
NOAA	National Oceanic and Atmospheric Adminstration
NWP	numerical weather prediction
PDF	Probavility Density Function

PILOT	observations from pilot sounding
PPA	Power purchase agreements
PSA	Plataforma Solar de Almeria
QC	quality control
QS	quantile score
R&D	research and development
REFIT	Renewable Energy Feed-in Tariff
REIPPP	Renewable Energy Independent Power Producer Procurement programme
relMAD	relative mean absolute difference
relRMSD	relative root mean square difference
relSD	relative standard deviation of the residuals
REST2	a radiative transfer model
RMSD	root mean square difference
RMSE	root mean square error
ROC	relative operating characteristic curve
RPS	Ranked Probability Score
RPSS	ranked probability skill score
RR	Ramp Rate
RRTM	Rapid Radiation Transfer Model
RSI	rotating shadowband irradiometers
RUC	relative user characteristic
RUC1	hourly rapid updated circle
RVD	GIZ Richtersveld (SAURAN station)
SAURAN	Southern African Universities Radiometric Network
SHIP	automatic ship observations
SLAF	scaled algged averaged forecast technique
SPPT	Stochastically Perturbed Parameterization Tendencies
STA	Mangosuthu Univ. of Technology STARlab (SAURAN station)
STDV	standard deviation
SUN	Stellenbosch University (SAURAN station)
SUT	Eskom Sutherland (SAURAN station)
SW	shortwave
SYNOP	synoptical observations
SZA	solar zenith angle
TEMP	Temp measurement observations
TKE	turbulent kinetic energy
U95%	uncertainty at 95%
UFS	GIZ University of Free State (SAURAN station)
UNV	USAid Venda (SAURAN station)
UNZ	University of Zululand (SAURAN station)
UPR	GIZ University of Pretoria (SAURAN station)
UV	ultraviolet
VAN	Vanrhynsdorp (Station in South Africa)

VAN	GIZ Vanrhynsdorp (SAURAN station)
VRY	GIZ Vryheid (SAURAN station)
WCRP	World Climate Research Program
WMO	World Meteorological Organisation

1. Site assessment - How special is Évora?

In this section we want to understand the meteorological conditions in Évora in general. This study relies on existing, historic observations from ground and satellites. It allows a characterisation of Évora and to compare this to other stations in Portugal/Spain, but also in other regions of the world. Fig. 1-1 illustrates the location of Évora, Badajoz and the Plataforma Solar de Almeria (PSA) being the three stations in the focus of this first chapter.

Figure 1.1 Location of Évora Badajoz, and PSA (source GoogleMaps)

1.1 Ground observations

1.1.1 Station details - Évora

Mitra´s station is situated in the countryside of Évora (about 8km South from Évora), in the Renewable Energies Chair experimental site (University of Évora). The station geographical coordinates are 38°31'50.28"N and 8° 0'40.33"W and the altitude is 220m.

The current station was installed in December of 2014 and has the following instrumentation:

- 1 Kipp-Zonen CHP-1 pyrheliometer measuring DNI (direct normal irradiation)
- 2 Kipp-Zonen CM-11 pyranometers measuring GHI (global horizontal irradiation) and DHI (diffuse hemispherical irradiation)
- 1 Thies Combined Sensor, measuring air temperature and relative Humidity
- The Sun's apparent motion is tracked by a Soly 2 Suntracker.

This station has been measuring since mid-December of 2014. There are some missing measurements due to technical problems and maintenance operations.

Table 1: Station information Évora

Station	**Latitude**	**Longitude**	**Elevation (m)**	**Pyrheliometer**	**Period**	**Temporal resolution**
Évora	38.531 N	8.011 W	220	KIPP-ZONEN CHP1	From 2003 to date	1-min

Below, Fig.1-2 shows the map location in relation to EMSP (Évora Molten Salt Platform) and Fig.1-3 is a picture of the actual station.

Figure 1.2 Mitra's station location at the Évora site in the west of the EMSP site (image: Google)

Figure 1.3 Picture of the Évora station

There is an AERONET station in Évora, managed by the University of Évora. Level 1.5 (automatically cloud-screened) observations are available from July 2003 to May 2016.

1.1.2 Station details - Badajoz

Badajoz station (Fig. 1-6) is situated on the flat roof of the local AEMET building (Fig. 1-5), in the campus of Extremadura University, 4 km west of the city (Fig. 1-4). Its geographical coordinates are 38º 53' N, 07º 01' W, and it is at 190m altitude. Its distance to Évora station is approx. 85 km.

Figure 1.4 Location of Badajoz station approx. 85 km north-east of Évora (GoogleMaps)

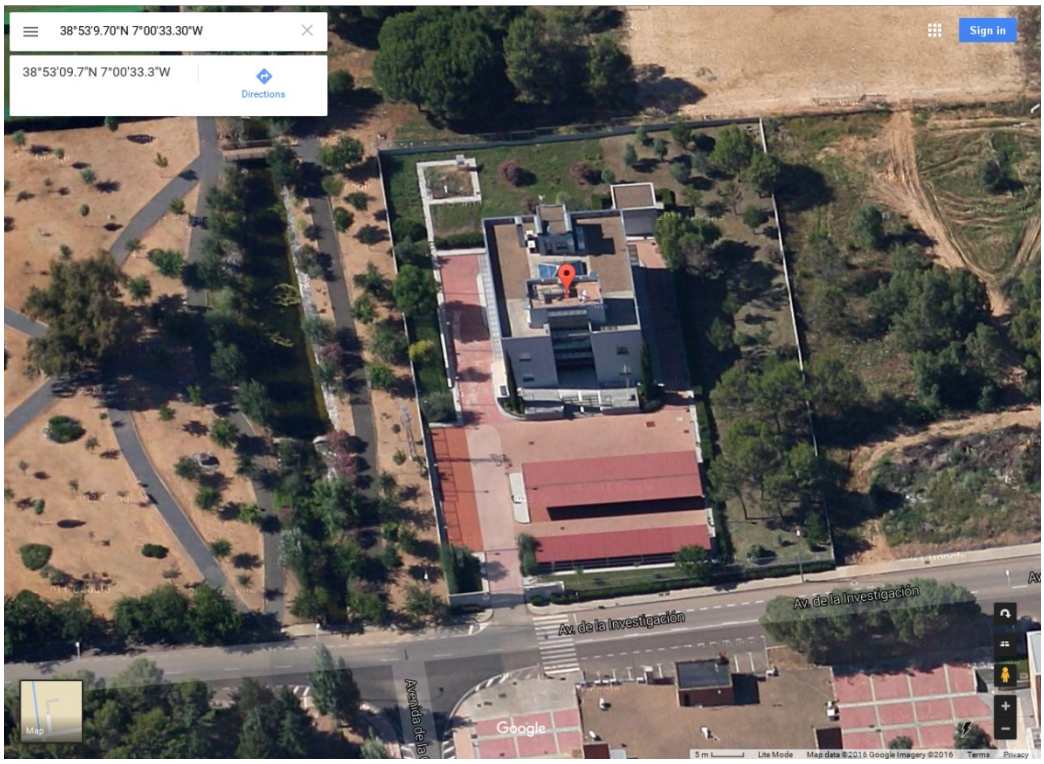

Figure 1.5 Location of Badajoz station on the roof-top of the AEMET building

Figure 1.6 Instrumentation at Badajoz station

The station is equipped with a Kipp-Zonen CMP-21 pyranometer, with GHI observations available since January 2005, and a Kipp-Zonen CH-1 pyrheliometer, which has given DNI measurements continuously

since January 2008 (there were non-continuous observations before). The other meteorological observations used in the project (2m temperature and 10m wind speed and direction) are measured by Thies Compact sensors, part of a standard meteorological station situated at ground level, very close to the AEMET building. There are observations for these variables since January 2001.

Table 2: Station information Badajoz

Station	**Latitude**	**Longitude**	**Elevation (m)**	**Pyrheliometer**	**Period**	**Temporal resolution**
Badajoz	38.883 N	7.017 W	190	KIPP-ZONEN CH-1	From 2008 to date	1-min

The following table show the number of invalid DNI days in Badajoz both caused by missing data and incorrectly measured data (see Annex B for QC procedures). Few missing days are found, as well as punctual tracking errors.

Table 2a: Station information Badajoz – data availability

	Badajoz (AEMET)												
Year	Jan	Feb	Mar	Apr	May	Jun	Jul	Aug	Sep	Oct	Nov	Dec	Annual
2015	2	1	1	1	1	0	1	0	0	1	0	0	8

There is a Cimel sun photometer nearby (approximately 300m away), managed by Extremadura University. AERONET observations (Level 1.5, automatically cloud-screened) are available from July 2012 to May 2016. It is part of the AERONET network. AOD (aerosol optical depth) measurements from this instrument will be used in the project as well.

1.1.3 Station details - PSA

DLR's radiometric station (Fig 1.7) at Plataforma Solar de Almería (PSA) collects data since February 2001. The data are recorded with first class pyrheliometers and secondary standard pyranometers as defined in ISO 9060. A pyrgeometer was installed in 2010. Data gaps are reduced to a minimum due the completive use of other meteorological stations with sensors of the same classes situated within 500 m of the main station. Until 2011 gaps were filled with co-located Rotating Shadowband Irradiometers (RSIs), with a posteriori spectral, temperature and air-mass correction. Several other radiometric stations exist at PSA. Intensive maintenance, including cleaning of the sensors on every working day, is provided.

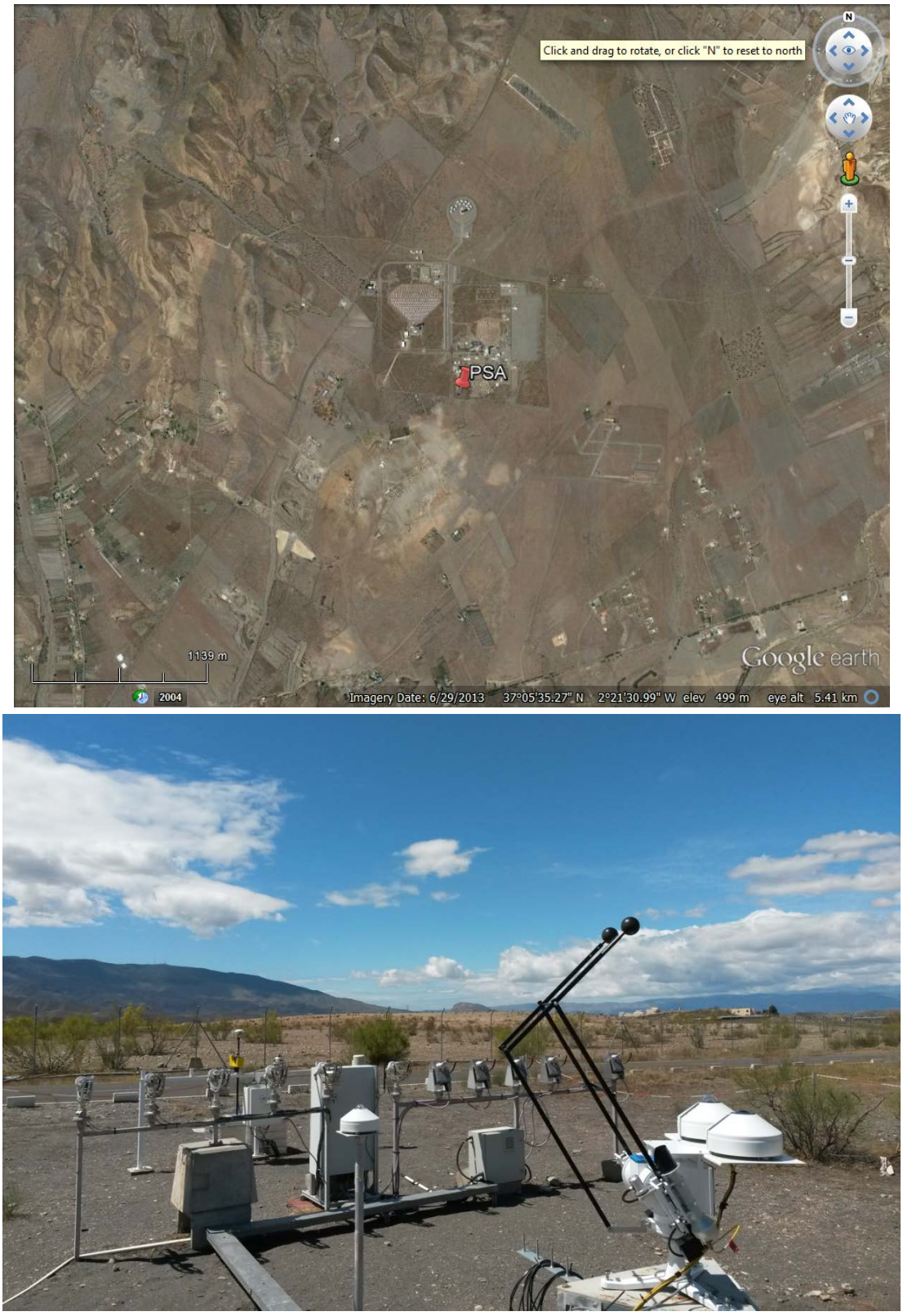

Figure 1.7 View of the PSA DLR radiometric station (source Google Maps, DLR)

In addition to the radiometric parameters just described, air temperature and relative humidity, wind speed, wind direction and air pressure are measured. In 2010, an AERONET sun photometer has been installed, as well as an all-sky imager that documents the state of the sky during measurements. A sun and aureole radiance measurement system, aerosol particle-counters, a 3D wind sensor and visibility measurement systems are operated since 2012. Since 2013 also ceilometer data are available.

Table 3: Station information PSA

Station	Latitude	Longitude	Elevation (m)	Pyrheliometer	Period	Temporal resolution
PSA_DLR	37.09081 N	2.35808 W	486	Kipp&Zonen	Feb 2001 onwards	1-min

The following table show the number of invalid DNI days at the PSA_DLR station both caused by missing data and incorrectly measured data (see Annex B for QC procedures). The following issues were found:

2005: There are no data on January, February and December 14th – 31st

2006: July: 7 days without data.

2007: No data on December 19th – 31st

2013: Tracking system failures

2014: There are no data from April 3rd

There is also an AERONET station available (named 'Tabernas_PSA-DLR'), operated by DLR. Level 1.5 (automatically cloud-screened) observations are available from March 2011 to April 2014.

1.1.4 Satellite-based irradiance information

The atmosphere service of Copernicus (CAMS, https://atmosphere.copernicus.eu/) combines state-of-the-art atmospheric modelling on aerosols with Earth observation data. It provides information services covering European air quality, global atmospheric composition, climate, and UV and solar energy. Within the radiation service (http://www.soda-pro.com/web-services/radiation/cams-radiation-service, Lefèvre et al., 2013 and Qu et al., 2016) the following time series of irradiances can be downloaded:

- Period of record: Feb 2004–present, data is provided with up to 2 days delay
- Temporal resolution: 1-minute, 15-minute, hour, day, month
- Spatial coverage: Europe/Africa/Middle East/Eastern part of South America/ Atlantic Ocean.
- Spatial resolution: Spatial resolution is the original pixel of the Meteosat Second Generation (MSG) image (approx. 3 km at satellite nadir and 5 km at mid-latitude).
- Data elements and sources: Global, direct, diffuse, and direct at normal incidence irradiances (GHI, DIR, DHI, DNI); global, direct, diffuse and direct normal irradiances in cloud free conditions; verbose mode with all atmospheric input parameters used for clouds, aerosols, ozone, water vapour and the surface reflective properties.
- Data quality control and assessment: Input quality control, regular quarterly benchmarking against ground stations, regular monitoring the consistency and detecting possible trends.
- Estimated uncertainties (Qu et al., 2016): The 15 min means of irradiance estimated by Heliosat-4 were compared to corresponding measurements made at 13 stations within

the Baseline Surface Radiation Network located in the field of view of MSG and in various climates. The bias for global irradiance was comprised between 2 and 32 W/m². The root mean square error (RMSE) ranged between 74 and 94 W/m². Relative RMSE values ranged between 15% and 20% of the mean observed irradiance for stations in desert and Mediterranean climates, and between 26% and 43% for rainy climates with mild winters. Correlation coefficients between 0.91 and 0.97 were found.

The bias for the direct irradiance at normal incidence was comprised between 163 and +50 W/m². The RMSE ranged from 160 W m 2 (29% of the mean observed irradiance) to 288 W/m² (63%). The correlation coefficient ranged between 0.67 and 0.87.

For this project, we have obtained 10 years of CAMS data (2006 to 2015) for each station where available.

1.1.5 Irradiance statistics – Évora

In the following we present the irradiances themselves, both from ground and satellite observations.

Ground observations

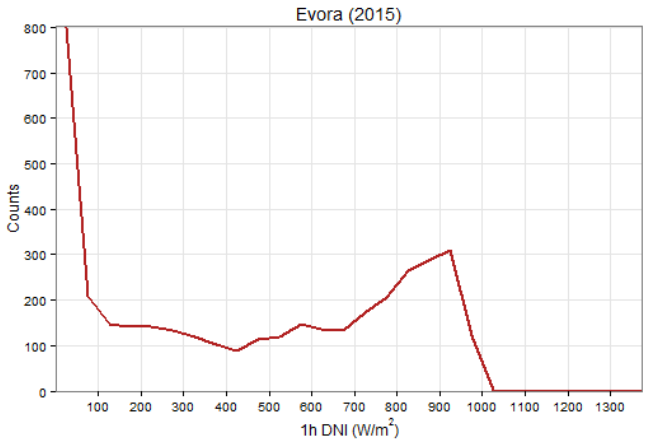

Figure 1.8: Frequency histogram of hourly DNI for daytime ground measurements in 2015 at Évora station.

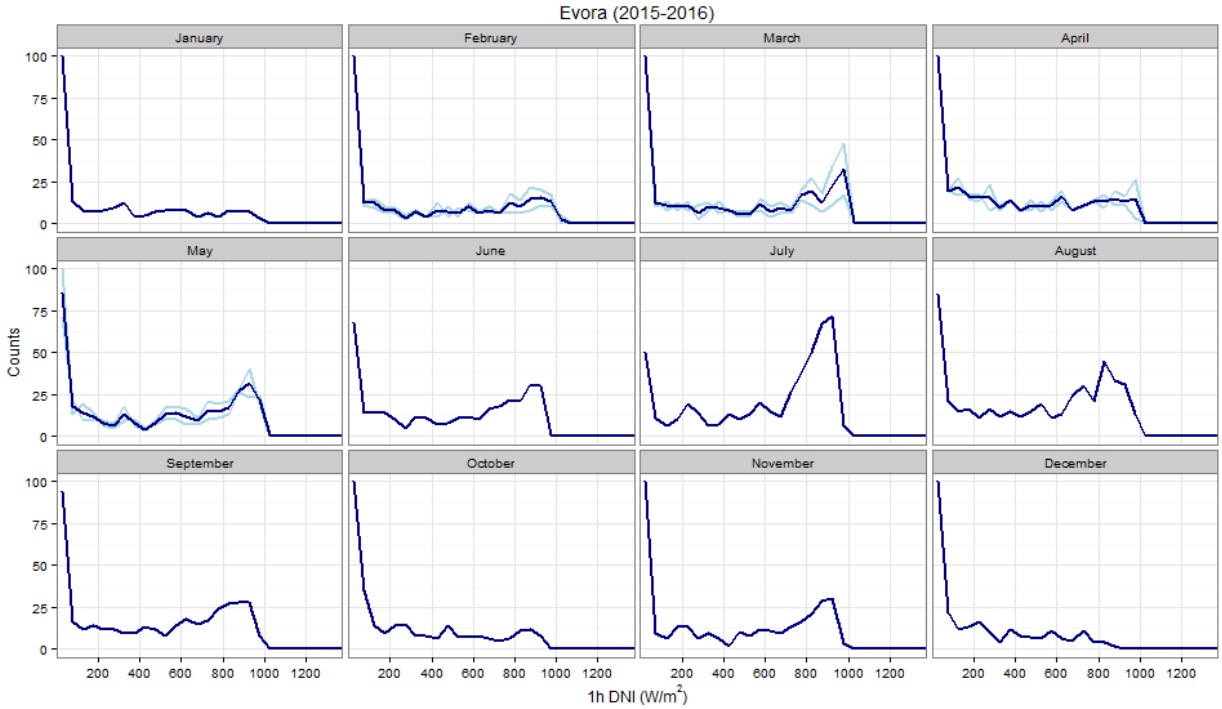

Figure 1.9 Ground observation based daytime hourly DNI values from 2015 and 2016 at Évora station and split in monthly frequency histograms.

First, we present all available observations from 2015 and 2016 jointly (Fig 1.8 and 1.9). It is worth to note that January and June 2015 are missing in the ground observations. For all other months the individual years are given in light blue, while the total dataset is given in dark blue. There is a clear seasonality, but due to the short time series of observations it is only an indication of weather pattern

having occurred in the respective months. It is no indication about the typical climate and the typical seasonal patterns.

Satellite/model based observations (CAMS)

Long-term satellite-based observations allow generating information on typical seasonal patterns. In order to ensure that CAMS data is sufficiently accurate in Évora, we compare the histograms for all months with available ground observations. We do not compare the annual histogram as the ground observations have missing data in January and June.

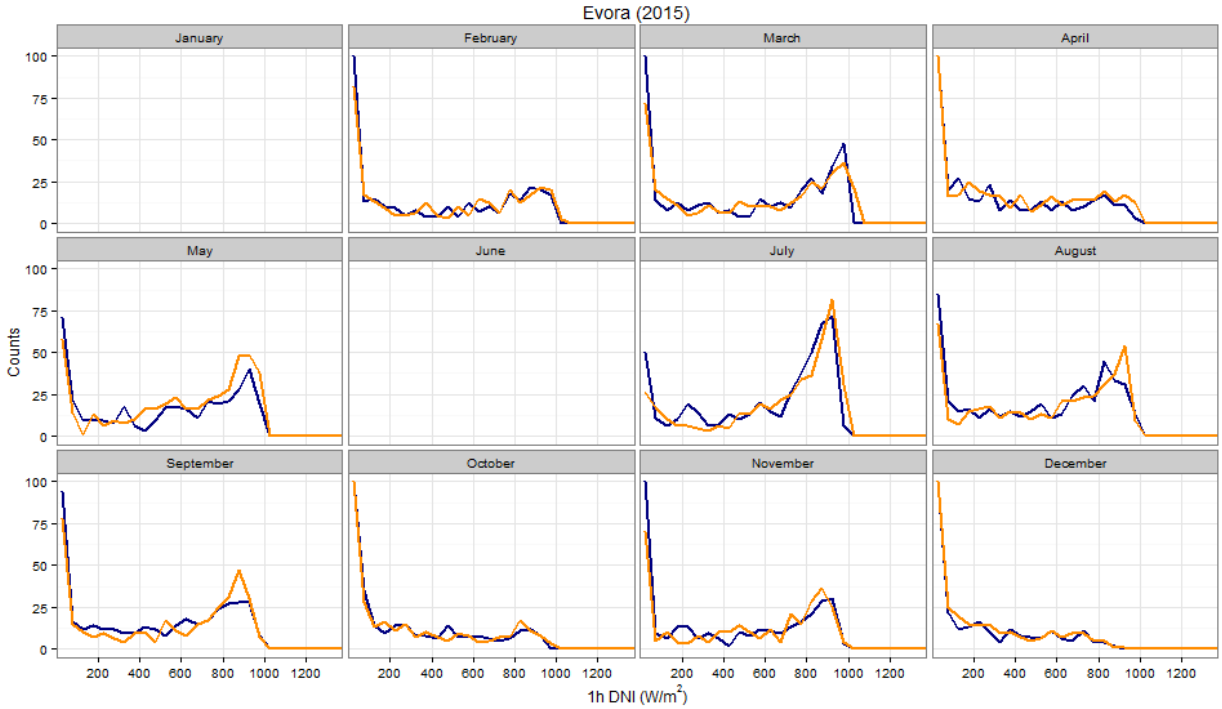

Figure 1.10 Ground based (blue) and CAMS-based (orange) daytime hourly DNI values from 2015 at Évora station and split in monthly frequency histograms.

Generally, the patterns are well met in the different months (Fig 1.10). Difference in the maximum peak values can be observed for May, August and September, but generally, the patterns agree very well.

Turning to look at the satellite observations, which provide a 10 year series, Fig 1.11 illustrates the mean histogram of 2006 to 2015 in red with the histograms of individual years in light grey. They indicate the year-to-year variability. The same is done in Fig. 1.12, but resolved over months.

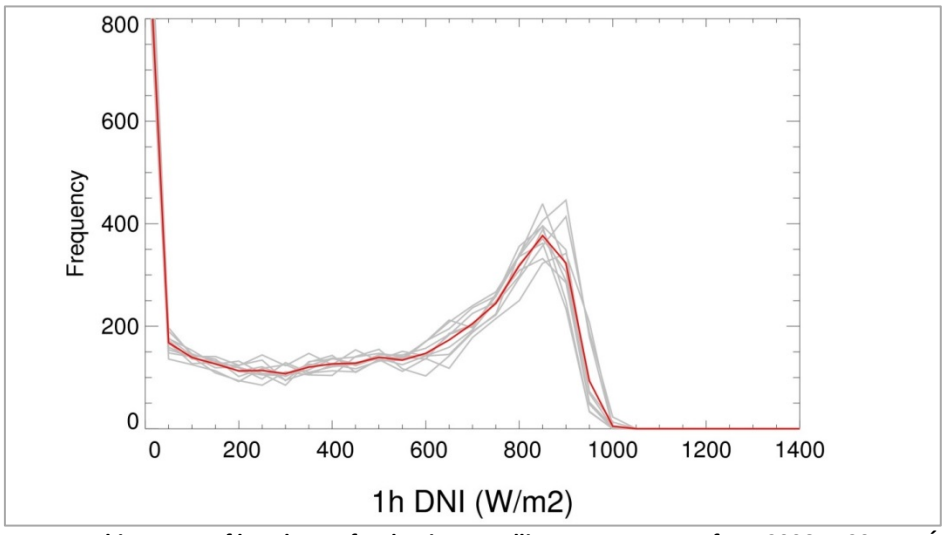

Figure 1.11 Frequency histogram of hourly DNI for daytime satellite measurements from 2006 to 2015 at Évora station. The mean is given in red and all individual years in grey.

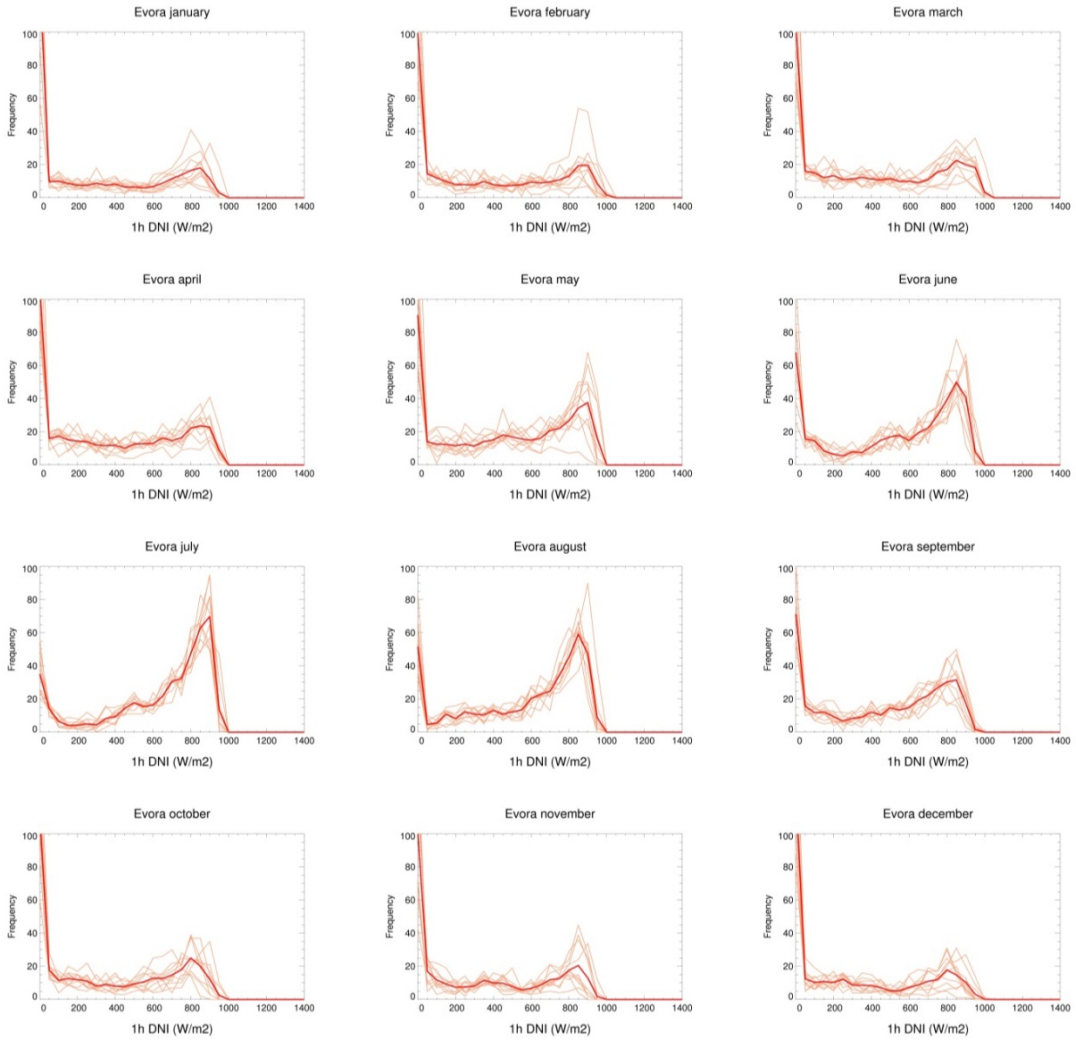

Figure 1.12 CAMS hourly DNI values from 2006 to 2015 at Évora station and split in monthly frequency histograms. The mean is given in bold red and all individual years in light red.

1.1.6 Irradiance statistics - Évora vs. Badajoz

In the following section we repeat the same statistics, but compare Évora with Badajoz. Évora is the PreFlexMS demo site, but Badajoz has a much longer record of ground observations. Therefore, forecast assessments will be based for Badajoz if longer time series are requested to gain significance and reliability in statistical results. Consequently, we want to understand how Badajoz and Évora stations differ.

Having only a short time overlap of ground observations, the direct comparison is only of restricted information content. We therefore use satellite observations at both locations to compare. First we have to understand if Badajoz conditions are met in the CAMS dataset before we compare long-term CAMS time series at the two locations.

Ground observations

Fig 1.13 and 1.14 present Badajoz ground observations as annual and monthly histograms derived from observations in 2015. Also in Badajoz a clear pattern over the months can be observed. We do not show multi-annual variability due to lack of observations.

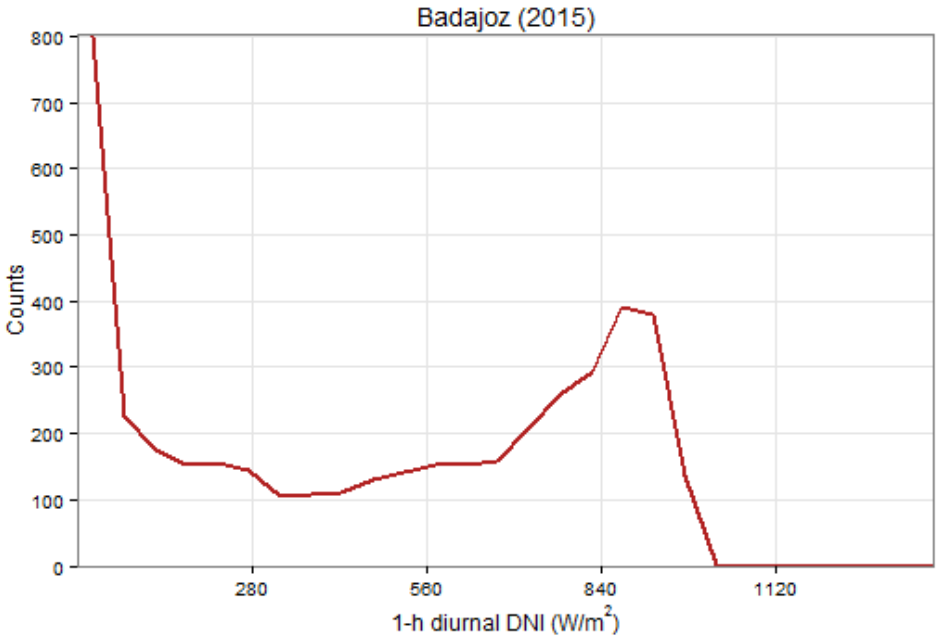

Figure 1.13 Frequency histogram of hourly DNI for daytime measurements in 2015 at Badajoz station.

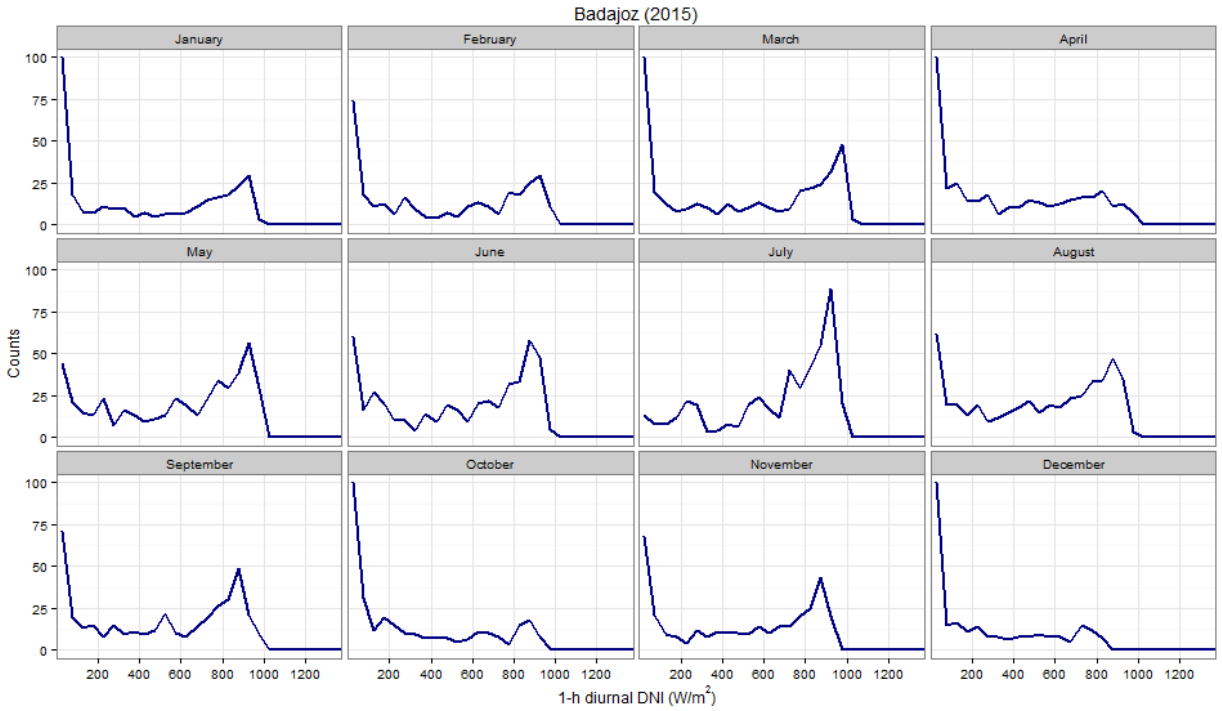

Figure 1.14 Ground observation based daytime hourly DNI values from 2015 at Badajoz station and split in monthly frequency histograms.

Satellite/model based observations (CAMS)

We compare the mean histograms for the years and months with available ground observations measured in 2015. We see an underestimation of small DNI values and a slight overestimation of values above 900 W/m2 in the annual histogram (Fig 1.15).

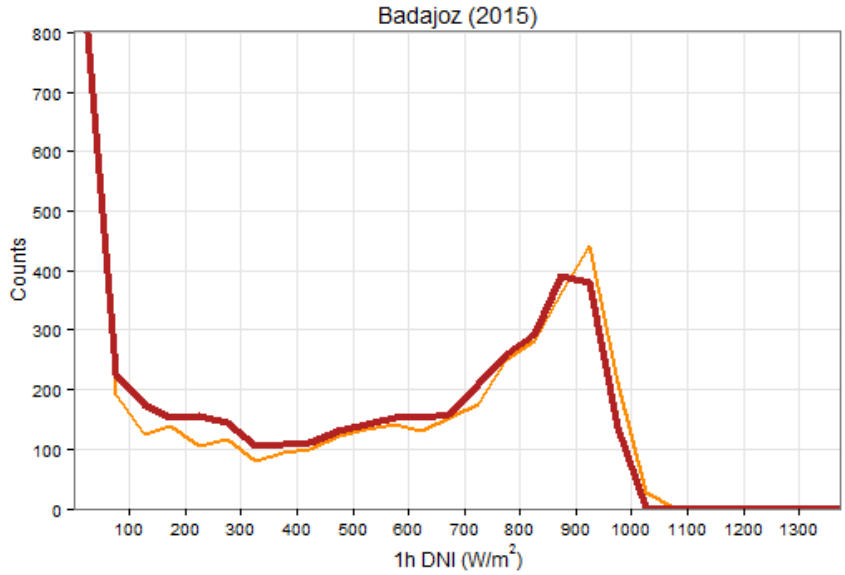

Figure 1.15 Ground (red) and CAMS-based (orange) hourly daytime DNI values from 2015 at Badajoz station.

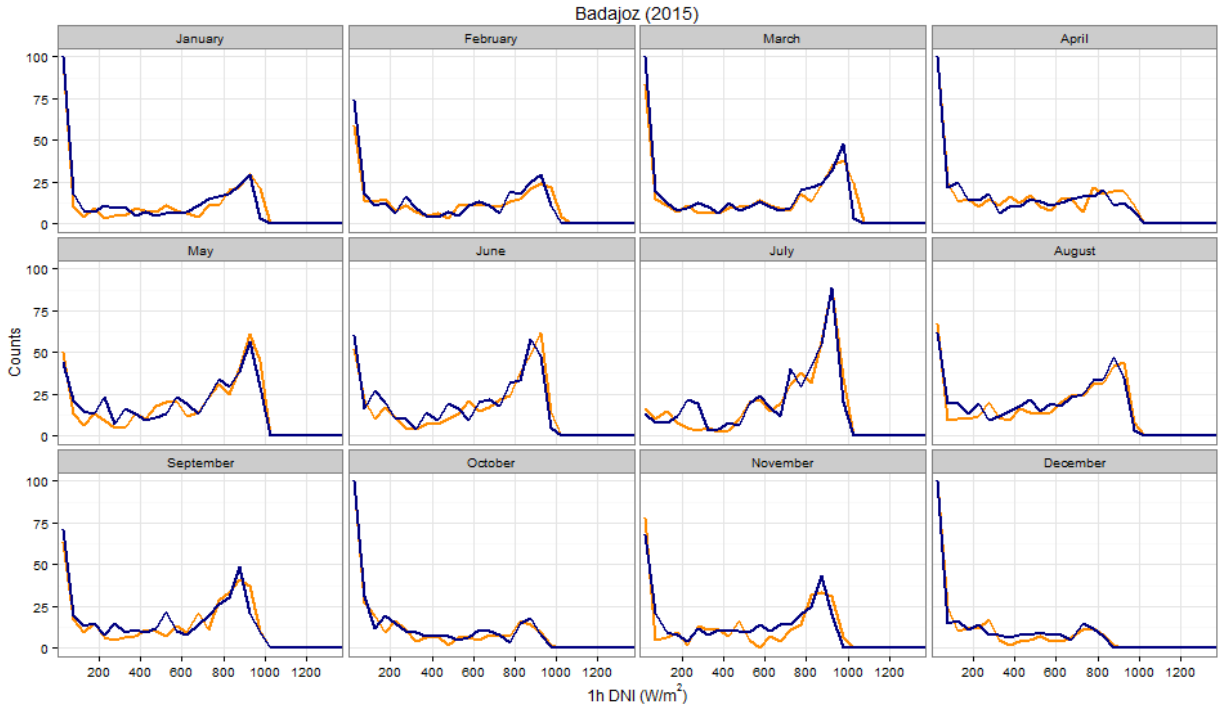

Figure 1.16 Ground (red) and CAMS-based (orange) daytime hourly DNI values from 2015 at Badajoz station (split in monthly frequency histograms)

Nevertheless, for our purpose of validating forecasts it is more relevant, that the monthly distribution of values is similar (Fig 1.16). We see that the variation from month to month is sufficiently met. This is an indication that the weather pattern is well met by the satellite observations. Therefore, CAMS observations may be used for forecast evaluations on a longer multi-annual forecast dataset.

Having discussed the difference between ground and satellite-based observations for the time series with available ground observations, we now continue to look at the satellite observations with their 10 year time series.

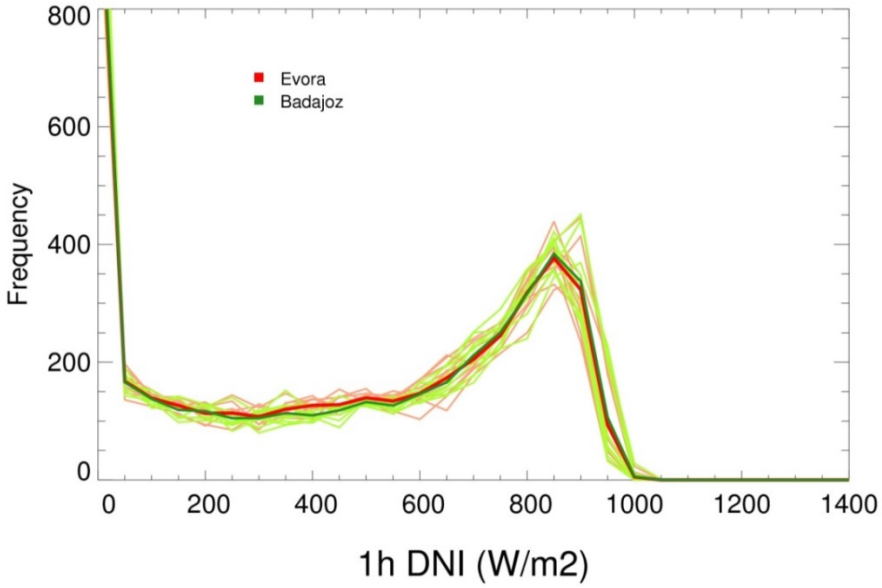

Figure 1.17 CAMS hourly daytime DNI values from 2006 to 2015 at Évora (red) and Badajoz (green) stations

Both stations have similar 10-year mean histograms, and also, the band of annual variability is very similar (Fig 1.17). Likewise, the monthly 10-year mean histograms are very similar (Fig 1.18). Small differences occur e.g. in January, May, or November, but the general seasonality is similar in both datasets. Therefore, Badajoz observations are well suited to be taken to evaluate numerical weather prediction (NWP) forecasts with respect to Évora. This statement is valid both for the ground observations being available from different periods only, but also for the long-term satellite observations.

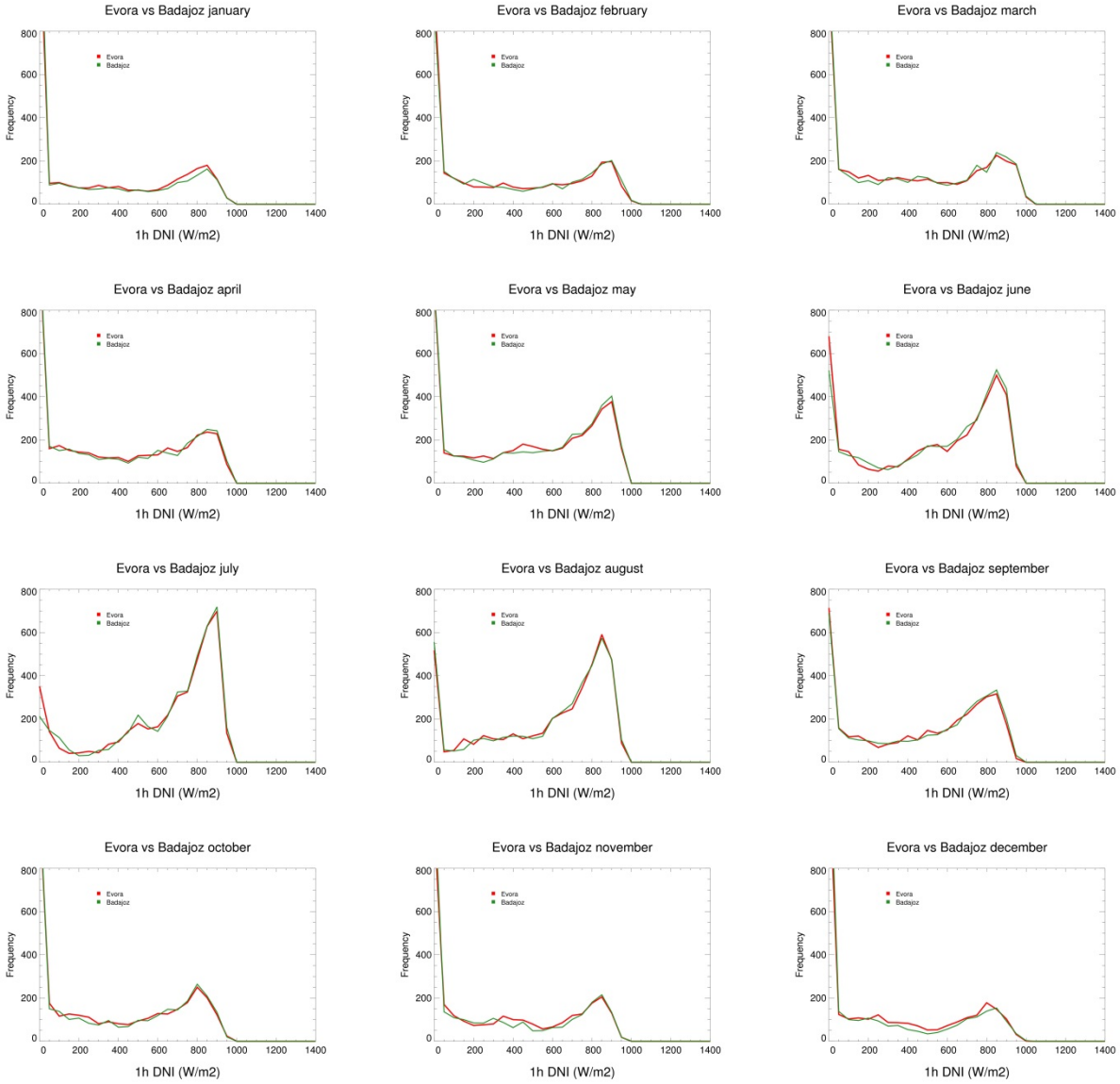

Figure 1.18 CAMS hourly daytime DNI values from 2006 to 2015 at Évora (red) and Badajoz (green) stations and split in monthly frequency histograms

1.1.7 Irradiance statistics - Évora vs. PSA

In a second comparison we want to assess the similarity of Évora versus the PSA station. While Évora is in the western part of the Iberian Peninsula, PSA is located in the East and within a desert and mountainous region. With this comparison we want to get an impression about the different climatic conditions for Concentrating Solar Power (CSP) on the Iberian Peninsula. Having CSP in mind, we omit any attempt to

compare Southern and Northern parts of the Iberian Peninsula. There are of course stronger differences expected, but the Northern part is less relevant for the CSP sector.

Ground observations

Thanks to the multi-annual data record based on ground observations at PSA, we can now assess the multi-annual variability in the period from 2006 to 2013 also based on ground observations (Fig 1.19 and 1.20). This had not been possible for Évora and Badajoz stations.

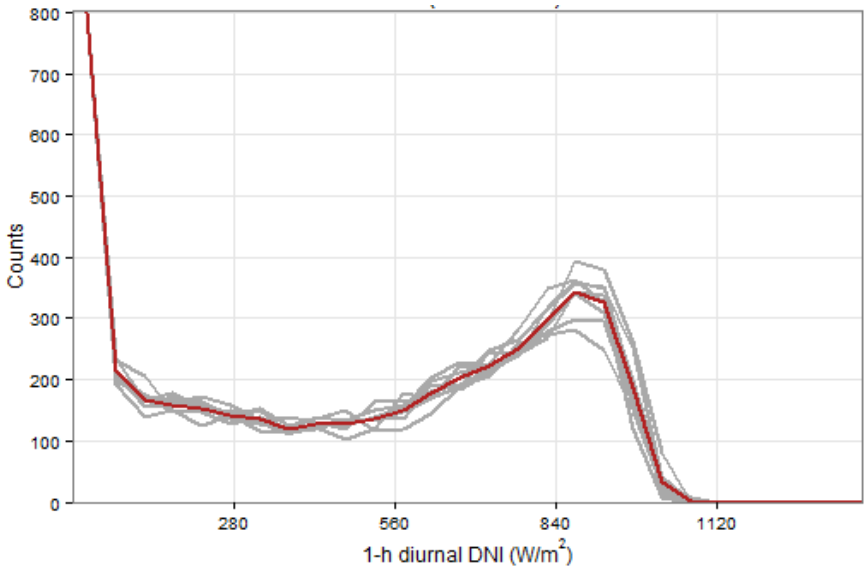

Figure 1.19 Ground observation daytime based hourly DNI values from 2006 to 2013 at PSA station. The mean is given in red and all individual years in grey.

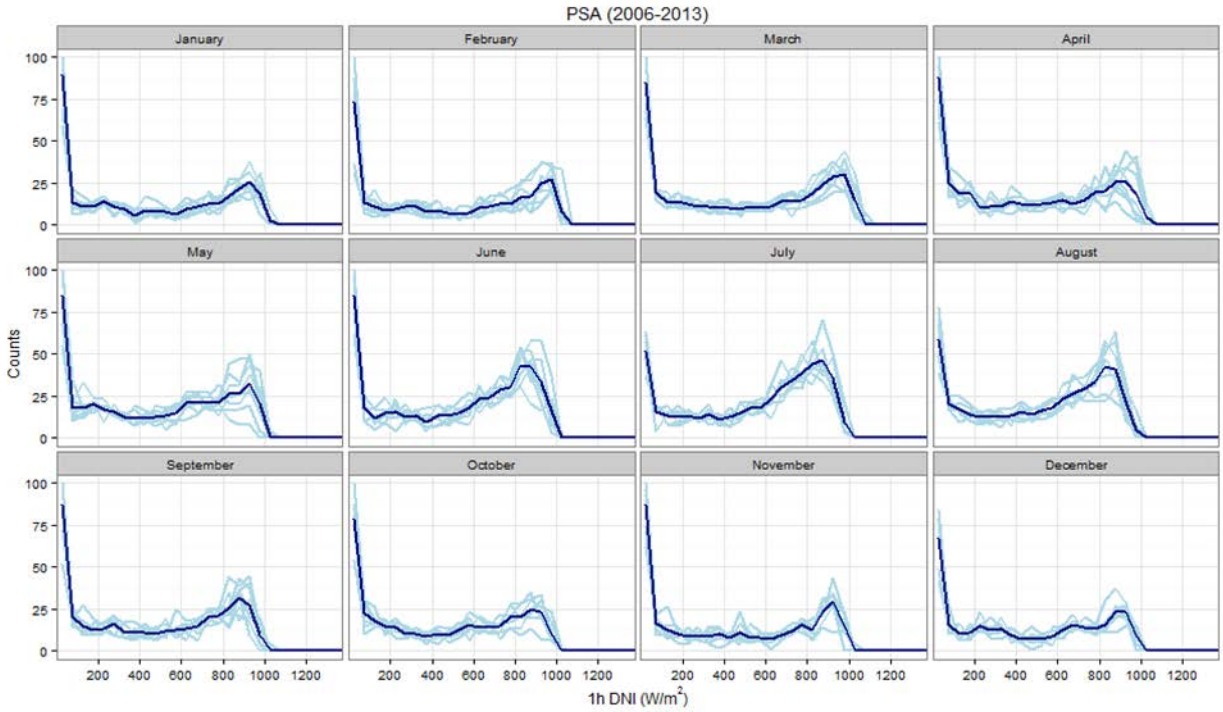

Figure 1.20 Ground observation based daytime hourly DNI values from 2006 to 2013 at PSA station and split in monthly frequency histograms. The mean is given in bold blue and all individual years in light blue.

Satellite/model based observations (CAMS)

In order to ensure that CAMS data is sufficiently accurate in PSA, we compare the mean histograms for the years and months with available ground observations (Fig 1.21 and 1.22).

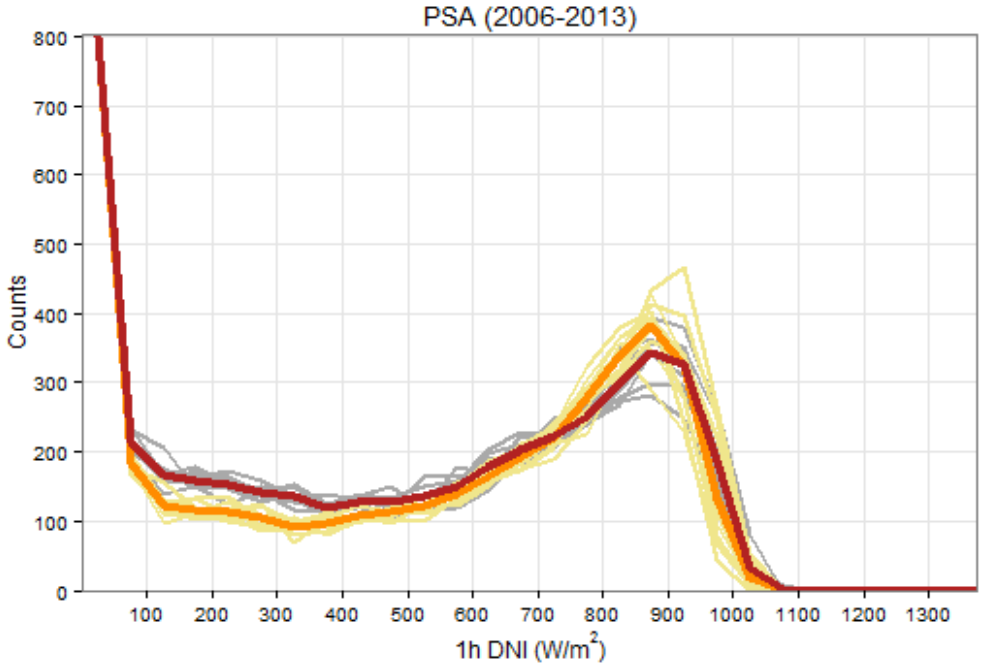

Figure 1.21 Ground based (red) and CAMS-based (orange) hourly daytime DNI values from 2006 to 2013 at PSA station. Individual years are given in thin lines (grey for ground observations, yellow for CAMS), while bold lines show the multi-annual average.

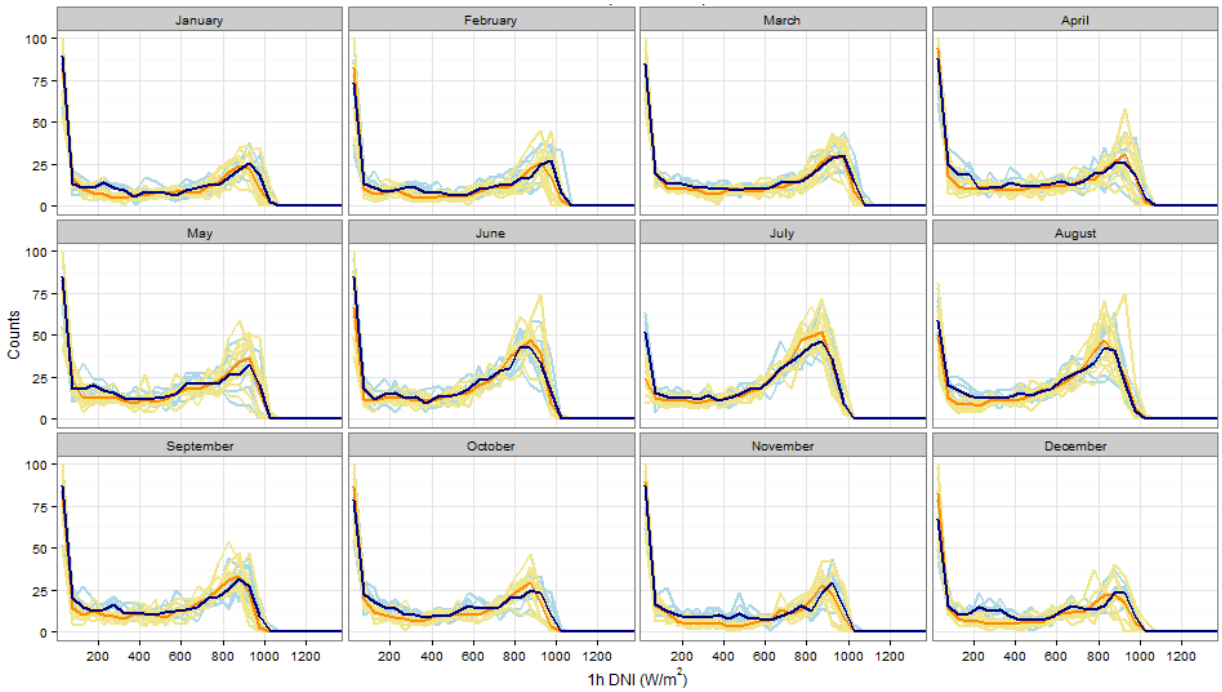

Figure 1.22 Ground based (dark blue) and CAMS-based (orange) hourly daytime DNI values from 2006 to 2013 at PSA station and split in monthly frequency histograms. The mean is given in bold and all individual years in thin lines.

In the annual mean histogram an underestimation of smaller DNI values and an overestimation of values between 800 and 900 W/m2 is seen in CAMS data. This difference originates from the months October to February, where also the monthly mean histograms show a similar shift. Especially in October, the shift in the 800 to 900 W/m2 range can be seen in several individual years.

Having discussed the difference between ground and satellite-based observations, we now continue to look at the satellite observations with their long-term time series. Comparing CAMS at Évora and PSA shows a larger occurrence of 200 to 550 W/m2 values in Évora, while values between 600 and 850 W/m2 occur less in Évora (Fig. 1.23). For DNI above 850 W/m2, the two locations show a similar long-term behaviour.

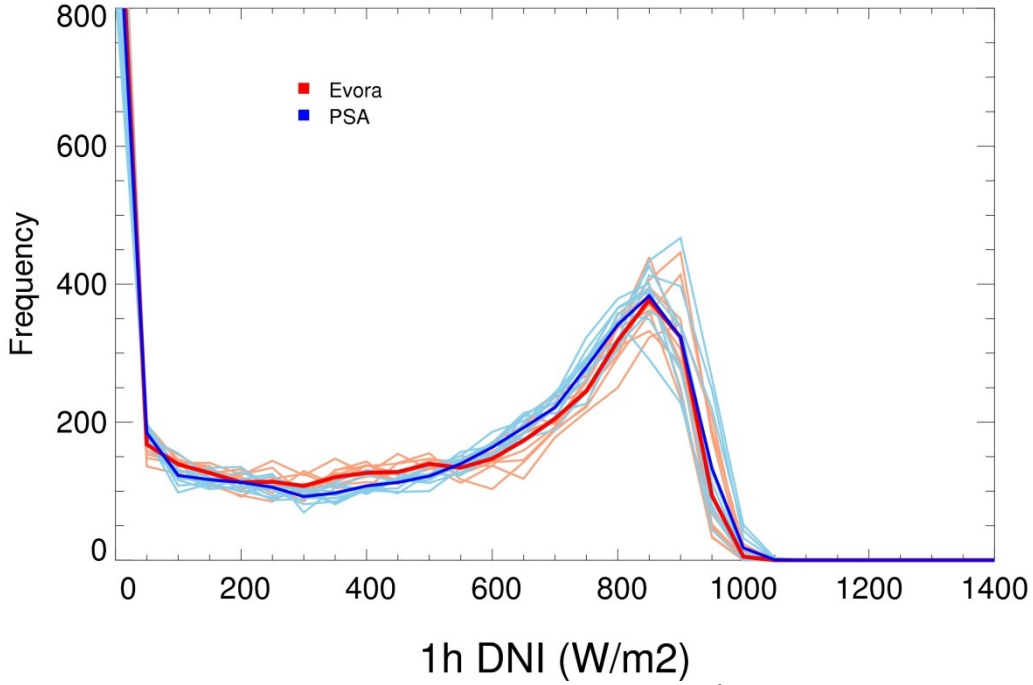

Figure 1.23 CAMS hourly daytime DNI values from 2006 to 2015 at Évora (red) and PSA (blue) stations. Multi-annual mean histograms are given in bold, while individual years are given in light colours.

Despite their rather similar multi-annual yearly histograms, the view on monthly histograms (Fig. 1.24) reveals significant differences. In July and August, Évora has much more high DNI values than PSA, while in October to April the PSA shows more high DNI values above 800 W/m2. This could be caused by a higher Saharan dust frequency in July and August (see chapter 2.3.2). Only in the transition months May, June and September both histograms are similar with respect to high DNI values.

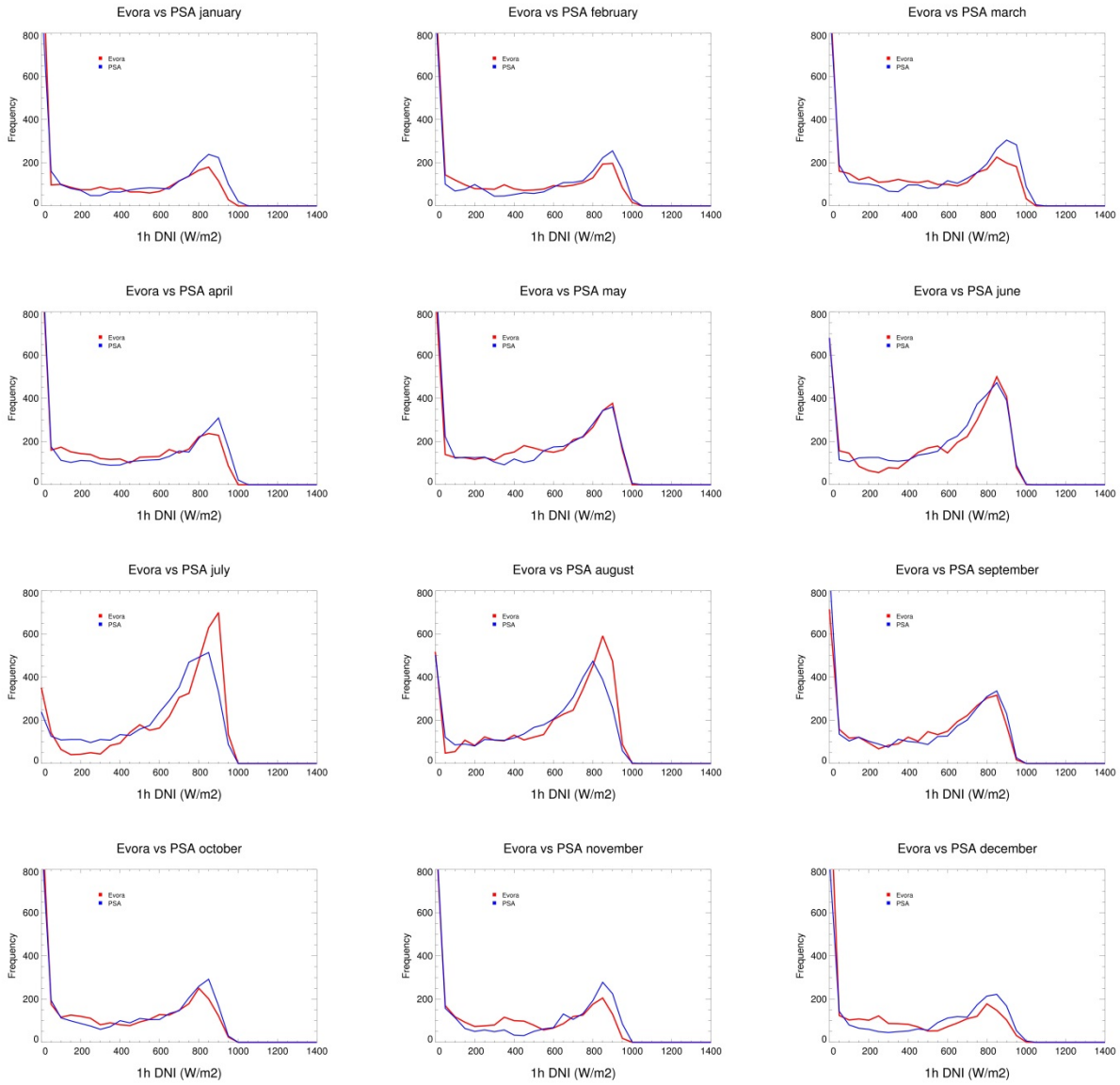

Figure 1.24 CAMS hourly daytime DNI values from 2006 to 2015 at Évora (red) and PSA (blue) stations and split in monthly frequency histograms.

1.2 Satellite-based cloud physical parameter statistics

1.2.1 Method

The APOLLO methodology (AVHRR Processing scheme Over cLouds, Land and Ocean; Saunders et al., 1988; Saunders, 1988; Gesell, G., 1989; Kriebel et al., 1989; Kriebel et al., 2003) uses multiple spectral channels of the MSG to discriminate between different cloud types and to provide cloud properties.

Fig. 1.25 provides an example image of MSG giving a visual impression how different cloud types look from space. Please note various colors – indicating low or high level clouds – and the thickness of various clouds. For some, the ground can be seen, for others, the ground is not visible due to the cloud optical thickness. The same applies for DNI – for some clouds the solar power plant will see the sun (which is related to DNI > 0), in other situations, the DNI is close to zero. Also, please note the spatial structures of

clouds and gaps in cloud cover. This is evaluated quantitatively by the APOLLO satellite retrieval and a post-processing of APOLLO results for cloud statistics.

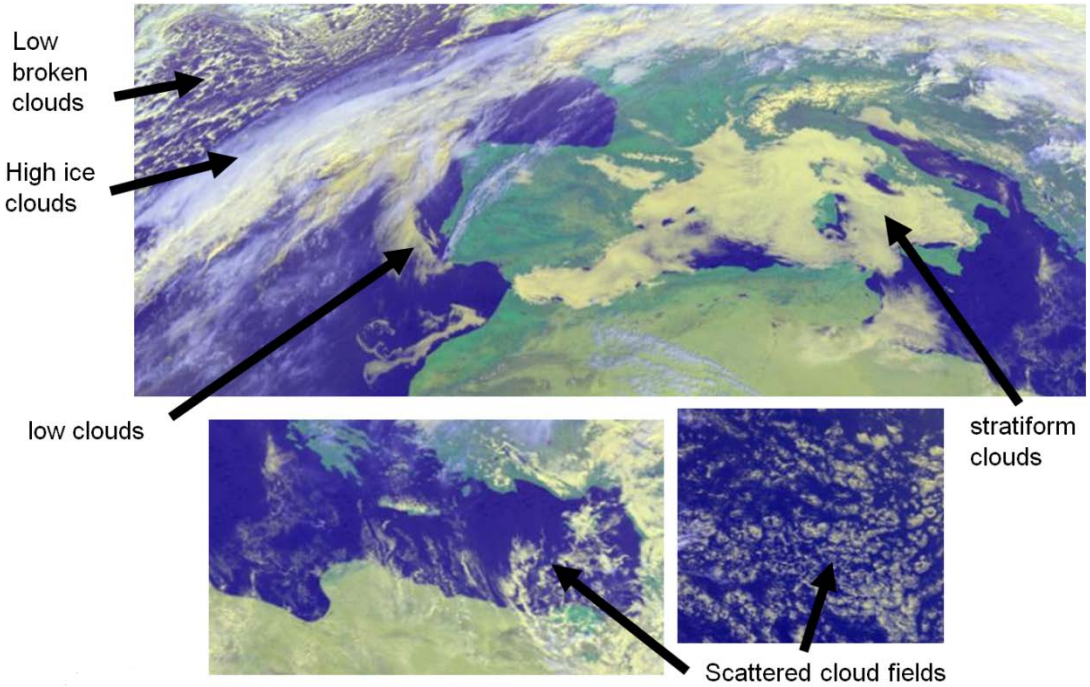

Figure 1.25 MSG example image (copyright EUMETSAT/DLR)

Below a picture of water/mixed phase clouds as seen from the ground is shown on the left image and an example for optically thin ice clouds is given on the right image (Fig. 1.26, left). It is expected that for water/mixed phase clouds in such an overcast case, both the global and the direct irradiance are low together with a low temporal variability.

For a more scattered case of water/mixed phase clouds (Fig. 1.27), the global irradiance varies quickly between medium and high values and even overshooting values above clear sky values occur. The direct irradiance jumps between zero, medium and high clear sky-like values.

For optically thin ice clouds (Fig 1.26, right), the situation is different: For global irradiances the influence is low and any temporal variability is typically fast, but low in the amplitude. On the other hand, direct irradiances are affected very significantly, with typically medium and high values together with a high fluctuation rate.

Figure 1.26 Clouds as seen from the ground – overcast (left) and thin cirrus (right; copyright Karlsruher Wolkenatlas, B. Mühr)

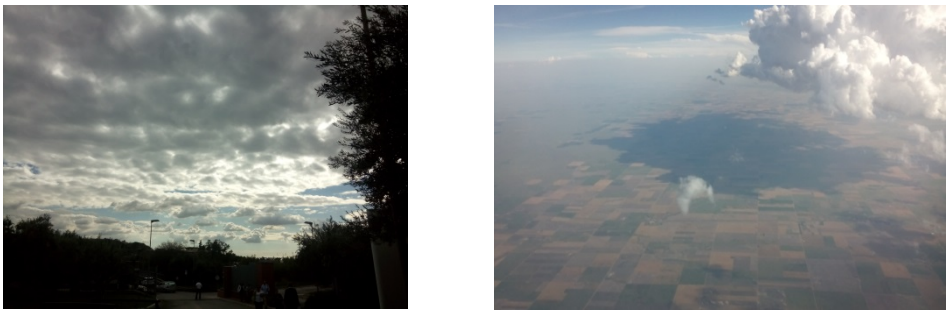

Figure 1.27 Overcast and scattered clouds (left) and a single cloud system with cloud shadow on the ground (right; copyright R. Ruf)

The APOLLO methodology delivers cloud mask, cloud optical depth, liquid and ice water path, and cloud top temperature as cloud parameter products for each MSG SEVIRI pixel in a temporal resolution of 15 minutes during daytime, for the period 2004 until today (>= 10 years). The covered zone is [60°N,60°S,60°E,60W], with a resolution of 3x3 km² at the nadir of the satellite [0°, 0°]. The resolution in Europe is about 4x5 km² to 5x6 km². The following parameters are computed and stored:

- Cloud mask (cloud/cloud-free) and snow
- Cloud coverage (0-100%)
- Cloud type (low, medium, high water/mixed water/ice phase clouds; optically thin ice clouds)
- Cloud optical depth
- Cloud top temperature

Additionally to the single pixel results, the surrounding 29x29 pixel window is evaluated in order to understand the medium scale cloud situation. In this window, several values are computed, mostly the number of cloud elements, the number of gradients in a binary cloud mask changing from cloud to non-cloud, the window cloud fraction, and the cloud shape complexity from the fractal box counting dimension. The main aspect highlighted by the fractal box dimension is its ability to identify different structures according to their level of aggregation, the circular patterns, and the isotropy of their pixel distribution (Carvalho and Dias, 1998). This fractal box counting dimension represents the complexity of the clouds shape and evolves from zero (a point) through one (a line) to two (an area). In most cases, it lies between one and two if the cloudy pixels clusters in the window are several pixels wide. Fig. 1.28 shows typical examples of these situations.

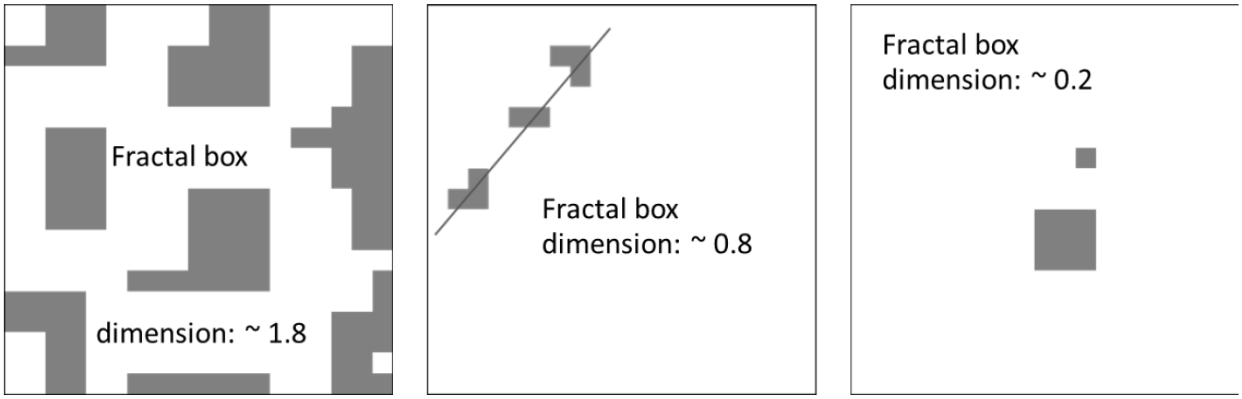

Figure1.28: Typical box dimensions of different cloud masks, source: S. Glas

Additionally, we discriminate between overcast/broken, scattered and isolated cloud fields and call this classification 'cloud area type'. If there are more than 10 individual cloud elements in the surroundings, the situation is classified as 'scattered' unless the total cloud fraction in the surroundings is above 80%, which classifies the case as 'broken/overcast'. If there are less than 10 cloud elements, the situation is classified as 'broken/overcast' unless there is a high number of more than 175 cloud/no cloud changes from pixel to pixel in any direction, which again results in a 'scattered' case. Also, any cloud/no cloud change from the central pixel to the direct neighbors always results in a 'scattered' classification.

1.2.2 Évora station

First of all, we quantify the occurrence of various clouds. Fig. 1.29 discriminates cloud-free from cloudy cases. Cloud-free, but snow on the ground cases are also given, as this evaluation tool is also used for more photovoltaic (PV) related studies in more snowy regions. The Évora station has about 35% of cloudy cases during daytime hours. The cloudy cases are further split in optically thick cases with low, medium and high cloud top levels (named 'low water', 'medium wat.', and 'high wat./mix.') and optically thin cirrus cases ('high thin ice'). With respect to DNI, the separation in optically thick and thin cloud types is most relevant, for meteorologists the further split into vertical levels is of further interest to assess the situation at a site. Évora has a majority of low level optically thick water clouds (approx. 15%), followed by the amount of thin ice clouds (approx. 10%), which allow parts of the DNI to reach the ground.

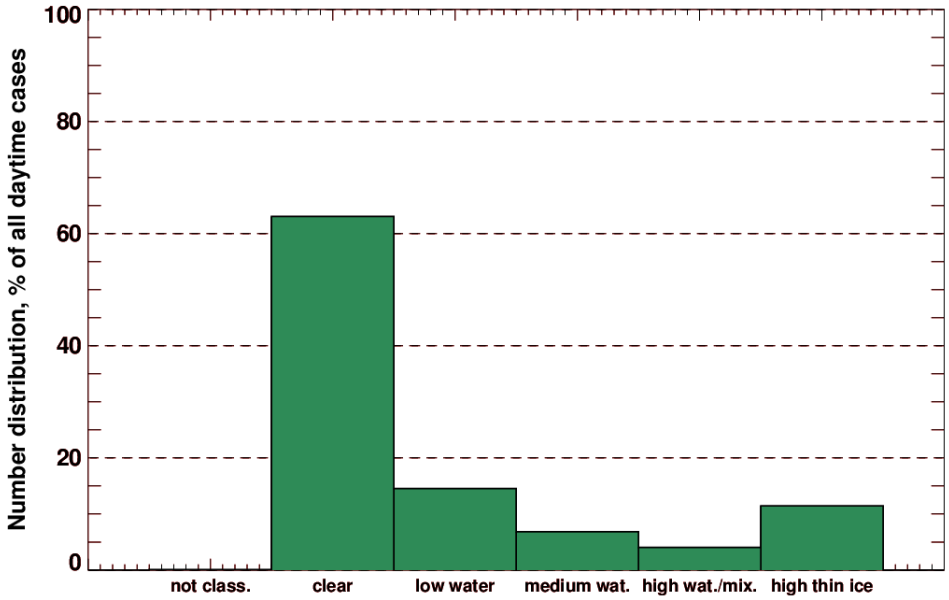

Figure 1.29 Cloud statistics at Évora stations: cloud type; frequency of occurrence in percentage of all daytime satellite images; split into cloud-free and cloudy cases – cloudy cases are separated in low, medium, high level cloud top height clouds (being optically thick) and optically thin ice cloud cases; based on 2005-2015.

Fig 1.30 provides the cloud type statistics as function of the month. We discriminate between scattered, broken/overcast, thin ice and cloud-free cases. During July and August a minimum of cloud cases is observed, while in other months the number of scattered cloud cases is quite constant over the year. The number of broken/overcast cases is reduced in May to September and also the number of thin cirrus cases is smaller from June to September.

Fig 1.31 provides the cloud type statistics as function of the time of the day. For scattered clouds there is no distinct diurnal cycle, but for the broken/overcast situations there is a dependency of the time of the day.

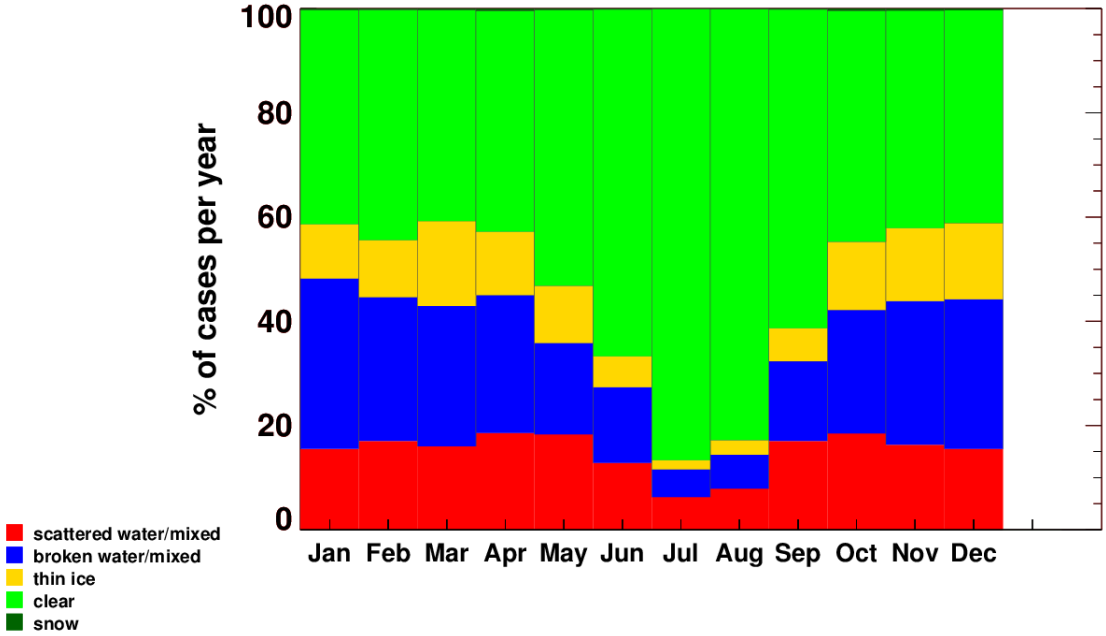

Figure 1.30 Cloud statistics at Évora station: cloud area type (red = scattered water/mixed phase; blue = broken/overcast water/mixed phase; yellow = thin ice phase; green = clear; dark green = snow); frequency of occurrence in percentage of all daytime satellite images; split into calendar month; based on 2005-2015.

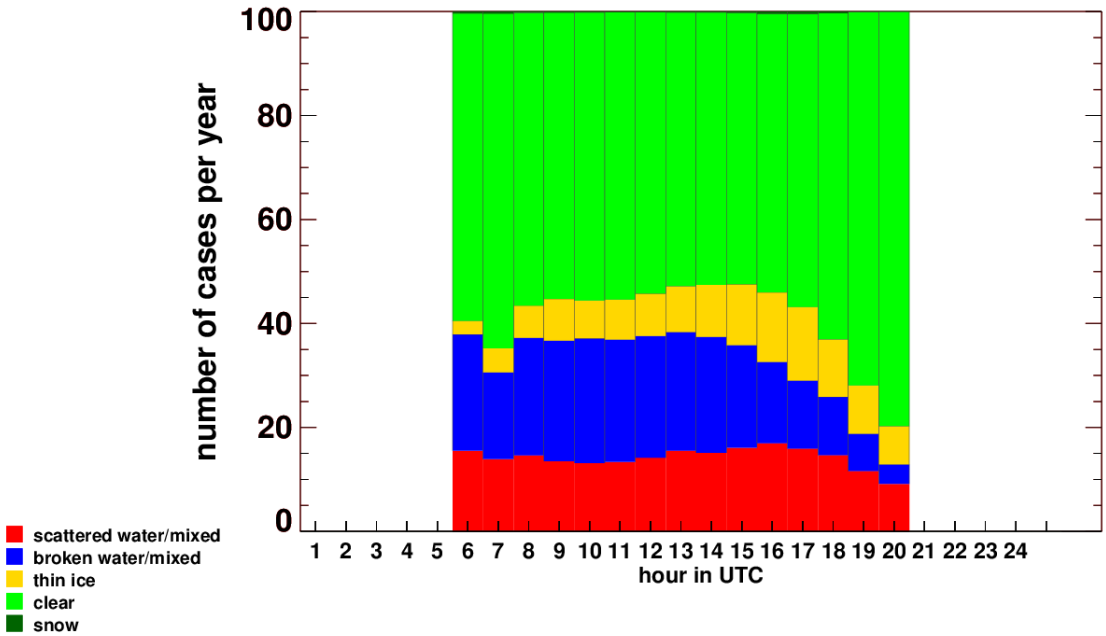

Figure 1.31 Cloud statistics at Évora station: cloud area type (red = scattered water/mixed phase; blue = broken/overcast water/mixed phase; yellow = thin ice phase; green = clear; dark green = snow); frequency of occurrence in percentage of all daytime satellite images; split into hour of the day; based on 2005-2015.

Fig 1.32 provides a split of Fig. 1.30 and 1.31 into months. The patterns over time of the day are highly variable. Some months show a dedicated diurnal cycle either in one of the cloud area type class or the overall cloud cases.

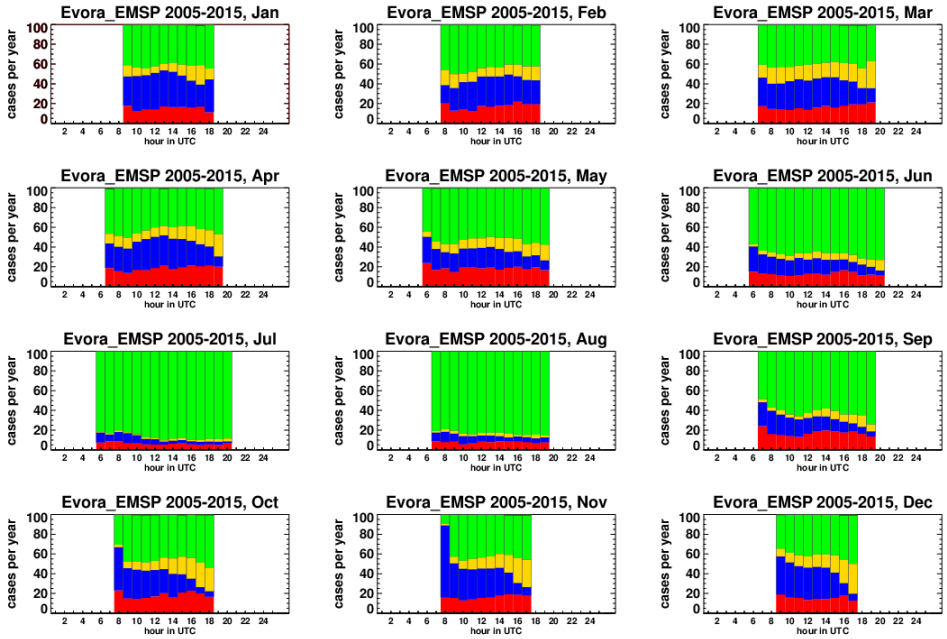

Figure 1.32 Cloud statistics at Évora station: cloud area type (red = scattered water/mixed phase; blue = broken/overcast water/mixed phase; yellow = thin ice phase; green = clear; dark green = snow); frequency of occurrence in percentage of all daytime satellite images; split into calendar month and hour of the day; based on 2005-2015.

1.2.3 Station Évora vs. Badajoz vs. PSA

Comparing cloud information from Évora vs Badajoz and PSA (Fig 1.33) shows that PSA has a larger fraction of clear cases. Badajoz and PSA have less low level water clouds but significantly more thin cirrus class cases.

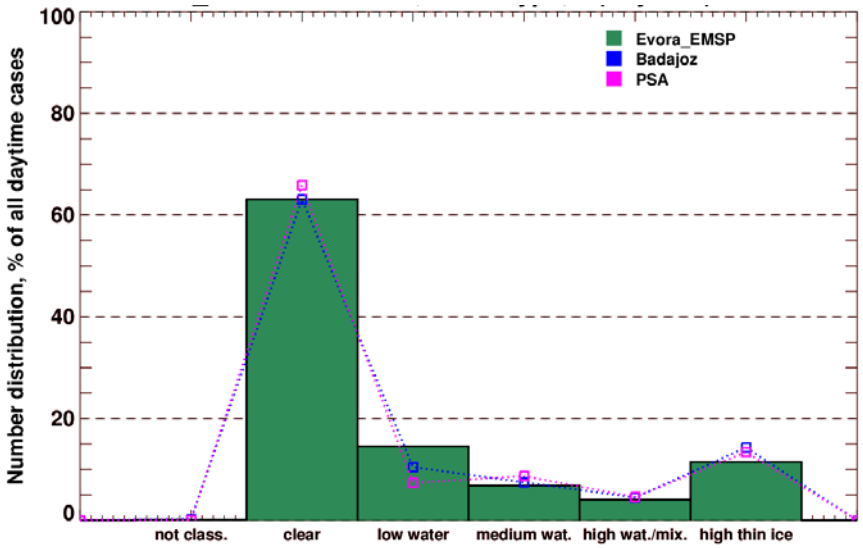

Figure 1.33 Cloud statistics at Évora stations vs. Badajoz and PSA: cloud type; frequency of occurrence in percentage of all daytime satellite images; split into cloud-free and cloudy cases – cloudy cases are separated in low, medium, high cloud top height clouds being optically thick and optically thin ice cloud cases; based on 2005-2015.

The pattern over the months is similar with exception of July and August, when there are more cloudy situations at the PSA then at the other stations. Also, the pattern over time of the day is similar. PSA has more clouds in the late afternoon, while at other times PSA is less cloudy.

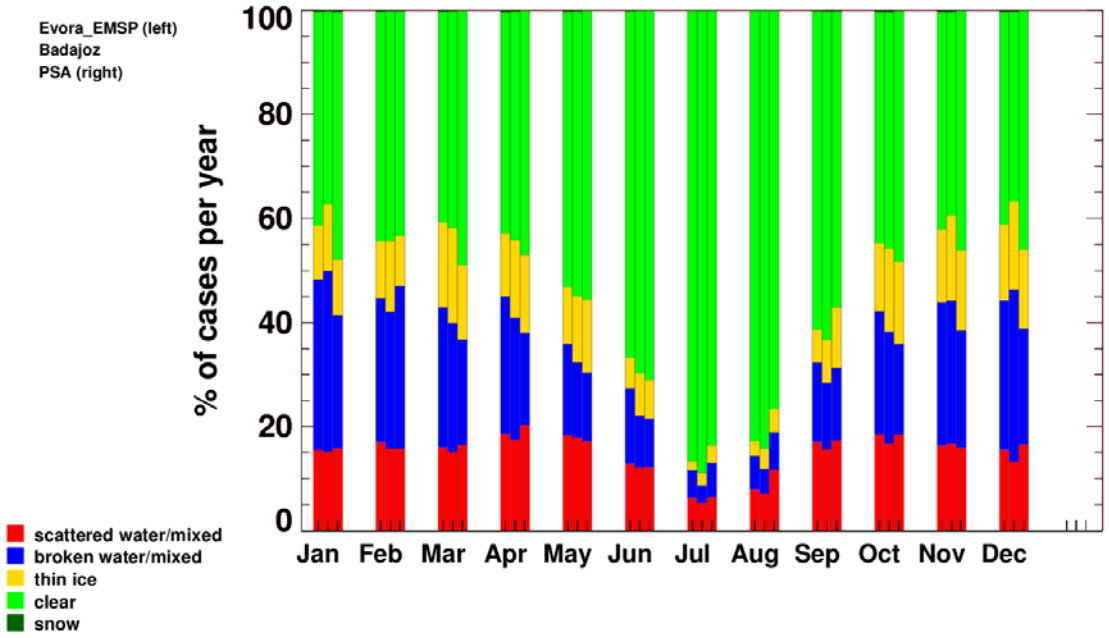

Figure 1.34 Cloud statistics at Évora station vs. Badajoz and PSA: cloud area type (red = scattered water/mixed phase; blue = broken/overcast water/mixed phase; yellow = thin ice phase; green = clear; dark green = snow); frequency of occurrence in percentage of all daytime satellite images; split into calendar month; based on 2005-2015.

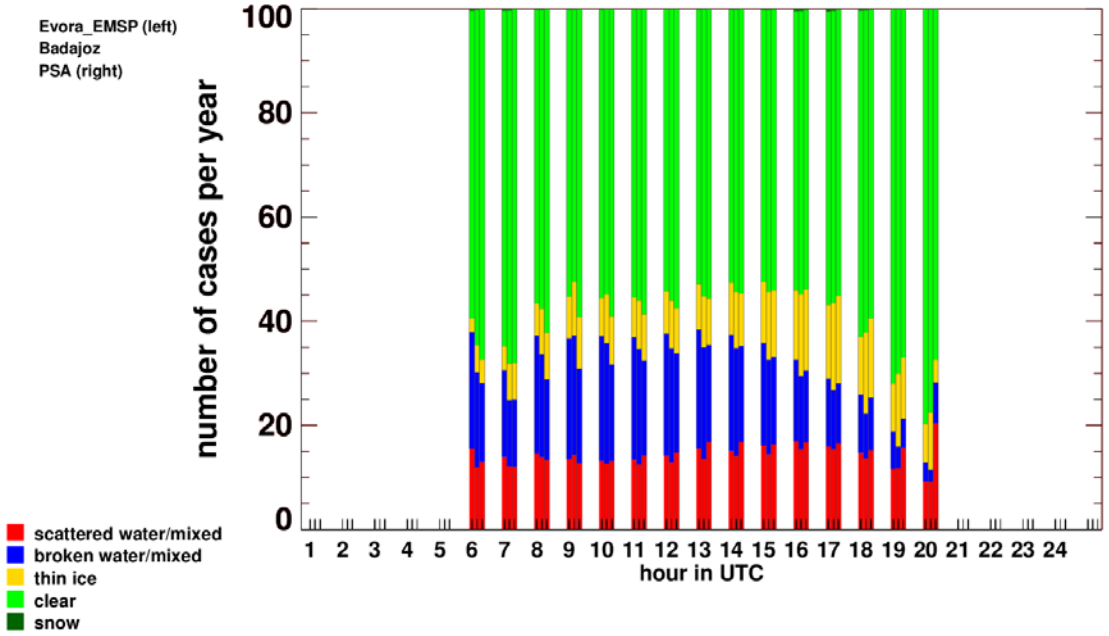

Figure 1.35 Cloud statistics at Évora station vs. Badajoz and PSA: cloud area type (red = scattered water/mixed phase; blue = broken/overcast water/mixed phase; yellow = thin ice phase; green = clear; dark green = snow); frequency of occurrence in percentage of all daytime satellite images; split into hour of the day; based on 2005-2015.

1.3 DNI variability classes

1.3.1 Method

Based on the indicators as defined in section 1.2.1, a number of satellite-based parameters with relation to DNI variability exist. The following section describes a development being performed in the DNICast project (http://www.dnicast-project.net) and is applied here. We summarize the development in order to explain the analysis done below.

Eight DNI variability classes have been selected due to their varying direct normal irradiation and the number of fluctuations. The selection is derived by a visual interpretation by three different scientists of a full year's time series. It also reflects the information of variability structures as being rated as important to know in various personal communications by power plant operators, by storage developers, by solar project planners and electricity grid operators. The selection has been made on the basis of 1-min temporally resolved DNI observations at the BSRN station in Carpentras, Southern France. Figure 1.36 provides example hours (marked by red boxes) which have been attributed to one of the eight classes. Yellow lines indicate the 1-min DNI observations, while the black line represents a 10-min moving DNI average. Dashed lines indicate the clear sky DNI.

Class 1 consists of cloud-free sky cases where the DNI follows the clear sky DNI.

Class 2 consists of cases with nearly clear sky values in the 10-min moving averages and nearly no difference in the 10-min moving averages and the individual 1-min values reflecting a small variability from minute to minute.

Class 3 also shows nearly clear sky values in the 10-min moving averages, but has a much stronger variability from minute to minute. Minute values may reach 30 to 50% of the clear sky DNI which is already a strong reduction in few minutes inside the hour.

Class 4 has both a large variability from minute to minute and among the consecutive 10-min moving averages. Individual minute values even reach DNI close to zero.

Class 5 has significantly lower 10-min moving averages than the clear sky values, mean k_{cDNI} (beam clear sky index being the ratio of DNI versus the clear sky DNI) of 0.66 are observed. Nevertheless, the additional variability from 1 minute to another minute is small.

Class 6 also has medium level DNI values like class 5, but additionally, the minute to minute ramps are very high. They may reach from zero to clear sky DNI values and provide the largest individual ramps.

Class 7 has very low medium k_{cDNI}, but still some large ramps from minute to minute.

Finally, class 8 consists of cases with zero DNI and now variability from minute to minute. Overall, the classes are sorted from largest k_{cDNI} to the smallest k_{cDNI}.

Classes 1, 2, and 8 have a small number of DCH, classes 3, 5, and 7 a medium number of DCH and classes 4 and 6 have a large number of DCH. The naming of classes is a combination of low, medium, high or very high DNI with a low, medium and high number of DCH.

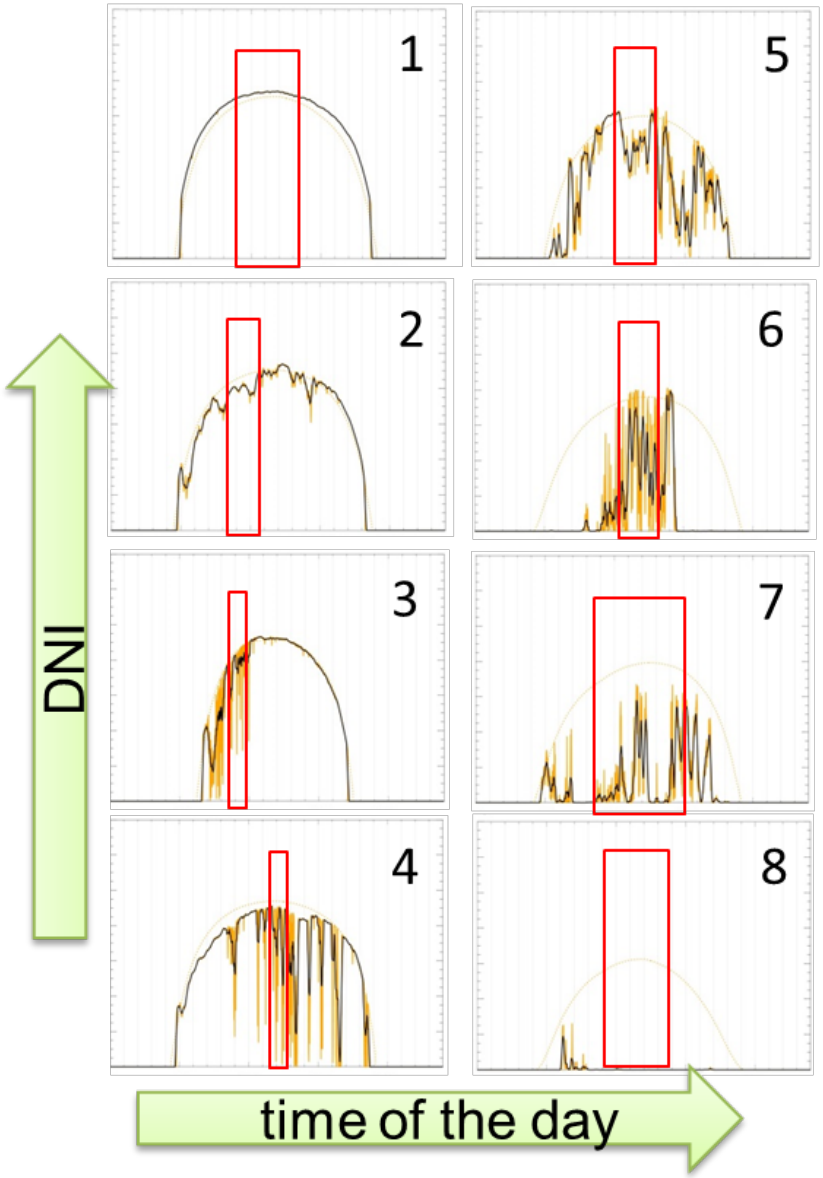

Figure1.36: Arbitrarily chosen examples of the variability cloud classes 1 to 8. Hours being classified in one of the classes are marked by a red box. For some classes, the red box extends the range of a single hour and illustrates several hours being included in the reference database. Minute values (yellow), 10 min moving averages (black) and CAMS clear sky values (thin) are given.

Based on visual interpretation, a number of cases for each variability class were selected out of the hours with high sun elevation between 9 and 14 UTC in 2012 and for the ground measurements at the station BSRN-Carpentras. Hours with varying conditions and changing their related variability class inside the hour have been excluded. Such transition situations are frequent in real time series, but are not suited for the inclusion in our reference database. The database shall contain only those hours which can be unambiguously attributed to a single variability class. The class characteristics can be quantified by their typical k_{cDNI} values and the number of direction changes (Tab. 4).

Table 4: Ground observation based variability class characterisation by $k_{cDNI,}$ the number of direction changes in DNI within the hour, and the number of cases in the reference database.

Class	name	mean k_{cDNI}	no. of DCH (#DCH) in DNI	no. of cases
1	very high DNI, low #DCH	0.99	0-2	61
2	high DNI, low #DCH	0.95	0-7, mean 1	44
3	high DNI, medium #DCH	0.92	0-18, mean 8	27
4	high DNI, high #DCH	0.71	6-33, mean 15	37
5	medium DNI and #DCH	0.66	0-13, mean 6	66
6	medium DNI, high #DCH	0.41	6-22, mean 14	41
7	low DNI, medium #DCH	0.18	0-20, mean 7	64
8	low DNI, low #DCH	0.0	0-2	67

Each of these variability classes can be also described by a distribution of occurring APOLLO cloud parameters. Fig. 1.37 gives e.g. the distribution of satellite-based variability parameters as being typical for variability class 3.

Performing the same analysis for all variability classes defines typical APOLLO parameter patterns for each class. Applying a distance criterion, the best fitting variability class is selected for each individual satellite pixel in a time series. The sum of all distances between the actual cloud parameter value for a satellite image and the median of the n-th class is calculated. For all 8 classes, the minimum distance is chosen and the respective class is allocated to the satellite image time instant.

Finally, we obtain every 15 minutes, so for every satellite pixel, an estimate of the variability class. The variability class is a characteristic of a 1-min resolved time series of 1-hour duration around the time of the satellite observation. The update of this classification can be obtained every 15 minutes.

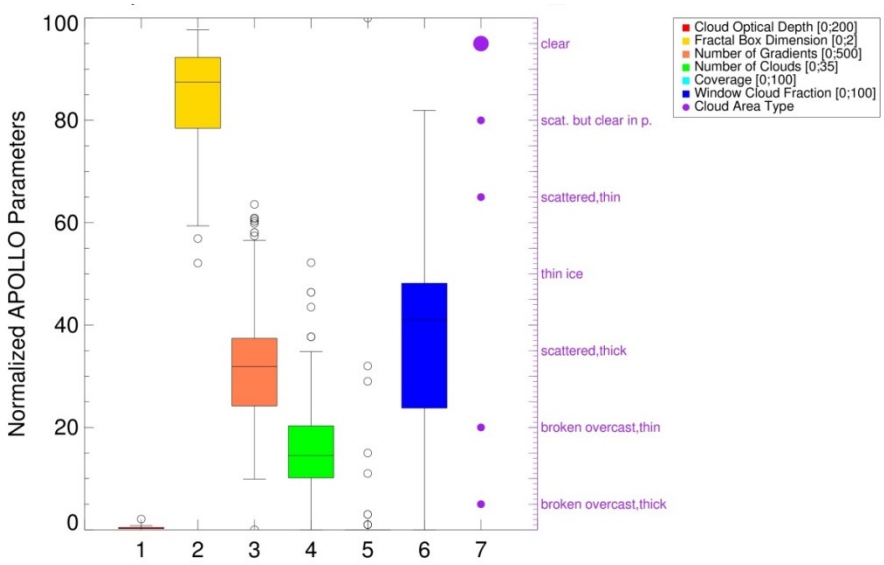

Figure1.37: Box-Whisker plot for the distribution of normalized satellite-based cloud parameters as found for class 3 related cases in the reference data base

1.3.2 Station Évora vs. Badajoz vs PSA

Évora is characterized by less variable conditions than Badajoz and PSA. Classes 2 to 7 are less populated than at the other locations and classes 2 to 4 are much less classified. Classes 4, 6 and 7 are the classes with highest variability – they occur much less at Évora. Especially, at PSA class 2 is more frequent. Assuming that perhaps class 1 and 2 can be misclassified into each other, the high DNI, but low variability situation is much more frequent at PSA and Badajoz than in Évora. On the other hand Évora has much more low variability and low DNI cases that PSA and Badajoz.

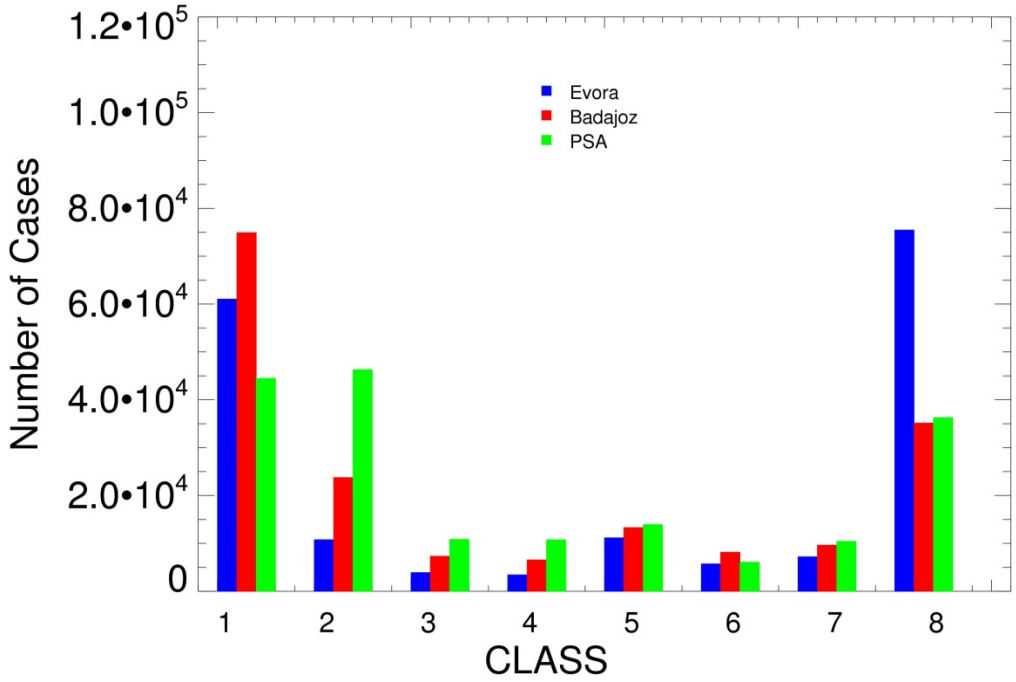

Figure1.38: DNI variability class statistics of Évora, Badajoz and PSA based on 2005-2015. The best fitting class is shown.

1.4 Aerosol variability Évora vs. Badajoz and vs. PSA

Based on AERONET observations, aerosol optical depth observations for the years 2013-2015 are available at all stations. First, we analyse the mean AOD found split into monthly values and for each of the years and the 3-years average (Fig. 1.39). Three-annual mean AOD of Évora and Badajoz is rather similar (with exception of November and December), while at PSA, the mean AOD in June to August is significantly higher. The inter-annual variability can be seen in the statistics of each year.

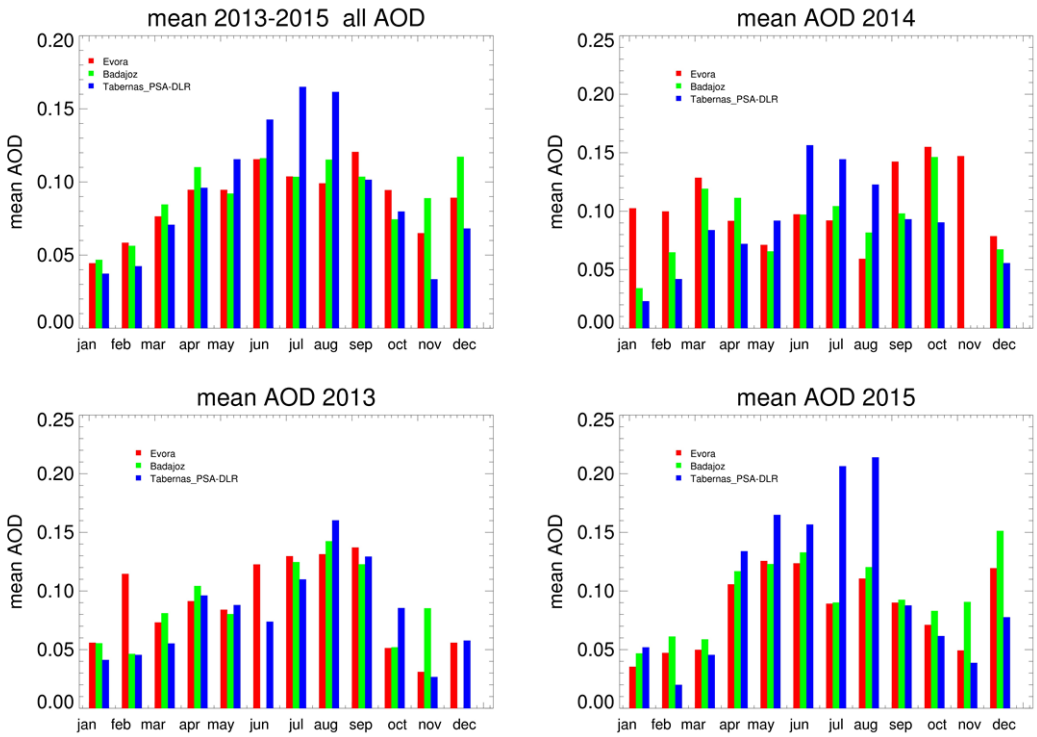

Figure 1.39: AERONET based mean aerosol optical depth (AOD) as found at stations Évora, Badajoz and PSA. Average over 2013-2015 (upper left) and the individual years.

Second, we split the dataset into large AOD cases with AOD values within 0.5 and 1.0, and with AOD values above 1.0. This is based on the assumption, that the occurrence of these events is affecting the CSP plant significantly (Schroedter-Homscheidt et al., 2010). Fig 1.40 illustrates that direct irradiance (not DNI in this plot) is reduced by 40% for an AOD of 0.5 and by 60% in case of an AOD of 1.0.

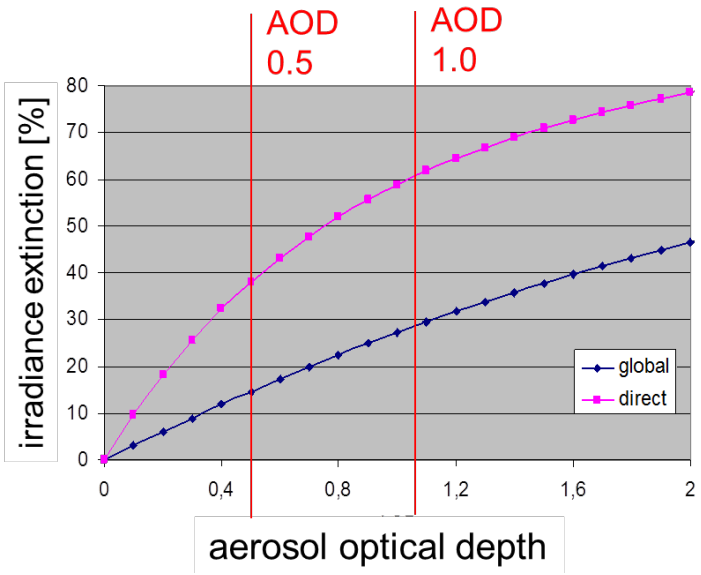

Figure 1.40: Extinction of direct and global irradiances due to dust aerosols for various aerosol optical depths (from Schroedter-Homscheidt et al., 2010)

Please note that despite the maximum in mean AOD per month in the summer (June-August), the number of strong events during the summer months does not show a similar pattern. The large events with AOD > 1.0 do not occur at all in these months and for the events with AOD between 0.5 and 1.0 are also more equally distributed over the months. These patterns are not unexpected due to the typical weather patterns. Atmospheric low pressure systems bringing dust aerosols from Northern Africa to the Iberian Peninsula are more frequent in the non-summer months.

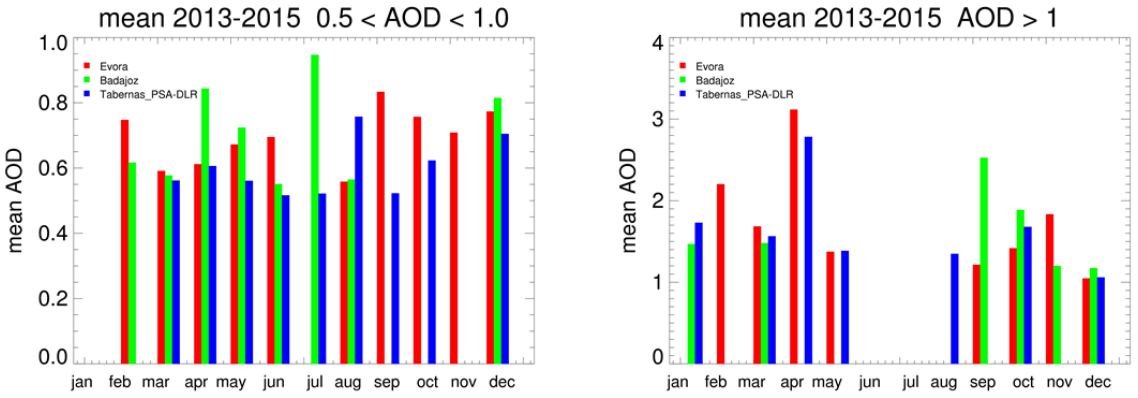

Figure 1.41: AERONET based mean aerosol optical depth (AOD) as found at stations Évora, Badajoz and PSA. Only AOD values between 0.5 and 1.0 (left) and AOD greater 1.0 (right) are evaluated.

2. Typical conditions in other regions of interest

2.1 South Africa

2.1.1 Available ground observations

The BSRN station in De Aar follows rules and measurement practises as described in (Ohmura et al., 1998). BSRN is a project of the World Climate Research Program (WCRP) that aims to measure surface radiative fluxes at the highest possible accuracy with well-calibrated state-of-the-art instrumentation at selected sites in the major climate zones (Ohmura et al., 1998). BSRN data underwent rigorous quality checks (Ohmura et al., 1998; Gilgen and Ohmura, 1999), to assure high accuracy as well as homogeneity in the data. The quality control procedures are described in a report of Long and Dutton (2012). The BSRN radiation variables are sampled at 1 Hz with a one-minute averaging time. Unfortunately, the data is only available until January 2005.

The Southern African Universities Radiometric Network (SAURAN, http://www.sauran.net/, Brooks et al., 2015) provides DNI, global and diffuse horizontal irradiances in 1 minute resolution for South Africa, Namibia, Botswana and Reunion Island. Figure 2.1 shows Location of South African stations, which details can be found in Table 5.

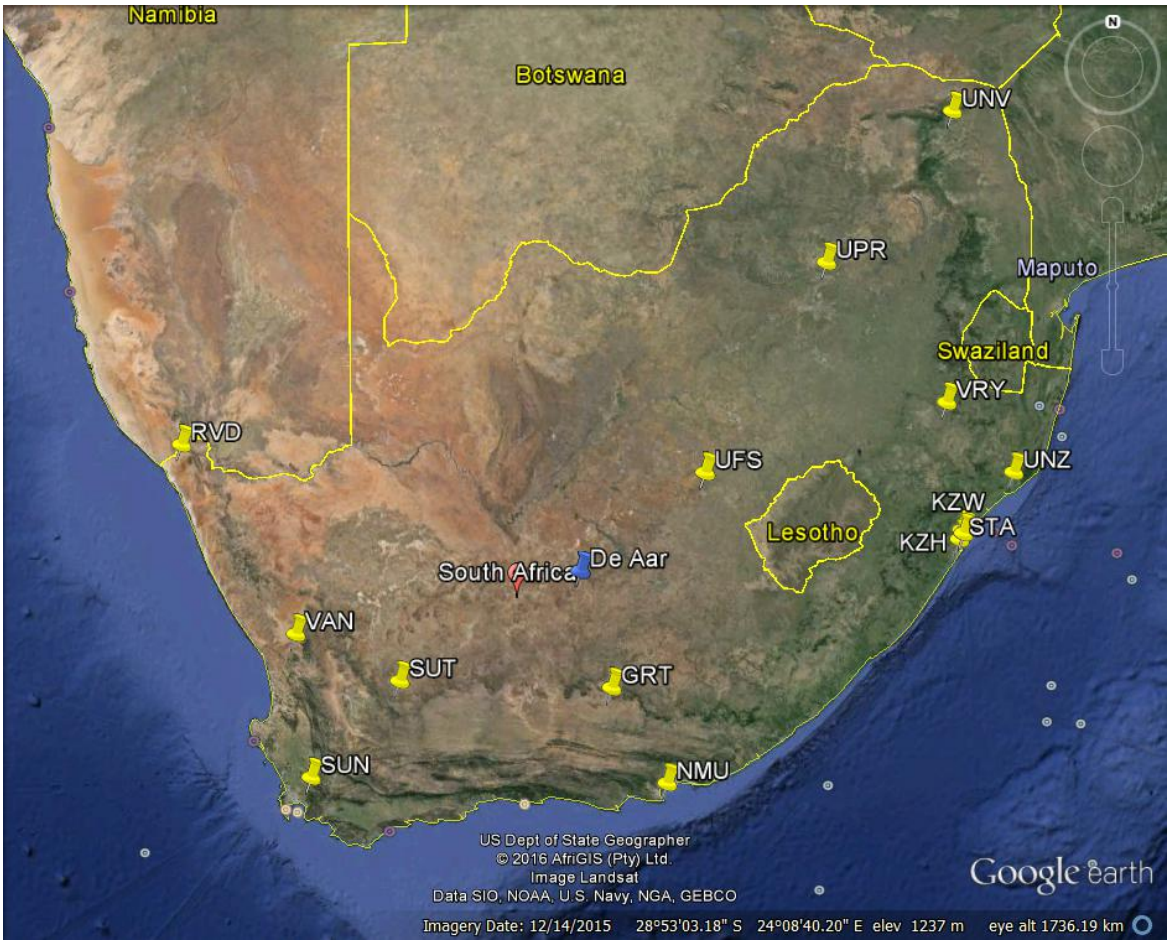

Figure 2.1 Location of South African stations (yellow = SAURAN network, blue = BSRN) Based on GoogleMaps as background.

Table 5: Station information South Africa

Name	Latitude (+N)	Longitude (+E)	Elevat-ion (m)	Period	Pyrhelio-meter	Temporal resolution	Net-work	Comments
De Aar	-30,67	23,99	1287	2000-07-01 to 2005-01-31	Kipp & Zonen CH1	1-min	BSRN	Data available in BSRN website
GRT	-32,49	24,59	660	2013-11-01 to 2016-01-31	Kipp & Zonen CHP1	1-min	SAURAN	Data available in SAURAN website
KZH	-29,87	30,98	150	2013-02-01 to date	Kipp & Zonen CHP1	1-min	SAURAN	Data available in SAURAN website
KZW	-29,82	30,94	200	2013-04-01 to date	Kipp & Zonen CHP1	1-min	SAURAN	Data available in SAURAN website
NMU	-34,01	25,67	35	2014-02-01 to date	Kipp & Zonen CHP1	1-min	SAURAN	Data available in SAURAN website
RVD	-28,56	16,76	141	2014-04-01 to date	Kipp & Zonen CHP1	1-min	SAURAN	Data available in SAURAN website
STA	-29,97	30,91	95	2014-08-01 to date	Eppley NIP	1-min	SAURAN	Data available in SAURAN website
SUN	-33,93	18,87	119	2010-03-01 to date	Kipp & Zonen CHP1	1-min	SAURAN	Data available in SAURAN website
SUT	-32,39	20,66	1450	2014-11-01 to date	Kipp & Zonen CHP1	1-min	SAURAN	Data available in SAURAN website
UFS	-29,11	26,19	1491	2013-10-01 to date	Kipp & Zonen CHP2	1-min	SAURAN	Data available in SAURAN website
UNV	-23,13	30,42	628	2015-04-01 to date	Kipp & Zonen CHP3	1-min	SAURAN	Data available in SAURAN website
UNZ	-28,85	31,85	90	2016-02-01 to date	Kipp & Zonen CHP4	1-min	SAURAN	Data available in SAURAN website
UPR	-25,75	28,23	1410	2013-09-01 to date	Kipp & Zonen CHP5	1-min	SAURAN	Data available in SAURAN website
VAN	-31,62	18,74	130	2013-10-01 to date	Kipp & Zonen CHP6	1-min	SAURAN	Data available in SAURAN website
VRY	-27,83	30,50	1277	2013-09-01 to 2015-10-31	Kipp & Zonen CHP7	1-min	SAURAN	Data available in SAURAN website

Quality control has been performed as described in Annex B. In general, quality measurements have been found in SAURAN stations. The main problems found are due to missing data and (but in a lesser measure) tracking errors. The following tables show, in each station, the number of days of each month for which no suitable DNI measurements are available.

Measured data are available in GRT station from November 29th 2013. Most invalid data are due to missing days.

Table 5a: Station information South Africa – availability GRT

	GIZ Graaff-Reinet - GRT (SAURAN)												
Year	Jan	Feb	Mar	Apr	May	Jun	Jul	Aug	Sep	Oct	Nov	Dec	Annual
2013	-	-	-	-	-	-	-	-	-	-	-	0	**-**
2014	1	0	0	10	6	0	4	0	0	0	9	0	**30**
2015	0	0	0	0	2	14	31	31	30	31	30	31	**200**

Measured data are available in KZH station from April 9th 2013. In the period between 22 and 29 June 2013 there is an error in time scale.

Table 5b: Station information South Africa – availability KZH

	University of KwaZulu-Natal Howard College - KZH (SAURAN)												
Year	Jan	Feb	Mar	Apr	May	Jun	Jul	Aug	Sep	Oct	Nov	Dec	Annual
2013	-	-	-	8	0	8	0	0	0	0	0	0	**-**
2014	0	0	0	0	0	0	0	0	0	0	0	0	**1**
2015	4	3	3	1	3	8	3	4	2	3	2	2	**38**
2016	0	2	1	5	-	-	-	-	-	-	-	-	**-**

Measured data are available in KZW station from April 10th 2013. Most invalid data are missing days.

Table 5c: Station information South Africa – availability KZW

	University of KwaZulu-Natal Westville - KZW (SAURAN)												
Year	Jan	Feb	Mar	Apr	May	Jun	Jul	Aug	Sep	Oct	Nov	Dec	Annual
2013	-	-	-	9	0	7	0	0	3	0	5	0	**-**
2014	0	0	0	0	1	2	5	7	2	5	9	14	**45**
2015	0	0	1	0	12	30	31	31	30	23	3	0	**161**
2016	4	0	7	3	21	-	-	-	-	-	-	-	**-**

Measured data are available in NMU station from February 22th 2014. Main problems are due to missing data and (but in a lesser measure) tracking errors. From October to December 2014 they are found at noon DNI records slightly low (notwithstanding, these data have been considered as valid if it is not pronounced and if no tracking errors are appreciated).

Table 5d: Station information South Africa – availability NMU

	Nelson Mandela Metropolitan University - NMU (SAURAN)												
Year	Jan	Feb	Mar	Apr	May	Jun	Jul	Aug	Sep	Oct	Nov	Dec	Annual
2014	-	-	8	0	0	0	1	0	0	14	0	10	**-**
2015	6	8	2	3	0	0	0	11	0	0	16	31	**77**
2016	19	3	8	5	-	-	-	-	-	-	-	-	**-**

Measured data are available in RVD station from April 24th 2014. Most invalid data are tracking errors.

Table 5e: Station information South Africa – availability RVD

	GIZ Richtersveld - RVD (SAURAN)												
Year	Jan	Feb	Mar	Apr	May	Jun	Jul	Aug	Sep	Oct	Nov	Dec	Annual
2014	-	-	-	-	0	0	0	2	2	0	0	0	**-**
2015	0	0	0	8	0	1	1	0	2	0	0	0	**12**
2016	0	0	0	0	-	-	-	-	-	-	-	-	**-**

In STA station there are no DNI measurements in the whole period.

Table 5f: Station information South Africa – availability STA

	Mangosuthu Univ. of Technology STARlab - STA (SAURAN)												
Year	Jan	Feb	Mar	Apr	May	Jun	Jul	Aug	Sep	Oct	Nov	Dec	Annual
2014	0	0	0	0	0	0	0	0	0	0	0	0	**0**
2015	0	0	0	0	0	0	0	0	0	0	0	0	**0**
2016	0	0	0	0	0	0	0	0	0	0	0	0	**0**

Measured data are available in SUN station from May 25th 2010. Also, there are not available data from December 9th to February 16th 2012. Most invalid data are due to missing data and (but in a lesser measure) tracking errors.

Table 5g: Station information South Africa – availability SUN

	Stellenbosch University - SUN (SAURAN)												
Year	Jan	Feb	Mar	Apr	May	Jun	Jul	Aug	Sep	Oct	Nov	Dec	Annual
2010	-	-	-	-	-	22	0	0	0	0	0	22	**-**
2011	-	-	-	-	-	-	-	-	-	-	-	-	**-**
2012	31	15	0	0	0	12	31	17	6	5	1	31	**149**
2013	10	0	0	11	0	5	0	0	3	2	0	2	**33**
2014	0	5	2	1	0	8	0	0	2	0	0	28	**46**
2015	9	9	0	8	1	2	0	0	3	1	2	0	**35**
2016	0	0	0	0	-	-	-	-	-	-	-	-	**-**

Measured data are available in SUT station from November 26th 2014. Few invalid DNI days found are caused by missing data or tracking errors.

Table 5h: Station information South Africa – availability SUT

	Eskom Sutherland - SUT (SAURAN)												
Year	Jan	Feb	Mar	Apr	May	Jun	Jul	Aug	Sep	Oct	Nov	Dec	Annual
2014	-	-	-	-	-	-	-	-	-	-	-	0	**-**
2015	0	0	0	0	0	1	1	2	2	0	0	0	**6**
2016	0	0	0	0	-	-	-	-	-	-	-	-	**-**

Measured data are available in UFS station from October 13th 2013. Few invalid DNI days found are caused by missing data or tracking errors.

Table 5i: Station information South Africa – availability UFS

	GIZ University of Free State - UFS (SAURAN)												
Year	Jan	Feb	Mar	Apr	May	Jun	Jul	Aug	Sep	Oct	Nov	Dec	Annual
2013	-	-	-	-	-	-	-	-	-	13	0	0	**-**
2014	0	0	0	0	0	0	0	0	0	0	0	0	**0**
2015	0	0	0	0	0	4	0	1	4	0	0	0	**9**
2016	0	0	0	0	-	-	-	-	-	-	-	-	**-**

Measured data are available in UNV station from April 22th 2015. Few invalid DNI days found are caused by missing data.

Table 5j: Station information South Africa – availability UNV

	USAid Venda - UNV (SAURAN)												
Year	Jan	Feb	Mar	Apr	May	Jun	Jul	Aug	Sep	Oct	Nov	Dec	Annual
2015	-	-	-	-	0	2	0	8	1	1	0	0	**-**
2016	0	0	0	0	-	-	-	-	-	-	-	-	**-**

Measured data are available in UNZ station only from February 11st 2016 to May 22th 2016. In few days at the beginning of this period there are tracking errors.

Table 5k: Station information South Africa – availability UNZ

	University of Zululand - UNZ (SAURAN)												
Year	Jan	Feb	Mar	Apr	May	Jun	Jul	Aug	Sep	Oct	Nov	Dec	Annual
2016	-	17	0	0	-	-	-	-	-	-	-	-	**-**

Measured data are available in VAN station from November 6th 2013. Few invalid DNI days found are caused mainly by missing data.

Table 5l: Station information South Africa – availability VAN

	GIZ Vanrhynsdorp - VAN (SAURAN)												
Year	Jan	Feb	Mar	Apr	May	Jun	Jul	Aug	Sep	Oct	Nov	Dec	Annual
2013	-	-	-	-	-	-	-	-	-	-	5	0	**-**
2014	1	0	0	0	0	0	0	0	0	0	0	5	**6**
2015	0	0	0	0	2	0	0	0	0	0	0	0	**2**
2016	0	0	0	0	-	-	-	-	-	-	-	-	**-**

Measured data are available in VRY station from October 25th 2013. Few invalid DNI days found are caused mainly by tracking errors.

Table 5m: Station information South Africa – availability VRY

	GIZ Vryheid - VRY (SAURAN)												
Year	Jan	Feb	Mar	Apr	May	Jun	Jul	Aug	Sep	Oct	Nov	Dec	Annual
2013	-	-	-	-	-	-	-	-	-	-	5	1	**-**
2014	1	0	3	0	0	0	0	0	0	0	0	0	**4**
2015	0	1	2	1	0	0	0	1	0	-	-	-	**-**

Measured data are available in UPR station from September 20th 2013. Few invalid in 2014 are due to missing data, while in 2015 they are found also tracking and shadow errors. It is also appreciated a slight asymmetry to the left in measured DNI from some clear days (a deeper investigation is required for evaluating in this asymmetry is due to natural reasons or to tracking errors).

Table 5n: Station information South Africa – availability UPR

	GIZ University of Pretoria - UPR (SAURAN)												
Year	Jan	Feb	Mar	Apr	May	Jun	Jul	Aug	Sep	Oct	Nov	Dec	Annual
2013	-	-	-	-	-	-	-	-	19	0	1	0	-
2014	1	0	0	0	1	0	0	0	0	0	0	0	**2**
2015	0	0	0	0	2	1	0	0	0	0	0	0	**3**
2016	0	0	0	0	9	-	-	-	-	-	-	-	**-**

2.1.2 Irradiances

We concentrate on stations RVD, VAN, SUT, GRT, UFS, and UPR. We exclude UNV and UNZ as they are having only short ground observation data records. And we exclude stations VRY, KZW, KZH, STA, NMU, and SUN as being in regions where CSP is not expected to be built.

Ground observations

First we plot the histograms of existing ground observations (Fig. 2.2 for all observations, Fig 2.3 split in months). Please note that the number of years of the plots is different. Therefore, a direct comparison with respect to the y-axis is not suitable.

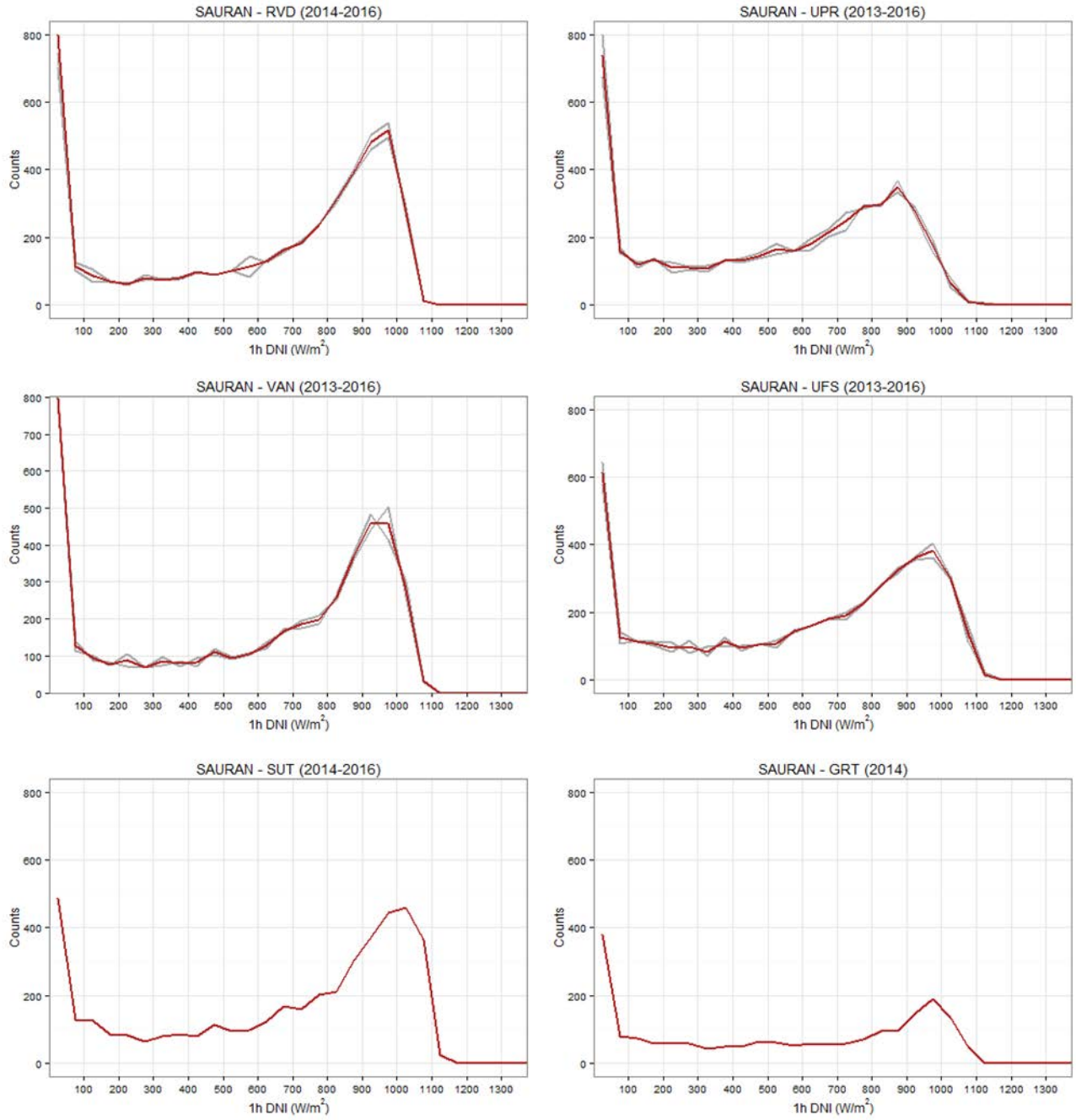

Figure 2.2: Ground-based frequency distributions of hourly daytime DNI at SAURAN stations RVD, VAN, SUT, GRT, UFS, UPR – data periods are as available, years vary.

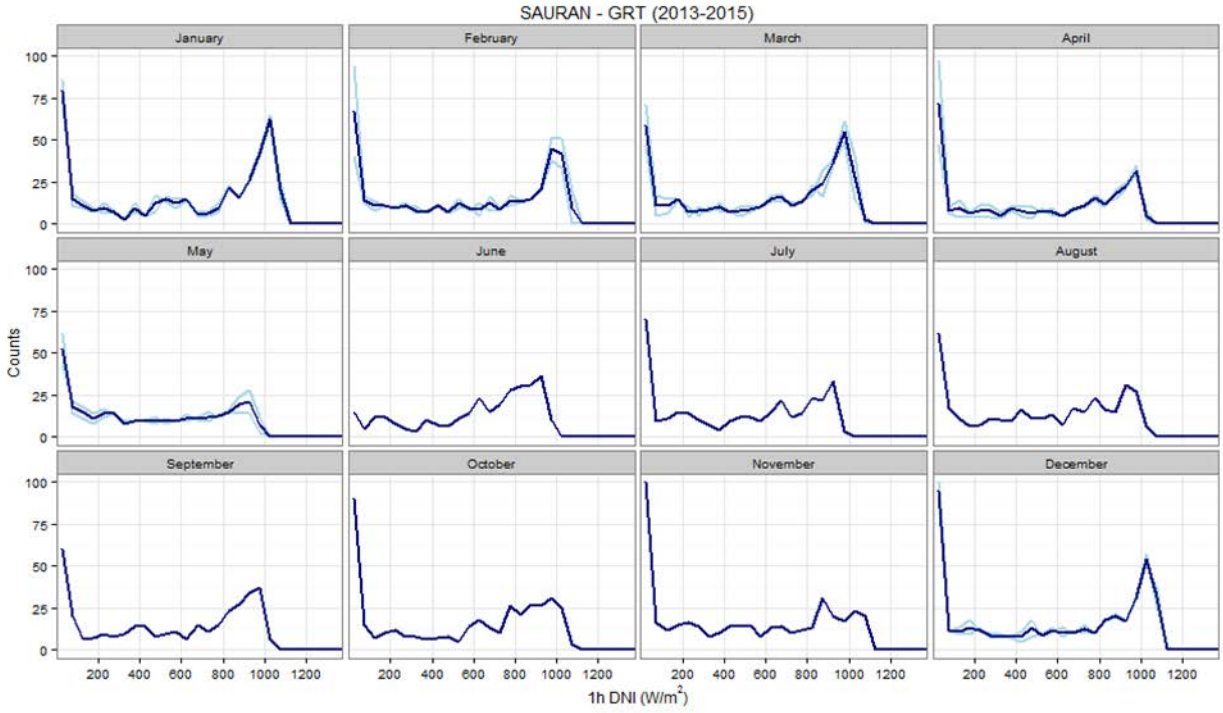

Figure 2.3: Ground-based frequency distributions of hourly daytime DNI at SAURAN station RVD (blue) for all calendar months.

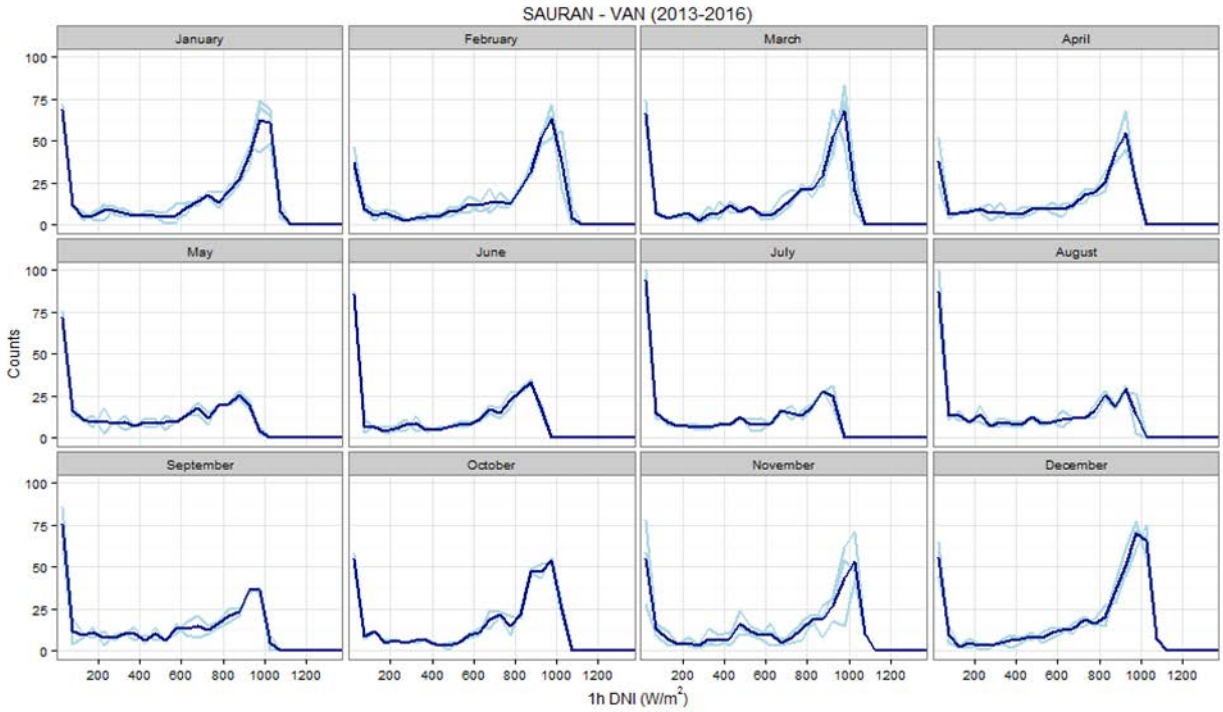

Figure 2.4: Ground-based frequency distributions of hourly daytime DNI at SAURAN station VAN (blue) for all calendar months.

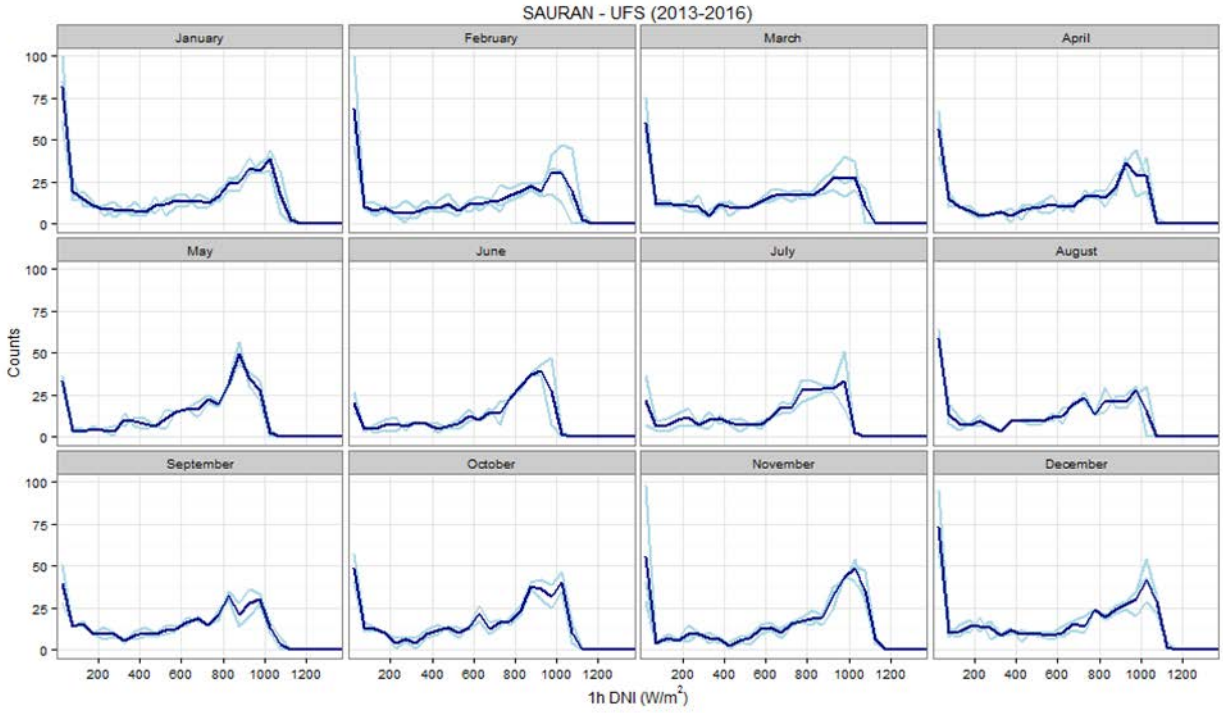

Figure 2.5: Ground-based frequency distributions of hourly daytime DNI at SAURAN station UFS (blue) for all calendar months.

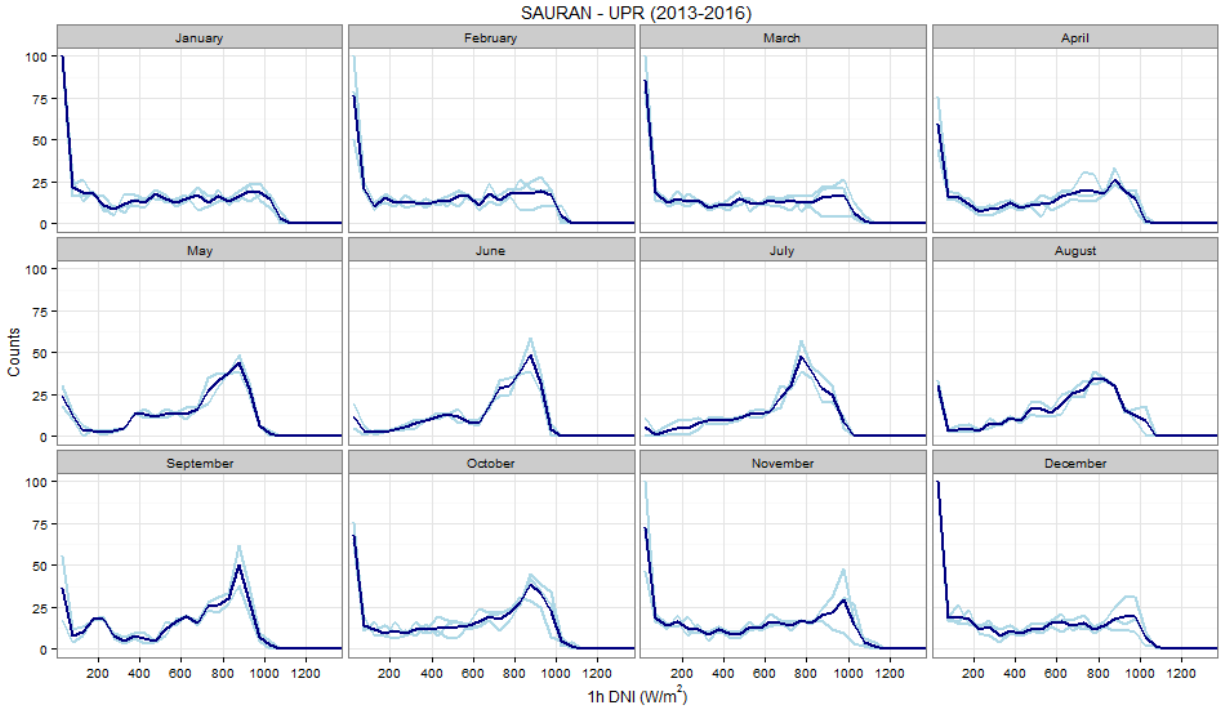

Figure 2.6: Ground-based DNI frequency distributions of hourly daytime DNI at SAURAN station UPR (blue) for all calendar months.

Satellite/model based observations (CAMS)

In order to ensure that CAMS data is sufficiently accurate at SAURAN stations, we compare the mean histograms for the years and months with available ground observations. We omit the stations SUT and GRT (as discussed below).

Figure 2.7 Ground based (red) and CAMS-based (orange) hourly daytime DNI values at SAURAN stations.

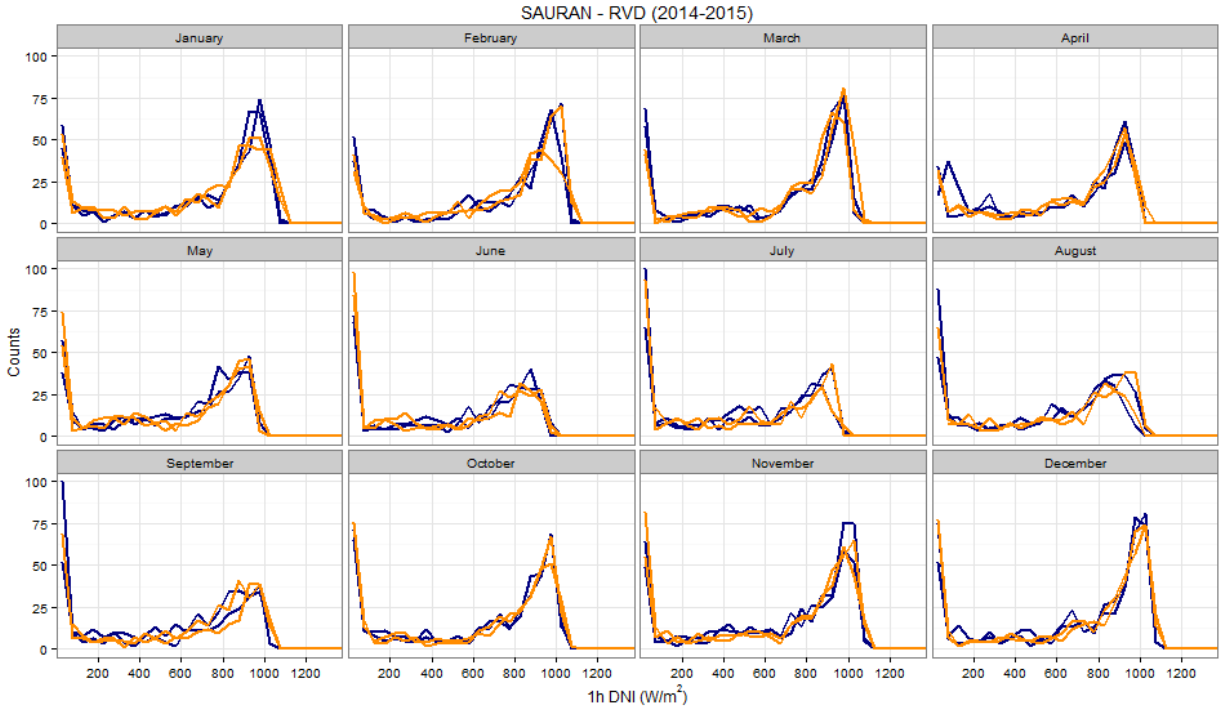

Figure 2.8 Ground based (blue) and CAMS-based (orange) hourly daytime DNI values at SAURAN station RVD and split in monthly plots. In case of several years of available data, all years are plotted separately.

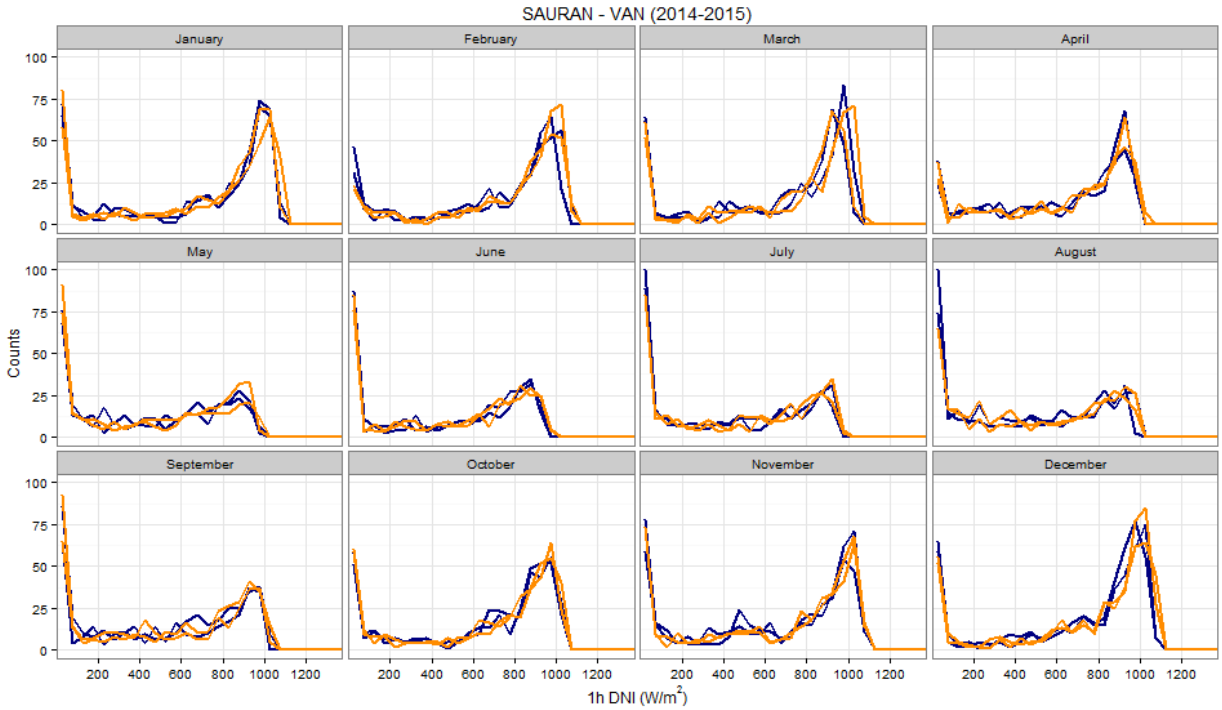

Figure 2.9 Ground based (blue) and CAMS-based (orange) hourly daytime DNI values at SAURAN station VAN and split in monthly plots. In case of several years of available data, all years are plotted separately.

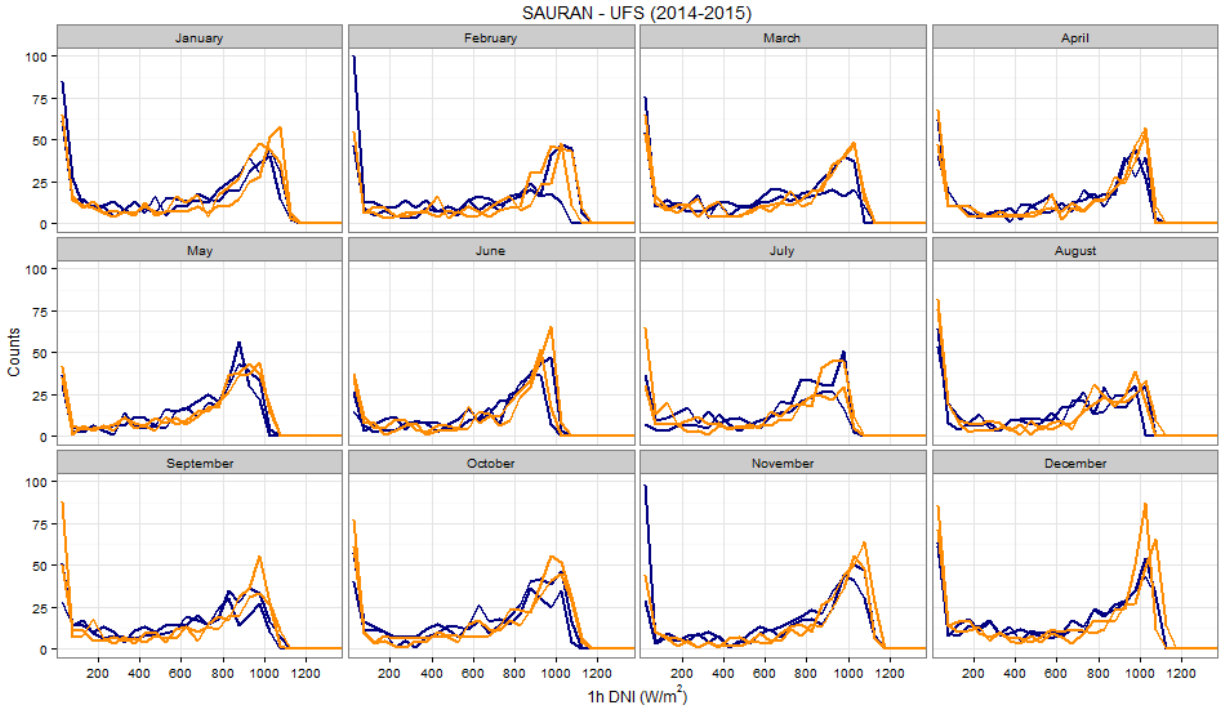

Figure 2.10 Ground based (blue) and CAMS-based (orange) hourly daytime DNI values at SAURAN station UFS and split in monthly plots. In case of several years of available data, all years are plotted separately.

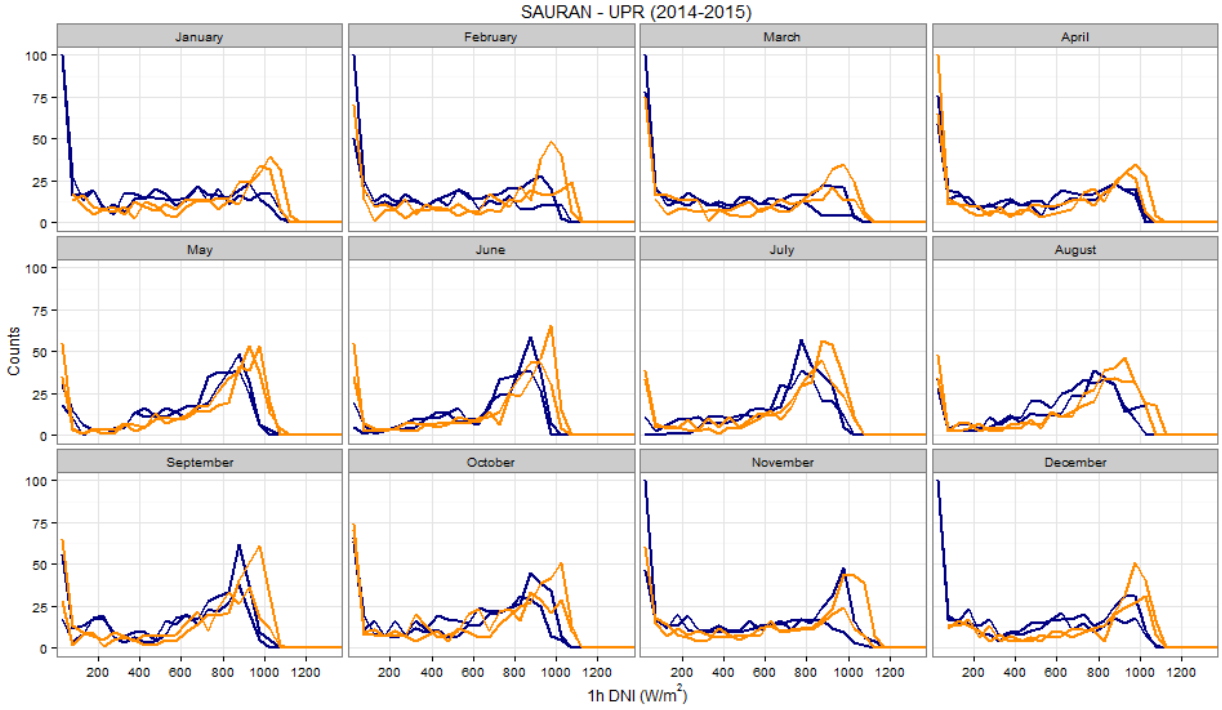

Figure 2.11 Ground based (blue) and CAMS-based (orange) hourly daytime DNI values at SAURAN station UPR and split in monthly plots. In case of several years of available data, all years are plotted separately.

Comparing CAMS satellite based DNI with the ground based DNI, a similar annual histogram is found for RVD and VAN stations. UPR is strongly overestimated in CAMS and also for UFS, CAMS is showing an overestimation of DNI.

The monthly histograms show a good agreement at station RVD with exception of January and February. But also these two months are not extremely off. The same applies for station VAN, where all months are sufficiently well met in the CAMS data. For UFS, an overestimation is visible in February, March, May, September, November, and December. For UPR, the same applies for all months.

Having discussed the difference between ground and satellite-based observations, we now continue to look at the long-term time series of satellite observations. They are available for a 10 years duration and at any point of interest in South Africa.

We compare results versus a location near of Upington (-28.157°N, 21.354°E) in the vicinity of various CSP power plant projects. Hourly resolved, satellite-based CAMS DNI is used from 2006 to 2015.

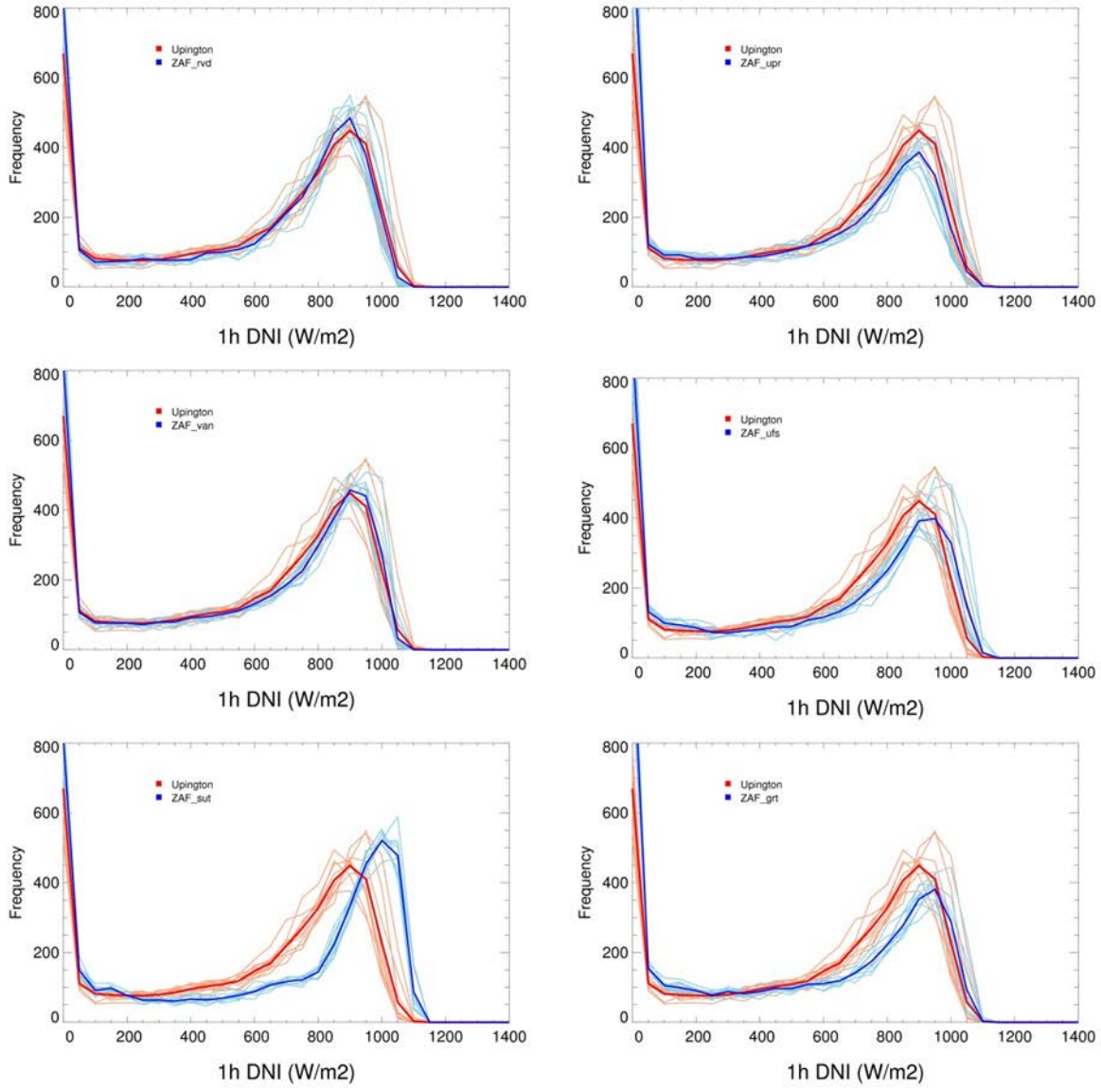

Figure 2.12: CAMS based DNI, frequency distributions of hourly daytime DNI at SAURAN stations RVD, VAN, SUT, GRT, UFS, UPR together with the Upington location; 2006-2015.

Based on this comparison, the stations SUT and GRT are excluded from the view on the monthly conditions as seen by the satellite as already the mean conditions differ strongly.

For the station RVD, the monthly structure is similar with respect to the DNI values occurring most frequently and the width of the histogram peak. Only small shifts are visible in February and March. Nevertheless, the number of the DNI cases in the histogram peak is higher than in Upington for January to April. For station VAN, the width of the peak is smaller in May to August, and the peak is higher in November to April, while it is lower in May to July.

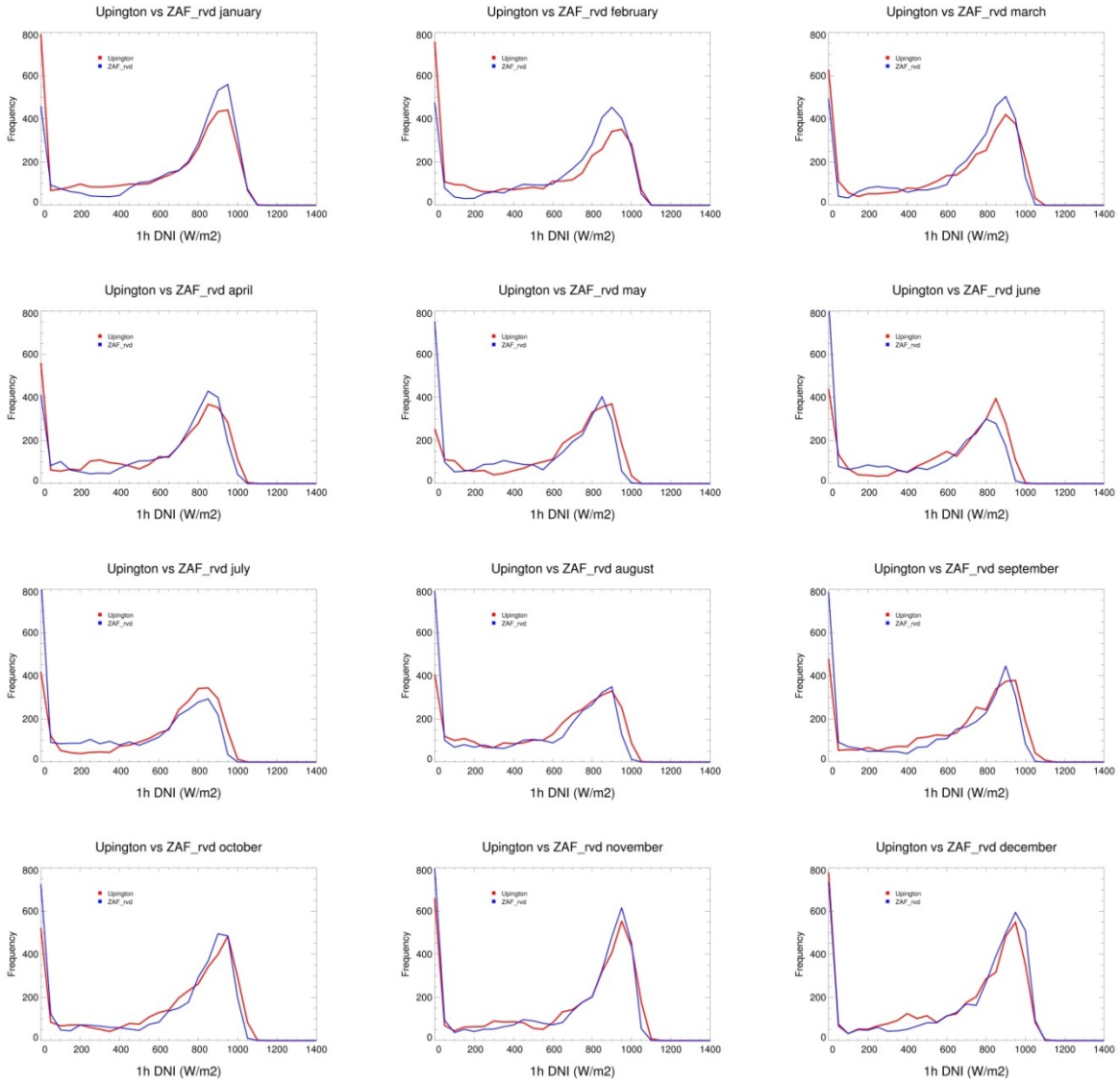

Figure 2.13: CAMS based DNI, frequency distributions of hourly daytime DNI at SAURAN station RVD (blue) and Upington (red) for all calendar months, based on data from 2006-2015.

For station UFS the position of the histogram peak is shifted toward higher DNI values in October to July, while the peak height is similar in all months. Only during August and September both histograms look different. For station UPR the location of the peak is similar for all months, but the height of the peak value is much smaller for October to April, while there are strong differences in the small DNI value part

of the histogram. On the other hand, for July and August, the peak height is higher than in Upington and in August, the frequency of small DNI values is much smaller than in Upington. Based on this comparison, stations RVD and VAN have more similarity to Upington than UPR and UFS.

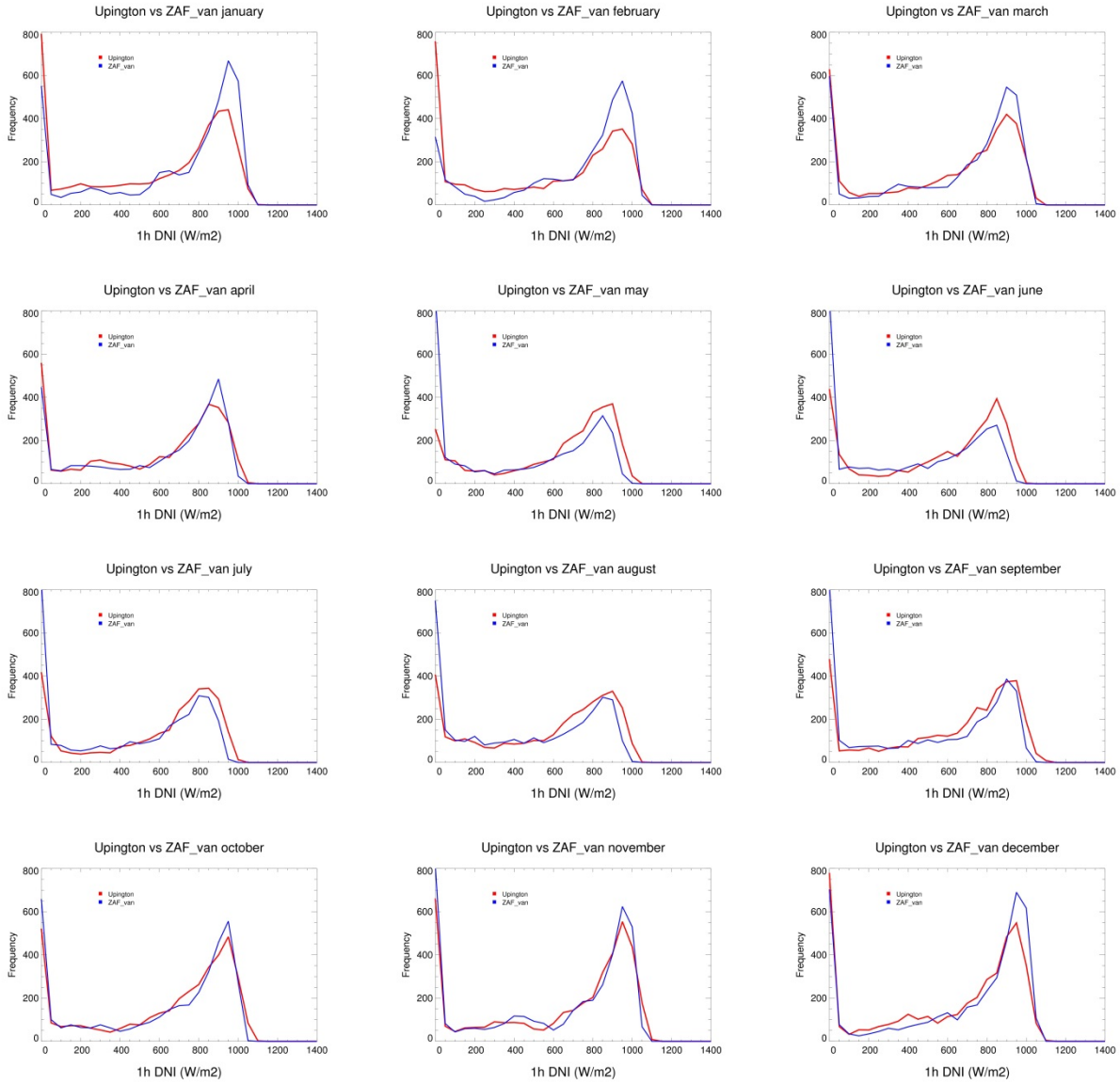

Figure 2.14: CAMS based DNI, frequency distributions of hourly daytime DNI at SAURAN station VAN (blue) and Upington (red) for all calendar months, based on data from 2006-2015.

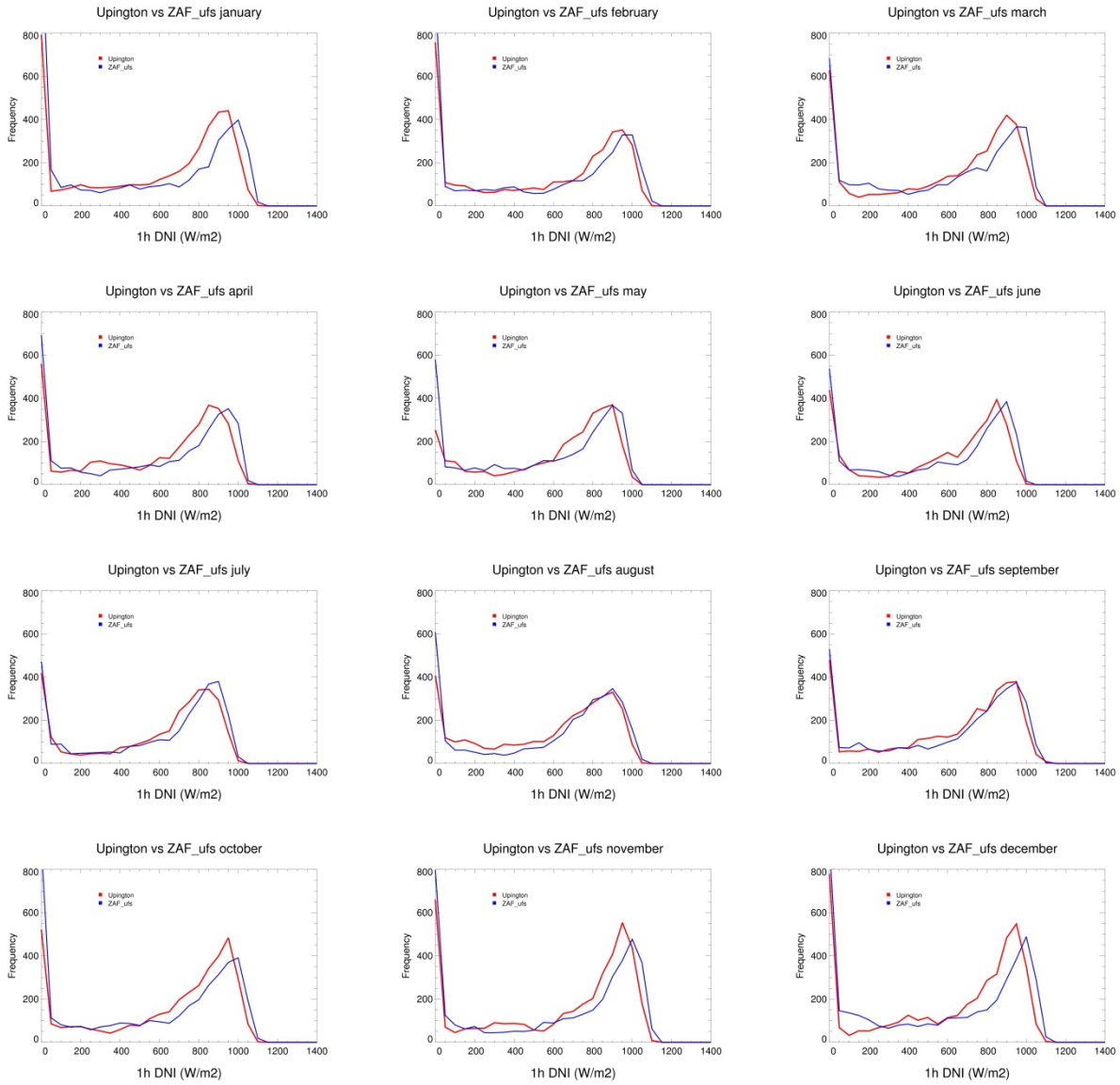

Figure 2.15: CAMS based DNI, frequency distributions of hourly daytime DNI at SAURAN station UFS (blue) and Upington (red) for all calendar months, based on data from 2006-2015.

f

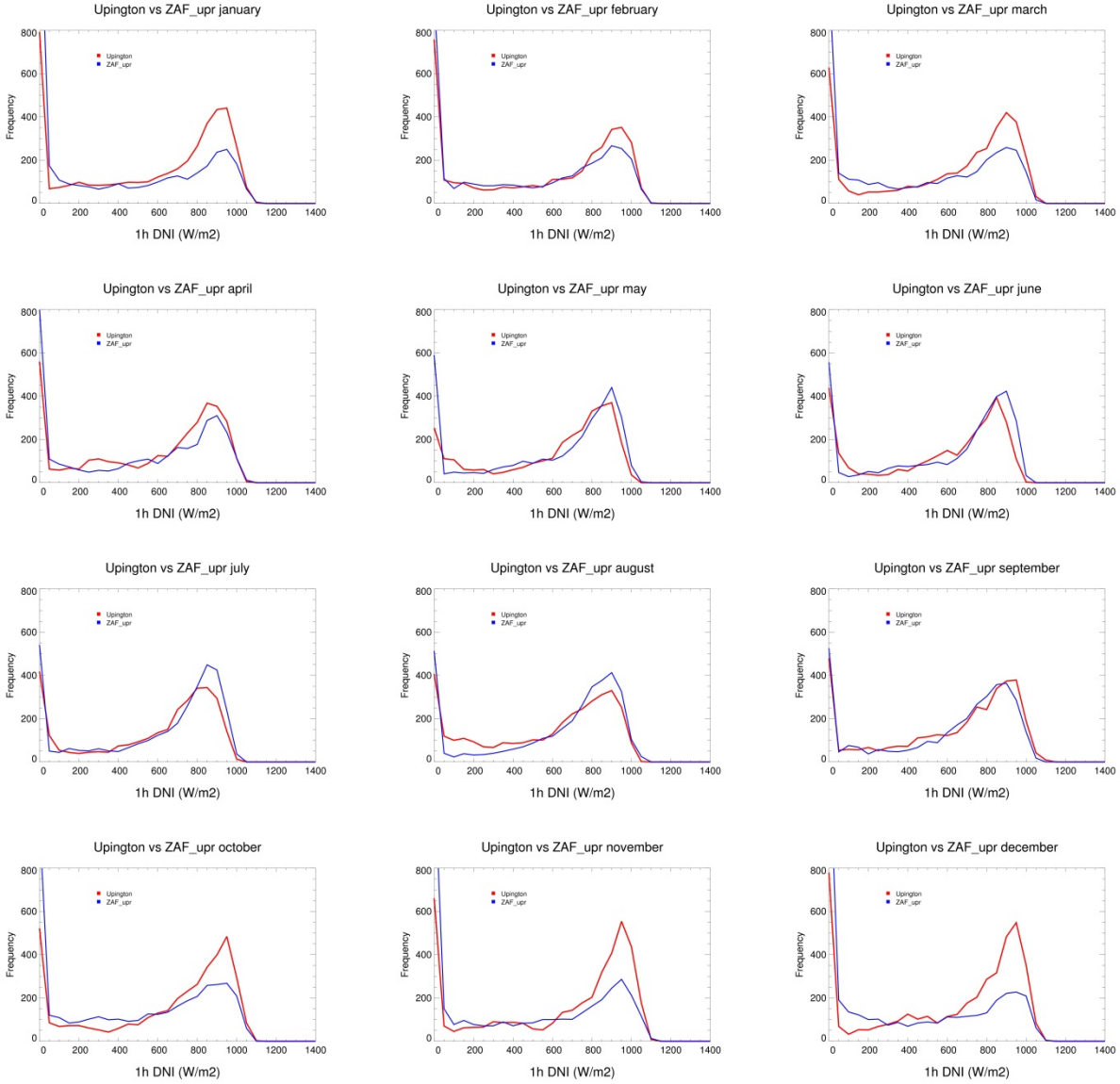

Figure 2.16: CAMS based DNI, frequency distributions of hourly daytime DNI at SAURAN station UPR (blue) and Upington (red) for all calendar months, based on data from 2006-2015.

2.1.3 Cloud conditions

First of all, we compare the stations with respect to the occurrence of clouds. We take the location of Upington as reference and compare the others against it – this selection is driven by the existence of several CSP power plant developments in this area. Fig. 2.17 discriminates cloud-free from cloudy cases. Cloud-free, but snow on the ground cases are also given, as this evaluation tool is also used for more PV related studies in more snowy regions. Upington has about 18% of cloudy cases during daytime hours, while all SAURAN stations show larger occurrence of clouds with increasing values for RVD, VAN, UFS/SUT (being equal), UPR and GRT with values up to 35%.

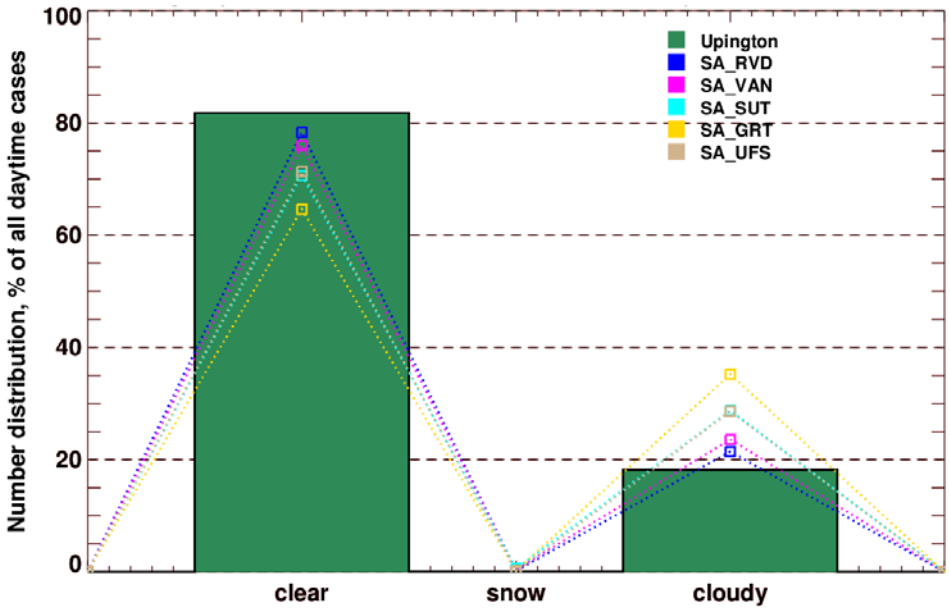

Figure 2.17 Cloud statistics of Upington and 5 SAURAN stations: cloud mask; frequency of occurrence in percentage of all daytime satellite images; split into cloud-free, cloud-free but snow on surface, and cloudy cases; based on 2004-2015.

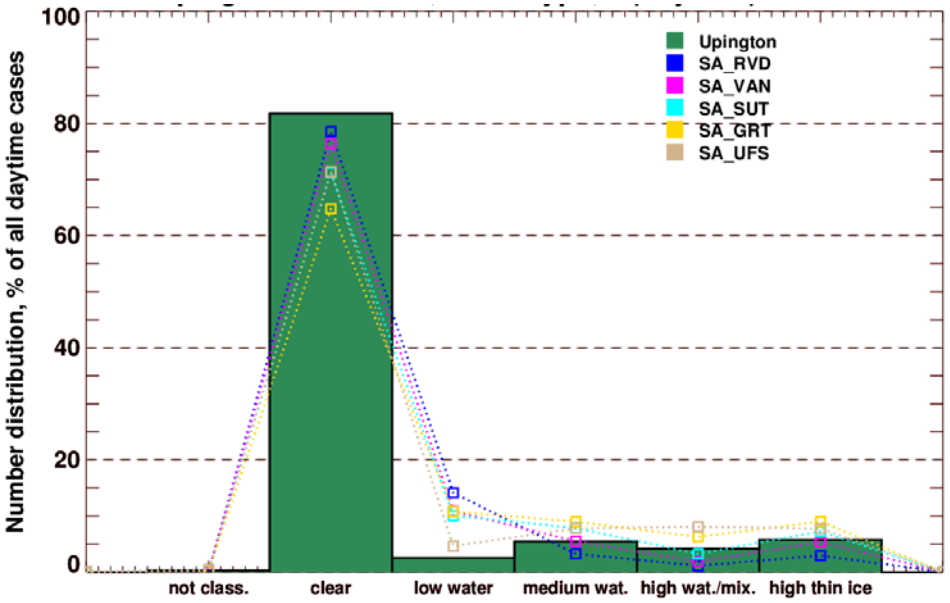

Figure 2.18 Cloud statistics of Upington and 5 SAURAN stations: cloud type; frequency of occurrence in percentage of all daytime satellite images; split into cloud-free and cloudy cases – cloudy cases are separated in low, medium, high cloud top height clouds being optically thick and optically thin ice cloud cases; based on 2004-2015.

In Fig. 2.18 the cloudy cases are further split in optically thick cases with low, medium and high cloud top levels (named 'low water', 'medium wat.', and 'high wat./mix.') and optically thin cirrus cases ('high thin ice'). With respect to DNI the separation in optically thick and thin cloud types is most relevant, for meteorologists the further split into vertical levels is of further interest to assess the situation at a site. The station RVD has the largest part of low level optically thick water clouds compared to other stations, while it has the lowest amount of thin ice clouds, which allow parts of the DNI to reach the ground. If adding all optically thick clouds to one group and comparing the thick and thin cloud groups, the station VAN is closest to Upington. The station RVD has too few thin cirrus cloud cases, while GRT and UFS show too many such cases.

The split of all cases in scattered, broken/overcast, thin ice clouds, clear and snow conditions is done first for each station separately, but split into time of the day and month of the year (Fig. 2.19 to 2.25) and normalized on the number of daytime cases in each bin. Several seasonal and daily cycles can be seen – some of them we discuss as examples before we compare the stations.

Please note that the first and last hours of the day are typically populated with less cases due to shorter days in winter time. But we prefer to give relative values here. If needed, absolute histograms can be provided as well.

Upington has a strong dependency of clouds as a function of hour of the day during summer months October to April, while this pattern is not available during winter months. Overall, the relative frequency of clouds is less in the winter months than in summer months.

RVD shows a clear seasonal cycle of having more clouds in winter months than in summer months. In all months, cloudy conditions dominate the morning hours, but the number of broken/overcast cases is more dominant in August to December, while in May to September also a strong contribution of scattered cases is found. Thin ice clouds during the whole day occur mostly in April to July and in the afternoon hours in September to October.

VAN shows a strong cycle over time of the day for many months, most pronounced in August to January. The months May to October are more cloudy, but in May to August the dependence of the time of the day is less pronounced.

SUT also has a very distinct daily cycle of cloud occurrence from April to October. In several months (e.g. October to May) a secondary maximum of cloud cover in afternoon hours is found.

Such an afternoon peak in cloud cover is strongly found as well at GRT. Here also a large number of thin cirrus cases over the whole day in most months is found. GRT is strongly affected by thin cirrus clouds from April to November. They will result in volatile DNI with frequent changes between approx. 50% DNI and 100% DNI values (percentages given in relation to the clear sky potential DNI value).

UFS is also strongly affected by both scattered and broken/overcast conditions in afternoon hours for October to April, while it has frequently cloud conditions in the morning in winter months.

And finally, UPR also shows the afternoon peak in cloud conditions for October to May, while in June to September only a morning peak in cloud cover exists in the first daytime hour of the day but not the rest of the day the cloud conditions are more flat. Note the increased number of scattered cloud cases in the afternoon from May to November – they will most likely produce a volatile DNI in the afternoon hours with frequent switches between zero and large DNI. Also, the occurrence of cirrus clouds from October to April will result in volatile DNI, but more between 50% of DNI and full DNI and not going down to 0% DNI frequently.

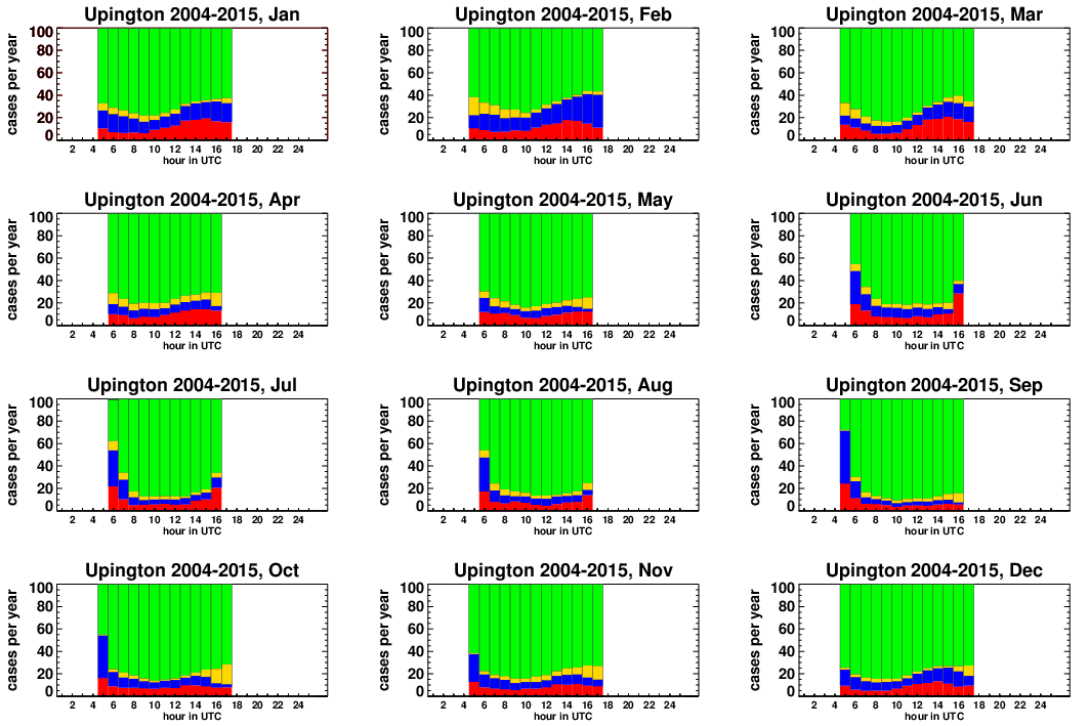

Figure 2.19 Cloud statistics Upington station: cloud area type (red = scattered water/mixed phase; blue = broken/overcast water/mixed phase; yellow = thin ice phase; green = clear; dark green = snow); frequency of occurrence in percentage of all daytime satellite images; split into calendar month and hours of the day; based on 2004-2015.

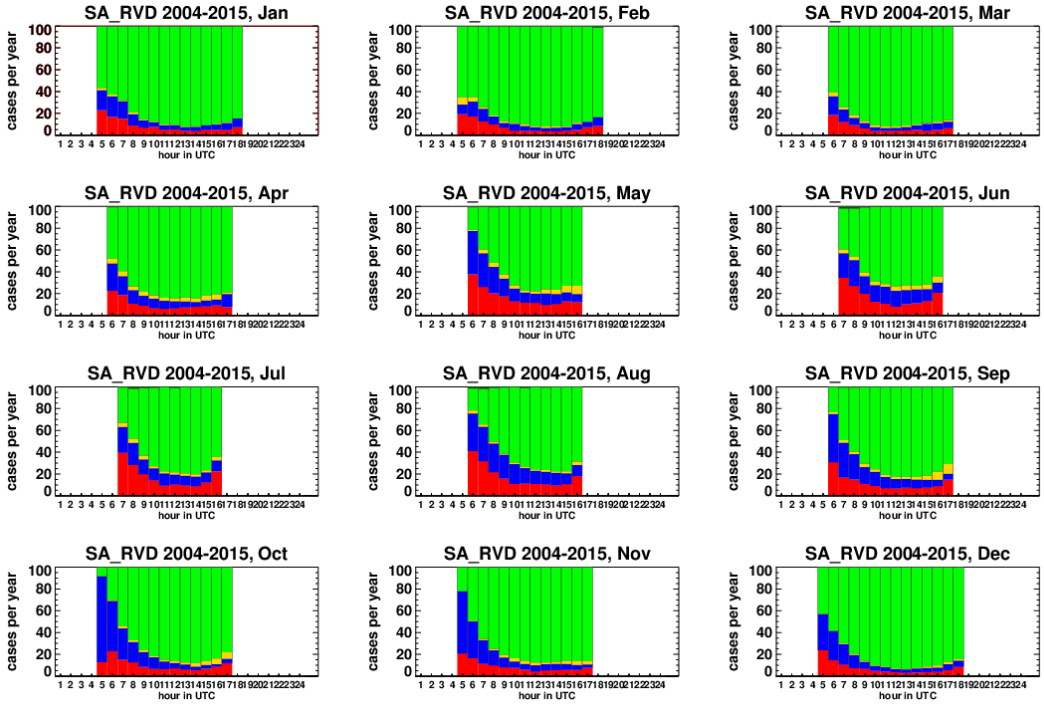

Figure 2.20 Cloud statistics SA-RVD station: cloud area type (red = scattered water/mixed phase; blue = broken/overcast water/mixed phase; yellow = thin ice phase; green = clear; dark green = snow); frequency of occurrence in percentage of all daytime satellite images; split into calendar month and hours of the day; based on 2004-2015.

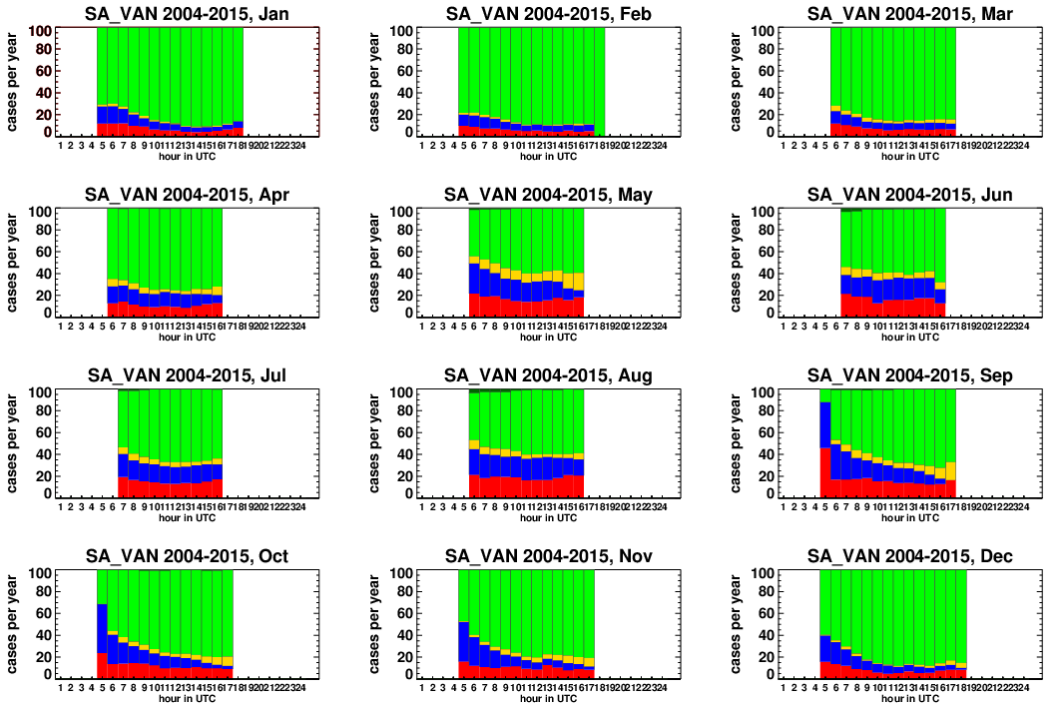

Figure 2.21 Cloud statistics SA-VAN station: cloud area type (red = scattered water/mixed phase; blue = broken/overcast water/mixed phase; yellow = thin ice phase; green = clear; dark green = snow); frequency of occurrence in percentage of all daytime satellite images; split into calendar month and hours of the day; based on 2004-2015.

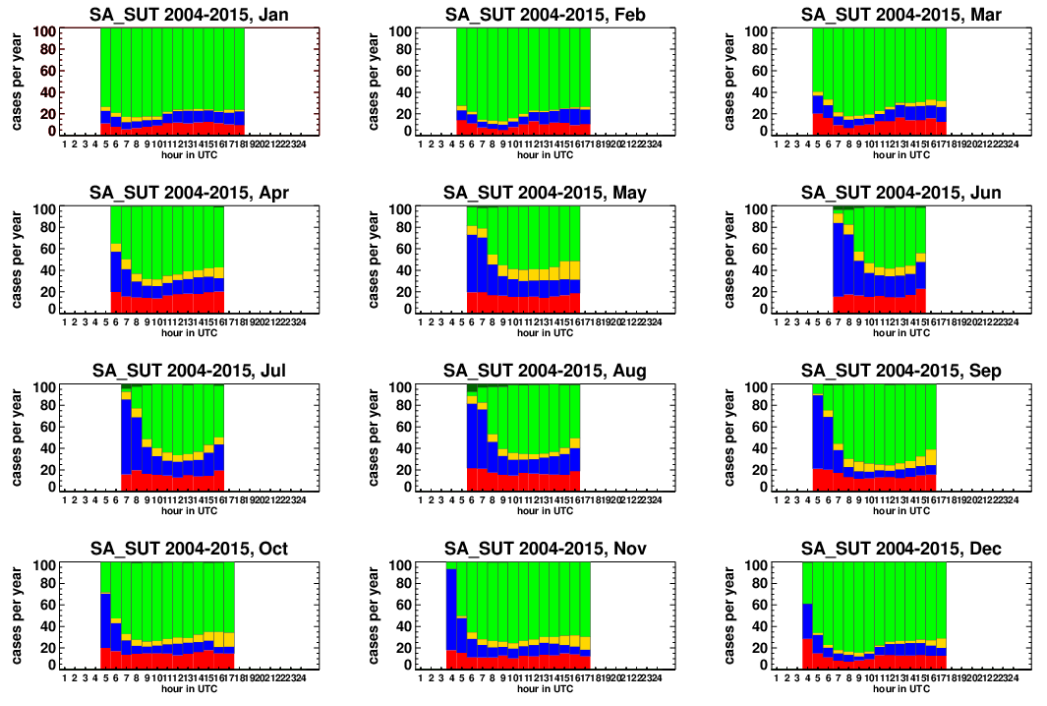

Figure 2.22 Cloud statistics SA-SUT station: cloud area type (red = scattered water/mixed phase; blue = broken/overcast water/mixed phase; yellow = thin ice phase; green = clear; dark green = snow); frequency of occurrence in percentage of all daytime satellite images; split into calendar month and hours of the day; based on 2004-2015.

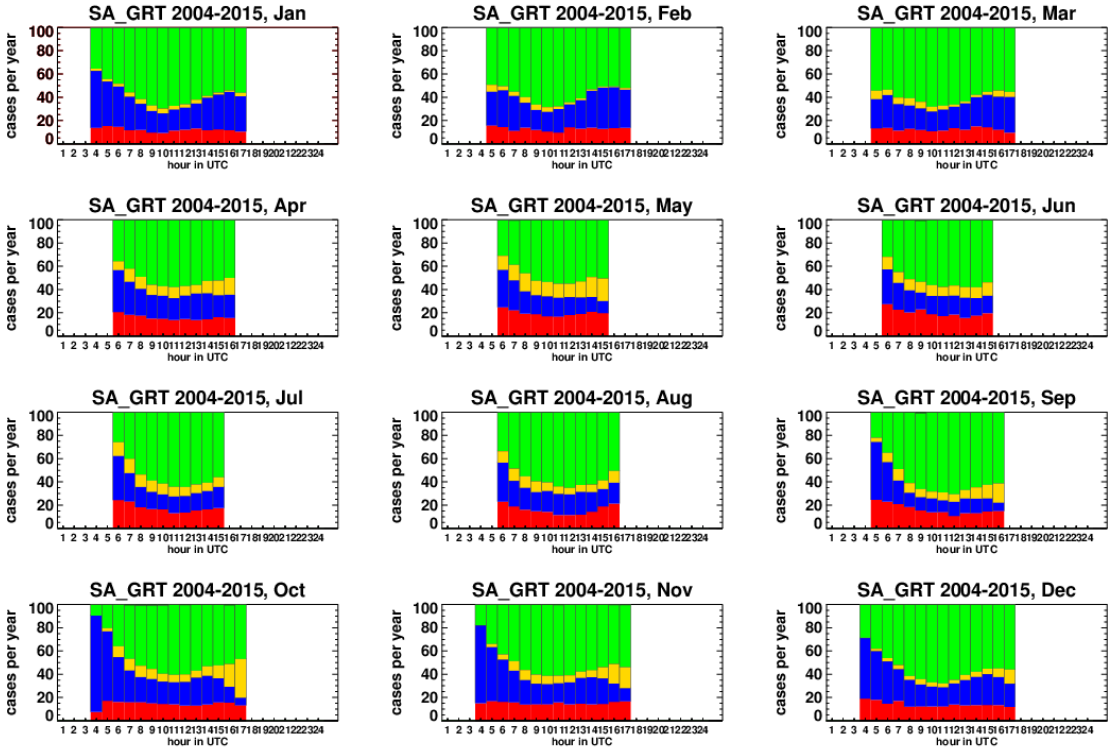

Figure 2.23 Cloud statistics SA-GRT station: cloud area type (red = scattered water/mixed phase; blue = broken/overcast water/mixed phase; yellow = thin ice phase; green = clear; dark green = snow); frequency of occurrence in percentage of all daytime satellite images; split into calendar month and hours of the day; based on 2004-2015.

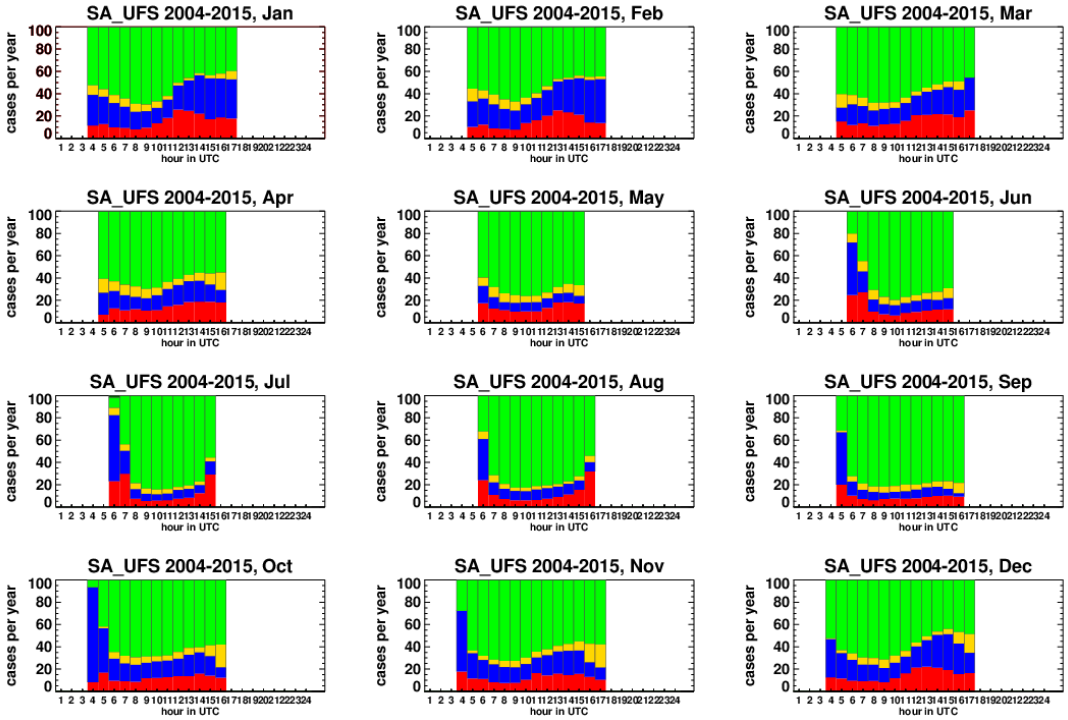

Figure 2.24 Cloud statistics SA-UFS station: cloud area type (red = scattered water/mixed phase; blue = broken/overcast water/mixed phase; yellow = thin ice phase; green = clear; dark green = snow); frequency of occurrence in percentage of all daytime satellite images; split into calendar month and hours of the day; based on 2004-2015.

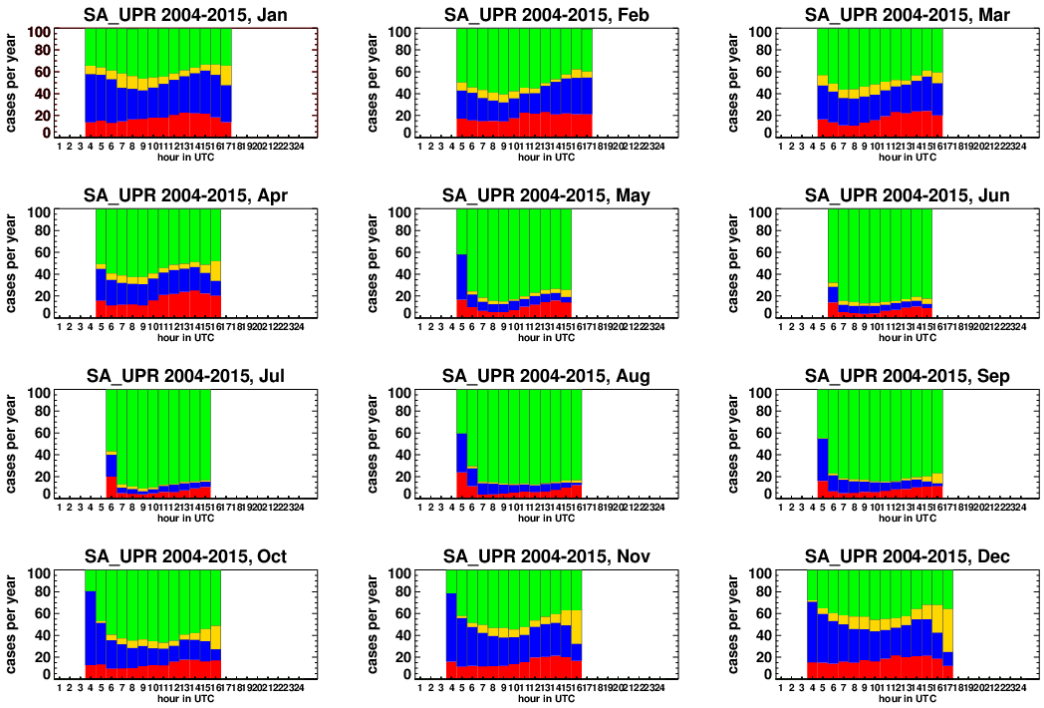

Figure 2.25 Cloud statistics SA-UPR station: cloud area type (red = scattered water/mixed phase; blue = broken/overcast water/mixed phase; yellow = thin ice phase; green = clear; dark green = snow); frequency of occurrence in percentage of all daytime satellite images; split into calendar month and hours of the day; based on 2004-2015.

Having discussed some seasonal and daily cycles which are different at the 6 stations, we now combine the monthly and hourly plots of all stations.

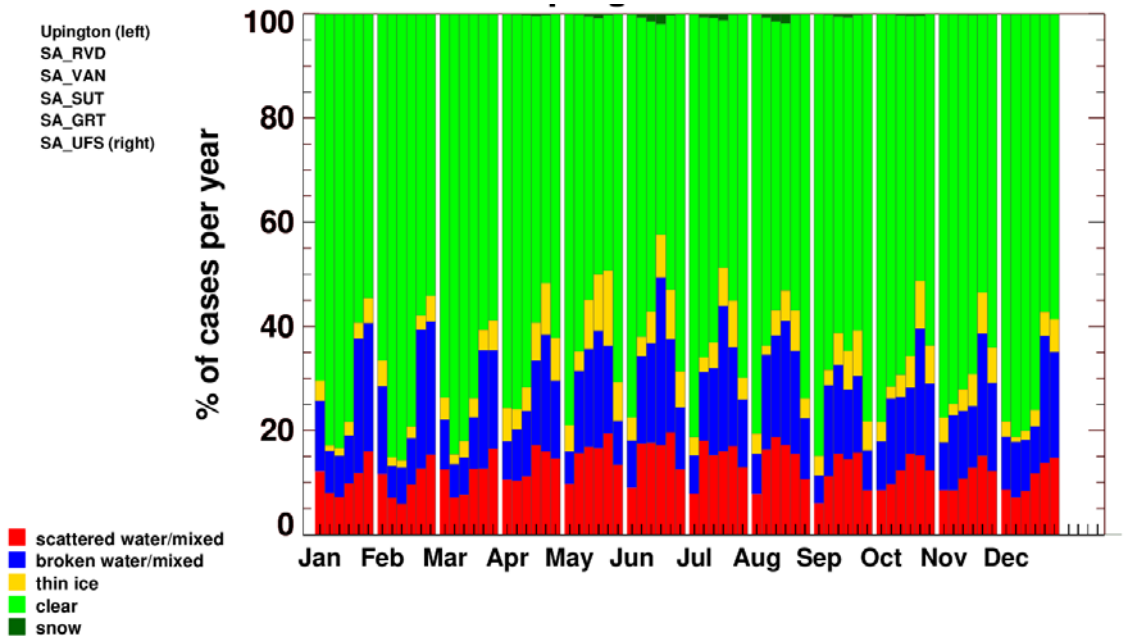

Figure 2.26 Cloud statistics of Upington and 6 SAURAN stations: cloud area type; relative frequency of occurrence over months; split into scattered, broken/overcast, thin ice, clear and snow cases; based on 2004-2015.

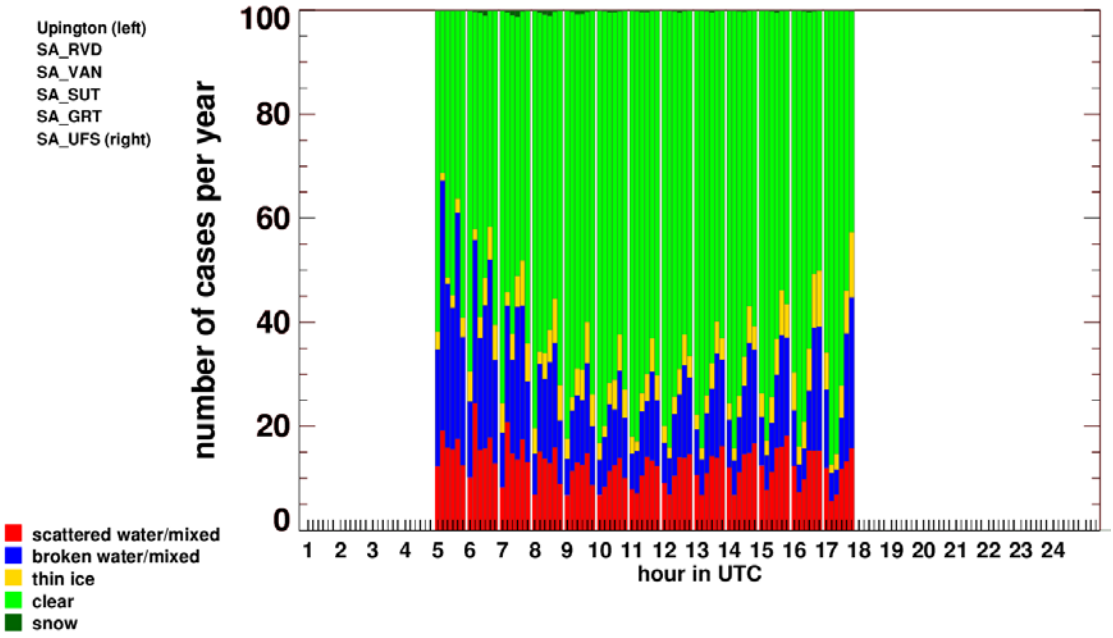

Figure 2.27 Cloud statistics of Upington and 6 SAURAN stations: cloud area type; relative frequency of occurrence over hours of the day; split into scattered, broken/overcast, thin ice, clear and snow cases; based on 2004-2015.

And finally, the duration of cloud periods inside a day is evaluated. We separate in optically thick (DNI < 200 W/m2) and optically thin (DNI reduced) cases. Based on these numbers none of the stations is very close to Upington in all characteristics. The values being closest to the Upington site are marked in green, but none of the sites is close in their characteristics with respect to all metrics.

Table 6: Length of cloud periods occurring in a day – optically thick clouds with DNI close to zero

Station	% of cloud< periods <= 15 min duration	% of cloudy periods <=1 hour duration	90% of cloud periods are <= X hours	98% of cloud periods are <= X hours
Upington	**34.92**	**66.80**	**4.0**	**9.5**
RVD	31.97	65.42	3.5	8.0
VAN	29.47	58.51	4.75	9.5
SUT	27.48	55.70	4.25	9.0
GRT	29.73	57.97	5.0	10.5
UFS	32.11	63.43	4.5	10.75
UPR	29.99	58.56	5.75	11.75

Table 7: Length of cloud periods occurring in a day – optically thin clouds with variable DNI

Station	% of cloud< periods <= 15 min duration	% of cloudy periods <=1 hour duration	90% of cloud periods are <= X hours	98% of cloud periods are <= X hours
Upington	**37.22**	**74.60**	**2.25**	**5.5**
RVD	28.54	67.37	3.0	6.5
VAN	33.58	71.77	2.75	6.25
SUT	33.74	70.82	3.0	7.0
GRT	32.35	66.93	3.5	7.75
UFS	36.83	71.67	2.75	7.25
UPR	34.88	69.64	3.0	7.25

2.1.4 DNI variability conditions

DNI variability classes are derived based on MSG cloud parameters as described in section 1.3. Histograms of their frequency in 2004-2015 cases are given (Fig 2.28). Upington is characterized by either no or small variation and cloud-free sky (class 1) or by no variation and cloudy sky (class 8). Class 2 is represented but significantly less than class 1 and 8. Class 2 is characterized by high DNI and a small amplitude variability. Very variable conditions (classes 4 and 6) and medium variable conditions (classes 3, 5, and 7) are also very seldom. This is confirmed by the 2nd best fitting class (Fig. 2.29) where classes 2 and 7 are most frequent.

None of the SAURAN stations has similar conditions. They all have a significant higher amount of variable cases in classes 2 to 7. Stations VAN and SUT have nearly the same frequency of class 1, but show only half of the occurrence of class 8, while variable classes occur more frequently. Station RVD on the other hand has a very high (doubled compared to Upington) occurrence of class 8, but only approx. 20% of the class 1 cases compared to Upington.

So, none of the SAURAN stations is similar with respect to the distribution of variability classes. For all locations we expect higher RMSE in the forecast verification due to their higher natural variability of DNI. From that perspective it is recommended to use the station RVD, VAN or SUT as they show the smallest amount of variable conditions. Even if the ratio of very low vs. very high DNI cases (class 1 vs 8) is very different from the Upington conditions at these stations, the number of variable situations is not too high. Otherwise, we would end with RMSE estimates which too pessimistic for the Upington site.

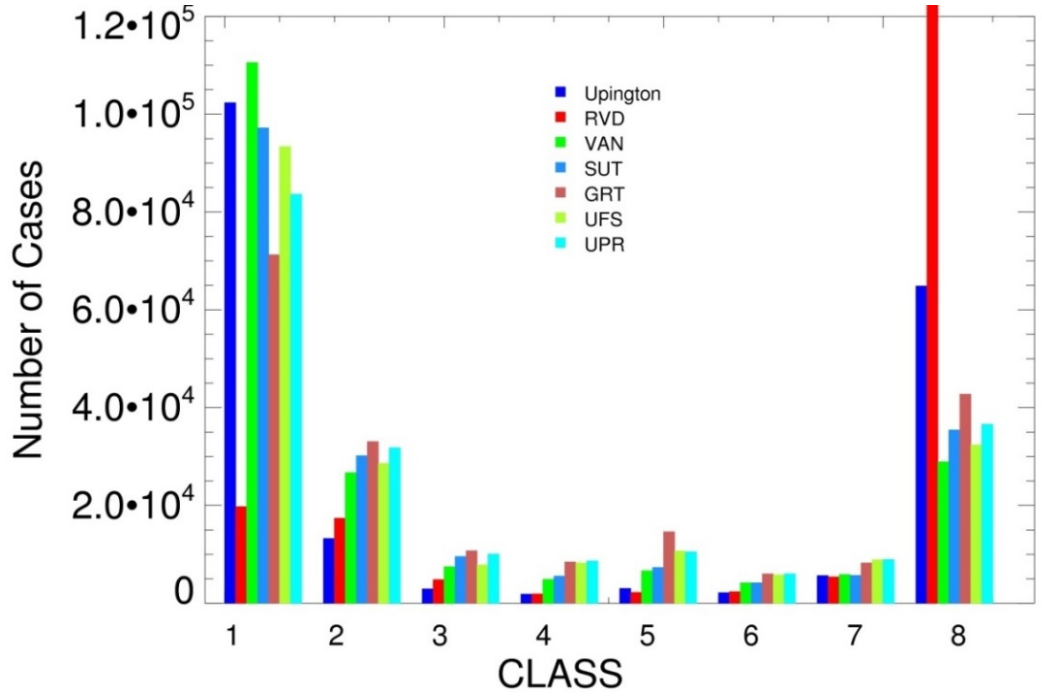

Figure 2.28 DNI variability class statistics of Upington and 6 SAURAN stations based on 2004-2015. The best fitting class is shown.

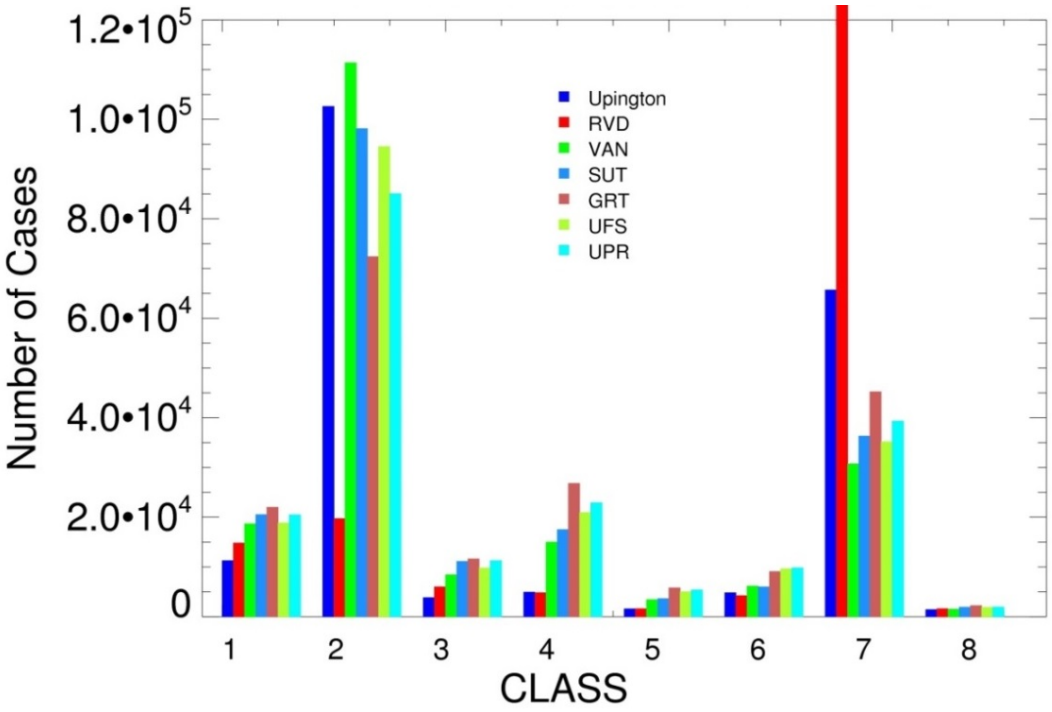

Figure 2.29 DNI variability class statistics of Upington and 6 SAURAN stations based on 2004-2015. The 2nd best fitting class is shown.

2.1.5 Aerosol conditions

There is an AERONET station available at the Upington reference station. Unfortunately, it went online only in the last few days of January 2016. We have obtained the standard data visualization as provided by AERONET (http://aeronet.gsfc.nasa.gov/cgi-bin/type_one_station_opera_v2_new?site=Upington&nachal=0&year=24&month=5&aero_water=0&level=2&if_day=0&if_err=0&place_code=10&year_or_month=0). Any further evaluation like done for the Iberian stations is not meaningful with only 4 months of data. Nevertheless, one gets a first impression of generally very low AOD around 0.1 to 0.2 (given as AOT_500 in green in the plots). Only late January and early March, there is a larger event reaching values up to 0.3 and 0.4, respectively.

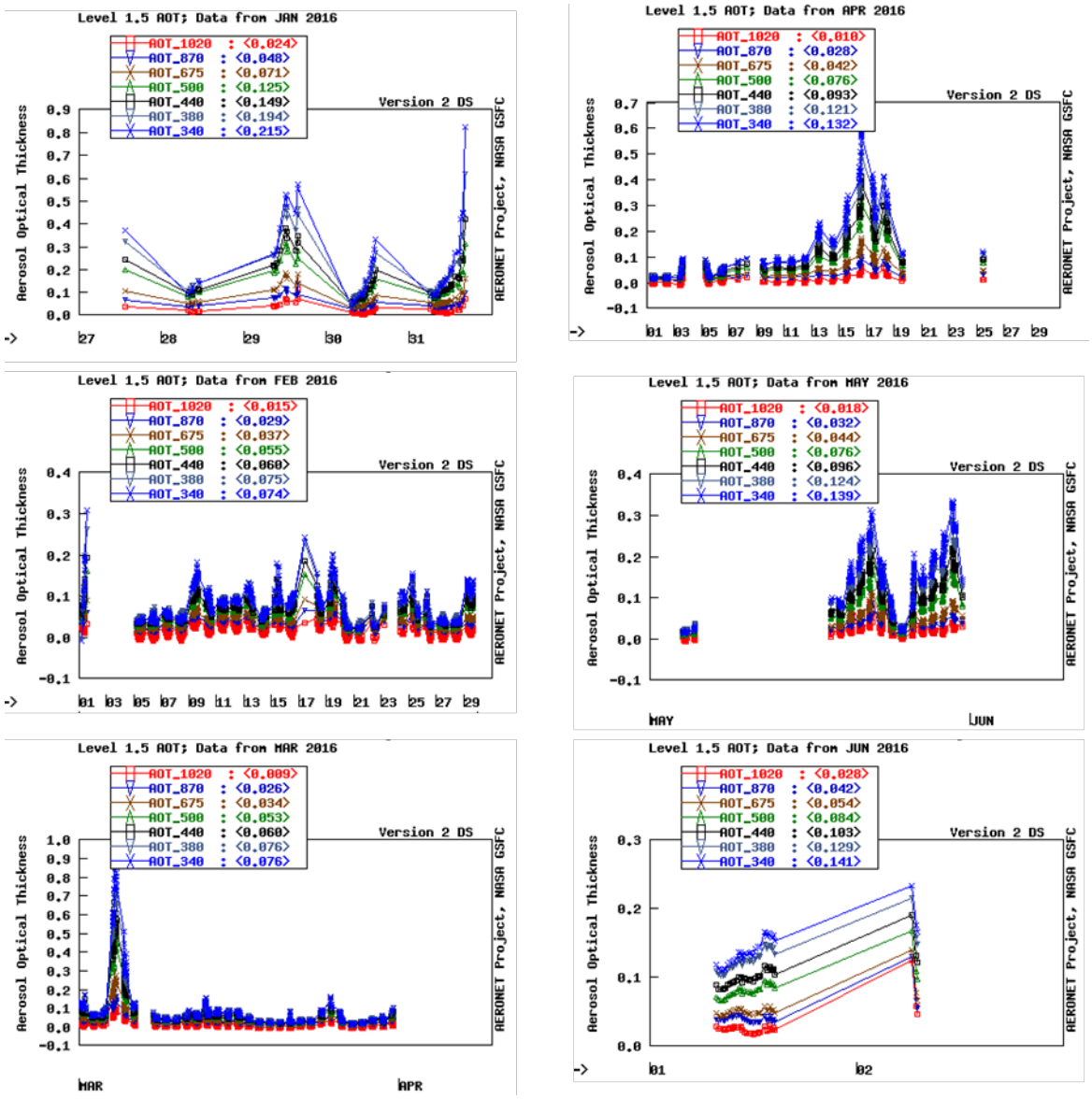

Figure 2.30 AERONET observations at Upington (source AERONET website)

2.1.6 Available meteo forecasts

AEMET does not provide any forecasts for South Africa routinely. Therefore, only ECMWF (European Centre for Medium-Range Weather Forecasts) based forecasts are available. Please note that from 2004 onwards ECMWF has applied a new aerosol climatology which changed the overall biases of GHI and DNI strongly (see section 2.5.1 for a more detailed discussion). Therefore, only the use of ECMWF forecasts after 2004 is recommended.

Table 8: Available NWP datasets

Available deterministic models	ECMWF/ IFS	AROME/ HARMONIE (RUC3 from 2016 onwards)	ECMWF/ IFS + post-processing	AROME/ HARMONIE + post-processing	AROME/ HARMONIE RUC1
Available probabilistic models	ECMWF EPS	gSREPS	ECMWF EPS + post-processing	gSREPS + post-processing	

Legend: Green = available, red = not available, orange = available if effort or upcoming verification results allows

2.2 India

2.2.1 Available ground observations

For India only BSRN candidate stations exist as public available data. They are not providing data so far due to their candidate status.

Table 9: Station information India

Name	Lati-tude (+N)	Longi-tude (+E)	Elevation (m)	Period	Pyrhelio-meter	Net-work	Comments
Gandhi-nagar	23,11	72,63	65	19-05-2014 to date	Not available	BSRN	BSRN Candidate stations. Data not available yet from BSRN website
Gurgaon	28,42	77,16	259	21-04-2014 to date	Not available	BSRN	BSRN Candidate stations. Data not available yet from BSRN website
Howrah	22,55	88,31	51	15-06-2014 to date	Not available	BSRN	BSRN Candidate stations. Data not available yet from BSRN website

Tiruvallur	13,09	79,97	36	16-04-2014 to date	Not available	BSRN	BSRN Candidate stations. Data not available yet from BSRN website

Figure 2.31 Location of Indian stations (light blue = BSRN candidate stations, no data available yet) Based on GoogleMaps as background.

2.2.2 Ground based irradiances

Such data does not exist for these stations.

2.2.3 Cloud conditions

This country is outside the MSG field of view and cannot be analysed.

2.2.4 DNI variability conditions

This country is outside the MSG field of view and cannot be analysed.

2.2.1 Available meteo forecasts

Table 10: Available NWP datasets

Available deterministic models	ECMWF/ IFS	AROME/ HARMONIE (RUC3 from 2016 onwards)	ECMWF/ IFS + post-processing	AROME/ HARMONIE + post-processing	AROME/ HARMONIE RUC1
Available probabilistic models	ECMWF EPS	gSREPS	ECMWF EPS + post-processing	gSREPS + post-processing	

Legend: Green = available, red = not available, orange = available if effort or upcoming verification results allows

2.2.2 Aerosol conditions

As we have no ground observations we do not investigate this further.

2.3 Morocco

2.3.1 Available ground observations

EnerMENA is a project being fully named 'Towards a Sustainable Implementation of Solar Thermal Power in the MENA Region'. The MENA acronym represents the Mediterranean Europe and Northern Africa regions. EnerMENA includes a dedicated ground measurement program 'enerMENA meteo network' applying ventilated CMP21 Secondary Standard Kipp & Zonen pyranometers and Kipp & Zonen CHP1 First Class pyrheliometer instruments at various locations in Algeria, Egypt, Jordan, Morocco, and Tunisia.

Table 11: Station information Morocco

Name	Latitude (+N)	Longitude (+E)	Elevation (m)	Period	Pyrheliometer	Temporal resolution	Network
Oujda	34,65	-1,9	617	2011-08-18 to date	Kipp & Zonen CHP1	1-min	enerMENA
Missour	32,86	-4,107	1107	2013-05-27 to date	Kipp & Zonen CHP1	1-min	enerMENA
Tan-Tan	28,498	-11,322	75	2013-05-05 to date	Kipp & Zonen CHP1	1-min	enerMENA
Erfoud	31,491	-4,218	859	2013-05-30 to date	Rotating Shadowband Irradiometer	1-min	enerMENA
Zagora	30,272	-5,852	783	2013-05-31 to date	Rotating Shadowband Irradiometer	1-min	enerMENA

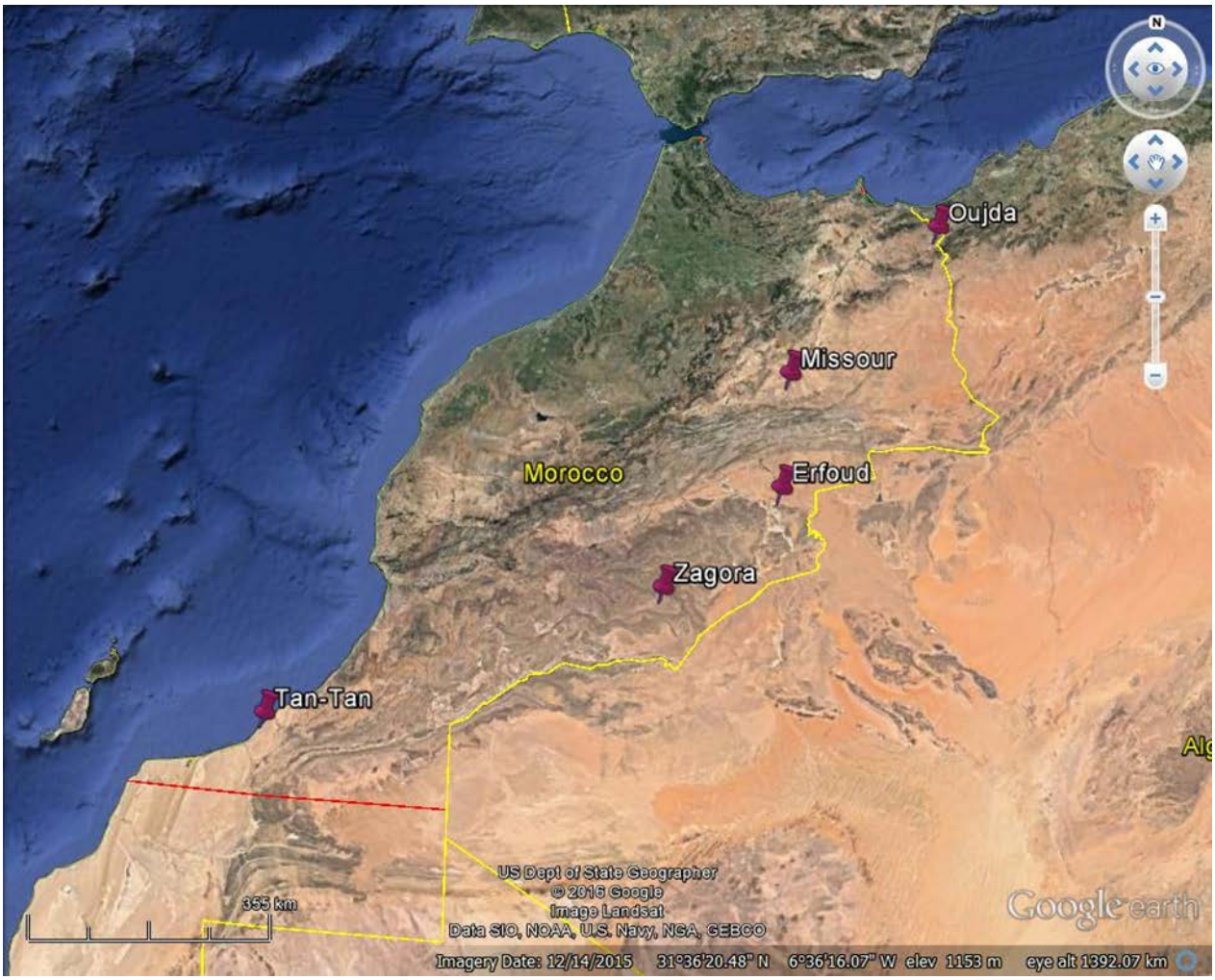

Figure 2.32 Location of stations in Morocco (red = EnerMENA stations) Based on GoogleMaps as background.

Quality control has been performed as described in Annex B. High quality measurements have been found in these stations. Practically all invalid DNI days are due to missing data. The following tables show, in each station, the number of days of each month for which no suitable DNI measurements are available.

Measured data are available in Oujda station from February 28th 2012. Main problems are due to missing data and (but in a lesser measure) tracking errors.

Table 11a: Station information Morocco – data availability Oujda

	Oujda (EnerMENA)												
Year	Jan	Feb	Mar	Apr	May	Jun	Jul	Aug	Sep	Oct	Nov	Dec	Annual
2012	-	-	0	0	0	0	2	4	0	4	0	0	**10**
2013	0	1	0	0	1	0	0	0	0	0	7	0	**9**
2014	2	0	1	1	6	16	5	-	-	-	-	-	**31**

Measured data are available in Missour station from June 1st 2013. Main problems are due to missing data.

Table 11b: Station information Morocco – data availability Missour

	Missour (EnerMENA)												
Year	Jan	Feb	Mar	Apr	May	Jun	Jul	Aug	Sep	Oct	Nov	Dec	Annual
2013	-	-	-	-	-	0	0	0	0	0	0	0	**0**
2014	0	0	0	7	5	0	0	0	0	0	0	1	**13**

Measured data are available in Erfoud station from June 3rd 2013. Main problems are due to missing data.

Table 11c: Station information Morocco – data availability Erfoud

	Erfoud (EnerMENA)												
Year	Jan	Feb	Mar	Apr	May	Jun	Jul	Aug	Sep	Oct	Nov	Dec	Annual
2013	-	-	-	-	-	2	0	0	0	0	0	0	**2**
2014	0	0	0	0	11	0	0	0	0	0	0	0	**11**

Measured data are available in Zagora station from June 3rd 2013. No problems are detected in this station.

Table 11d: Station information Morocco – data availability Zagora

	Zagora (EnerMENA)												
Year	Jan	Feb	Mar	Apr	May	Jun	Jul	Aug	Sep	Oct	Nov	Dec	Annual
2013	-	-	-	-	-	2	0	0	0	0	0	0	**27**
2014	0	0	0	0	0	0	0	0	0	0	0	0	**0**

Measured data are available in Tan-Tan station from June 6th 2013. Invalid DNI days in 2014 are due to missing data.

Table 11e: Station information Morocco – data availability Tan-Tan

	Tan-Tan (EnerMENA)												
Year	Jan	Feb	Mar	Apr	May	Jun	Jul	Aug	Sep	Oct	Nov	Dec	Annual
2013	-	-	-	-	-	5	0	0	0	0	0	0	**0**
2014	0	5	2	15	1	0	0	0	0	0	0	0	**23**

2.3.2 Irradiances

Ground observations

Fig. 2.33 provides the annual histograms of hourly daytime DNI at the EnerMENA stations. If more than a single complete year is available, the red line represents the mean and the other years are given as grey lines. Fig. 2.34 to Fig 2.37 present the monthly histograms of hourly daytime DNI observations at the stations Oujda, Missour, Erfoud, Tan-Tan, and Zagora.

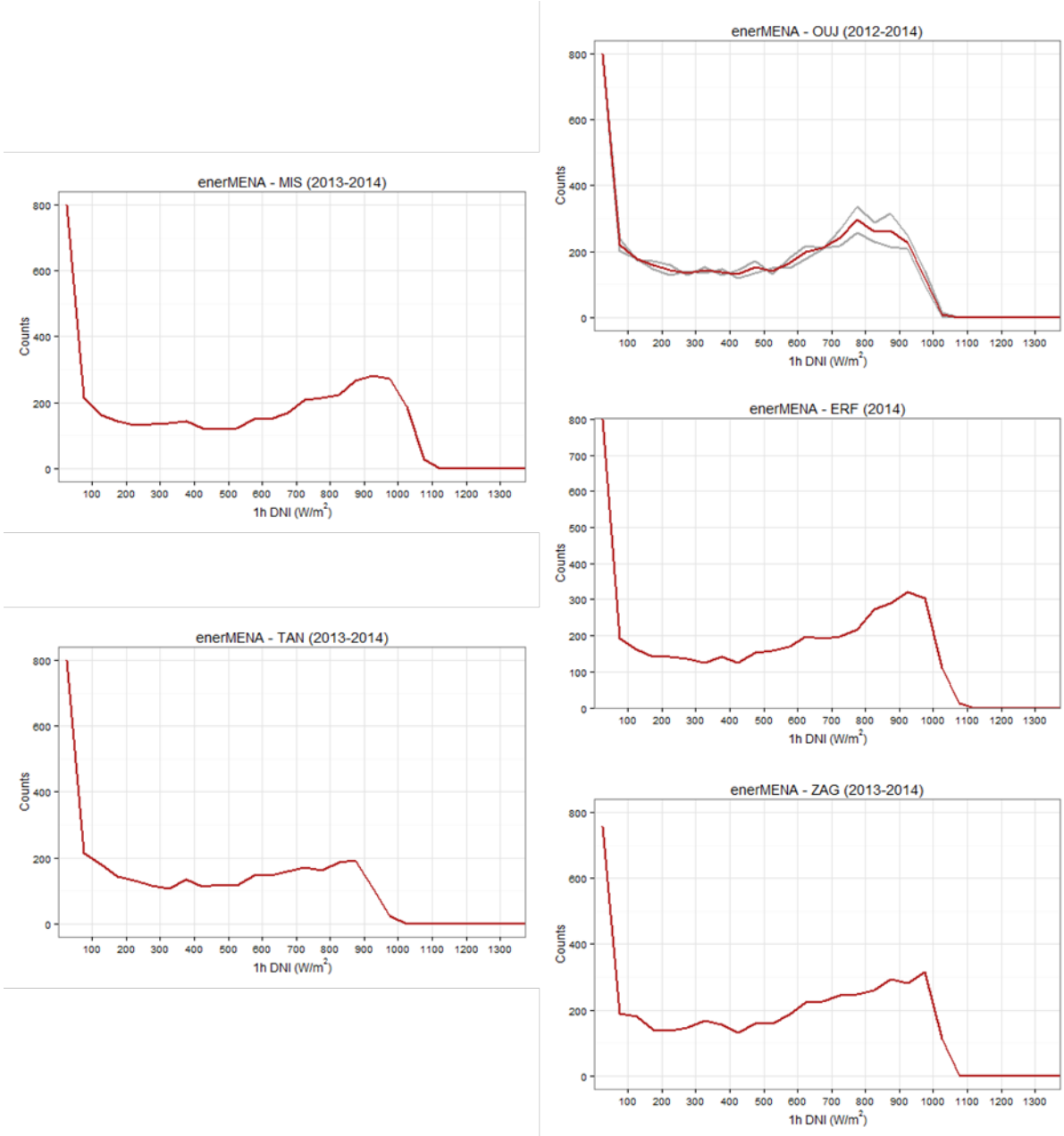

Figure 2.33: Ground-based DNI, frequency distributions of hourly DNI at EnerMENA stations Oujda, Missour, Erfoud, Tan-Tan and Zagora

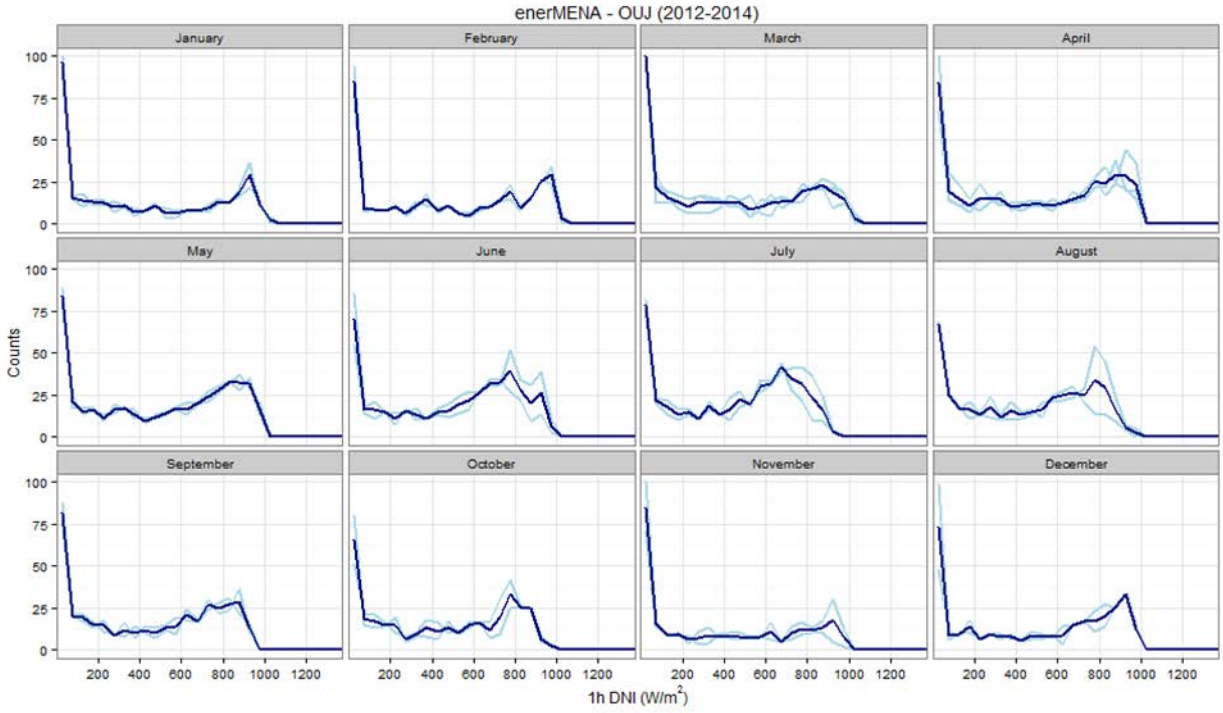

Figure 2.34: Ground-based DNI, frequency distributions of hourly DNI at EnerMENA station Oujda (blue) for all calendar months.

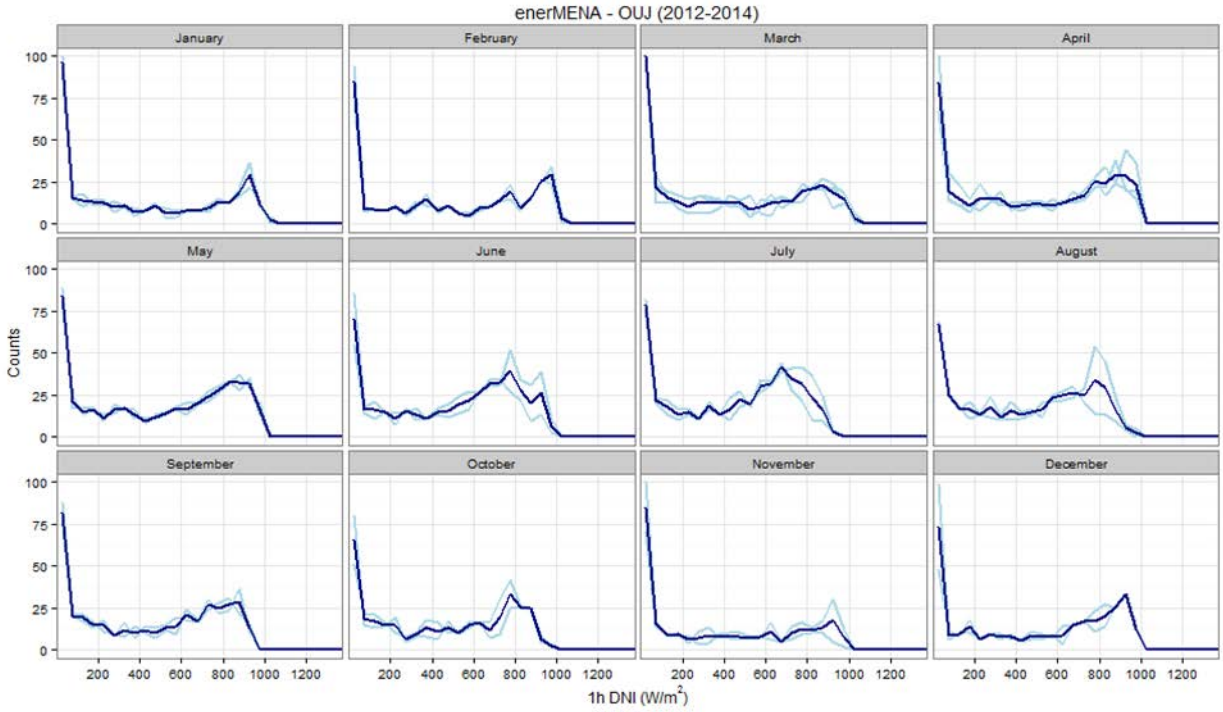

Figure 2.35: Ground-based DNI, frequency distributions of hourly DNI at EnerMENA station Missour (blue) for all calendar months.

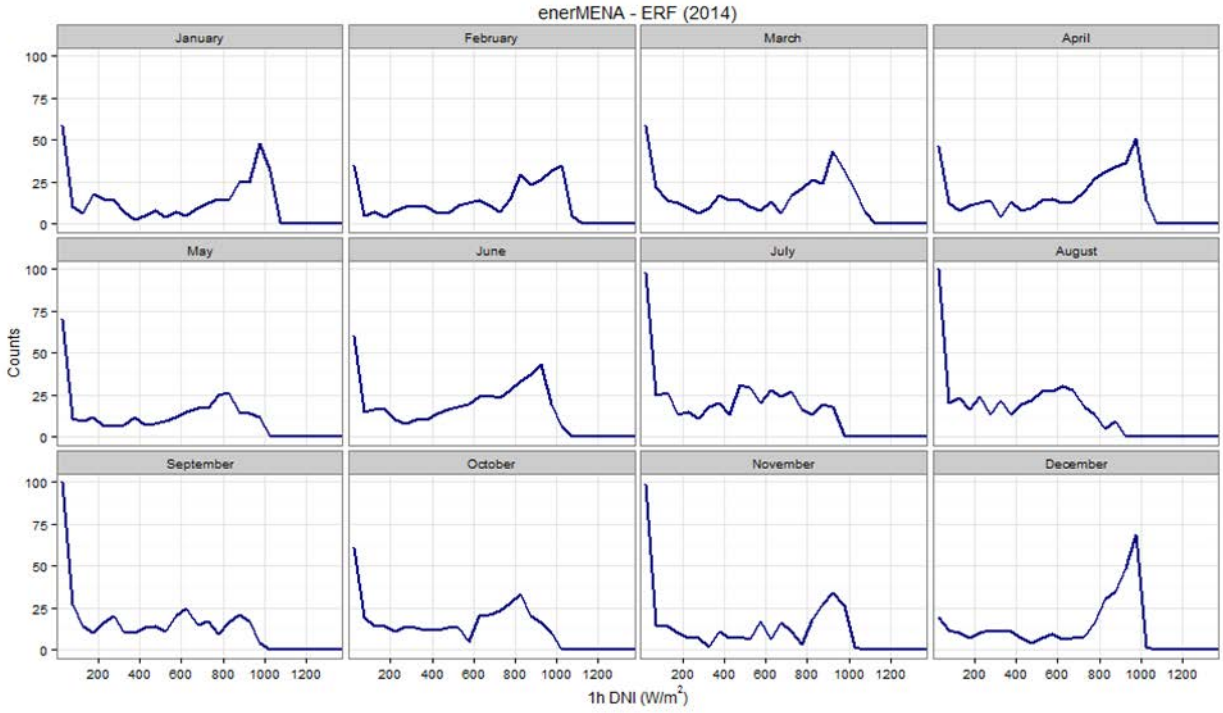

Figure 2.36: Ground-based DNI, frequency distributions of hourly DNI at EnerMENA station Erfoud (blue) for all calendar months.

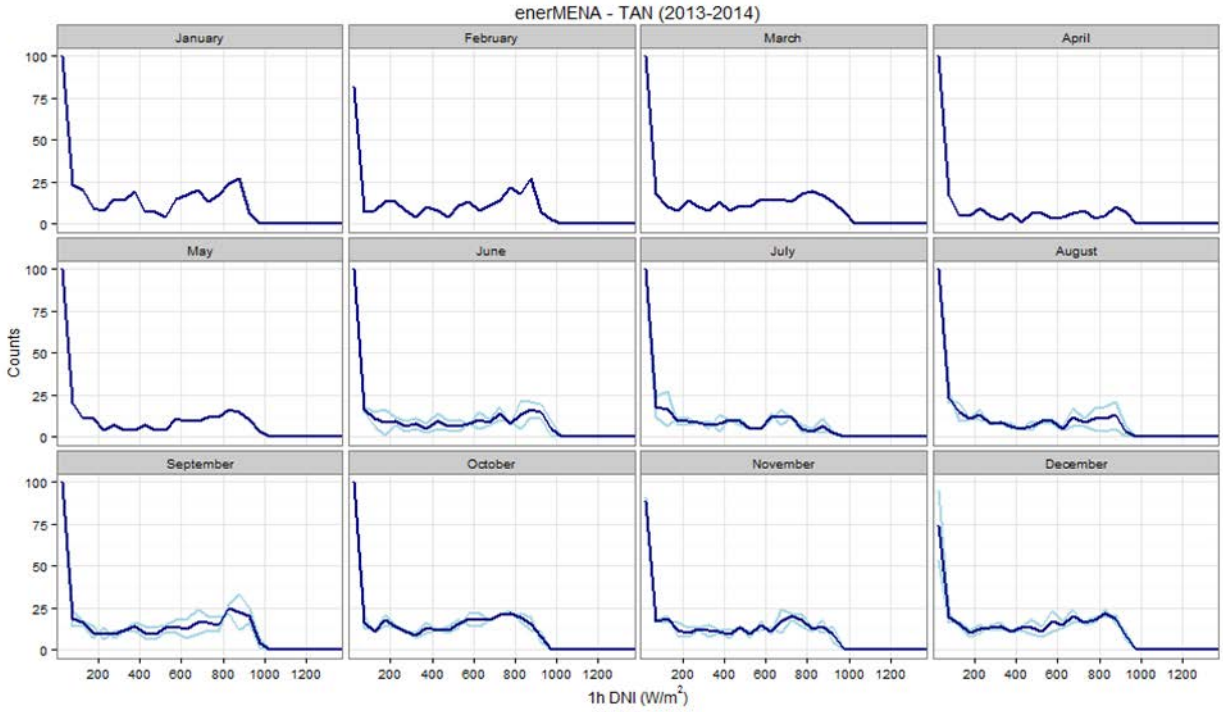

Figure 2.37: Ground-based DNI, frequency distributions of hourly DNI at EnerMENA station Tan-Tan (blue) for all calendar months.

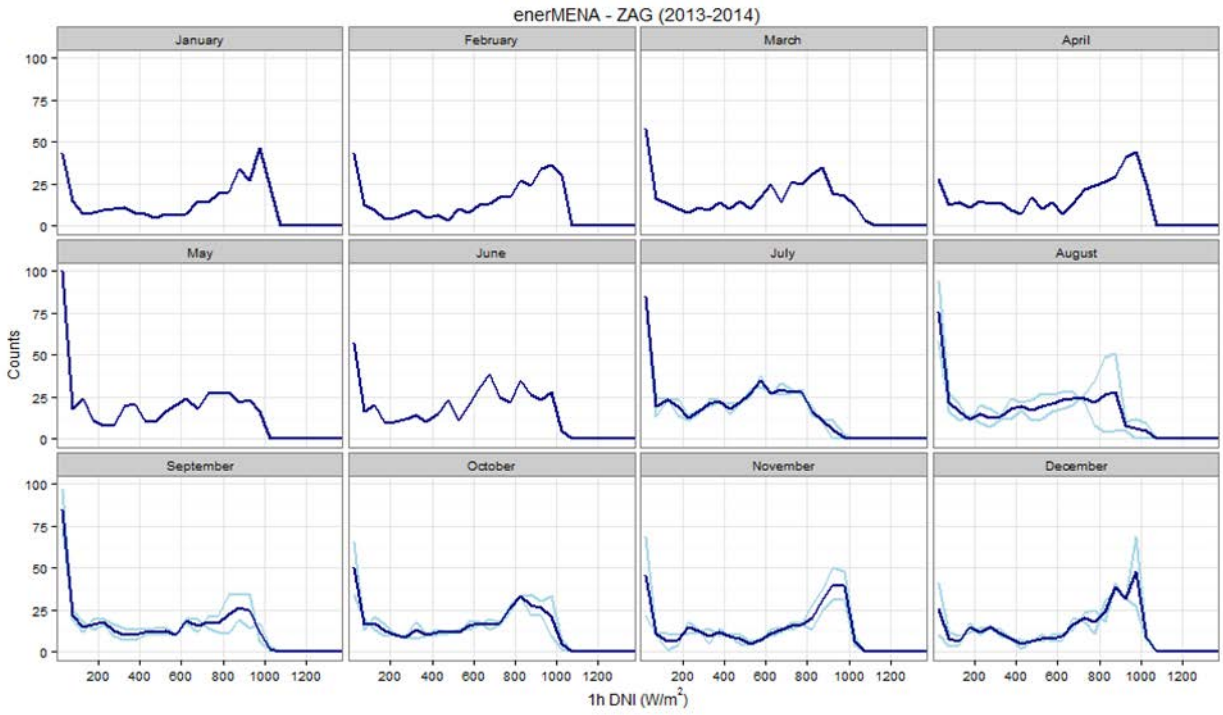

Figure 2.38: Ground-based DNI, frequency distributions of hourly DNI at EnerMENA station Zagora (blue) for all calendar months.

Satellite/model based observations (CAMS)

In order to ensure that CAMS data is sufficiently accurate at EnerMENA stations, we compare the mean histograms for the years and months with available ground observations.

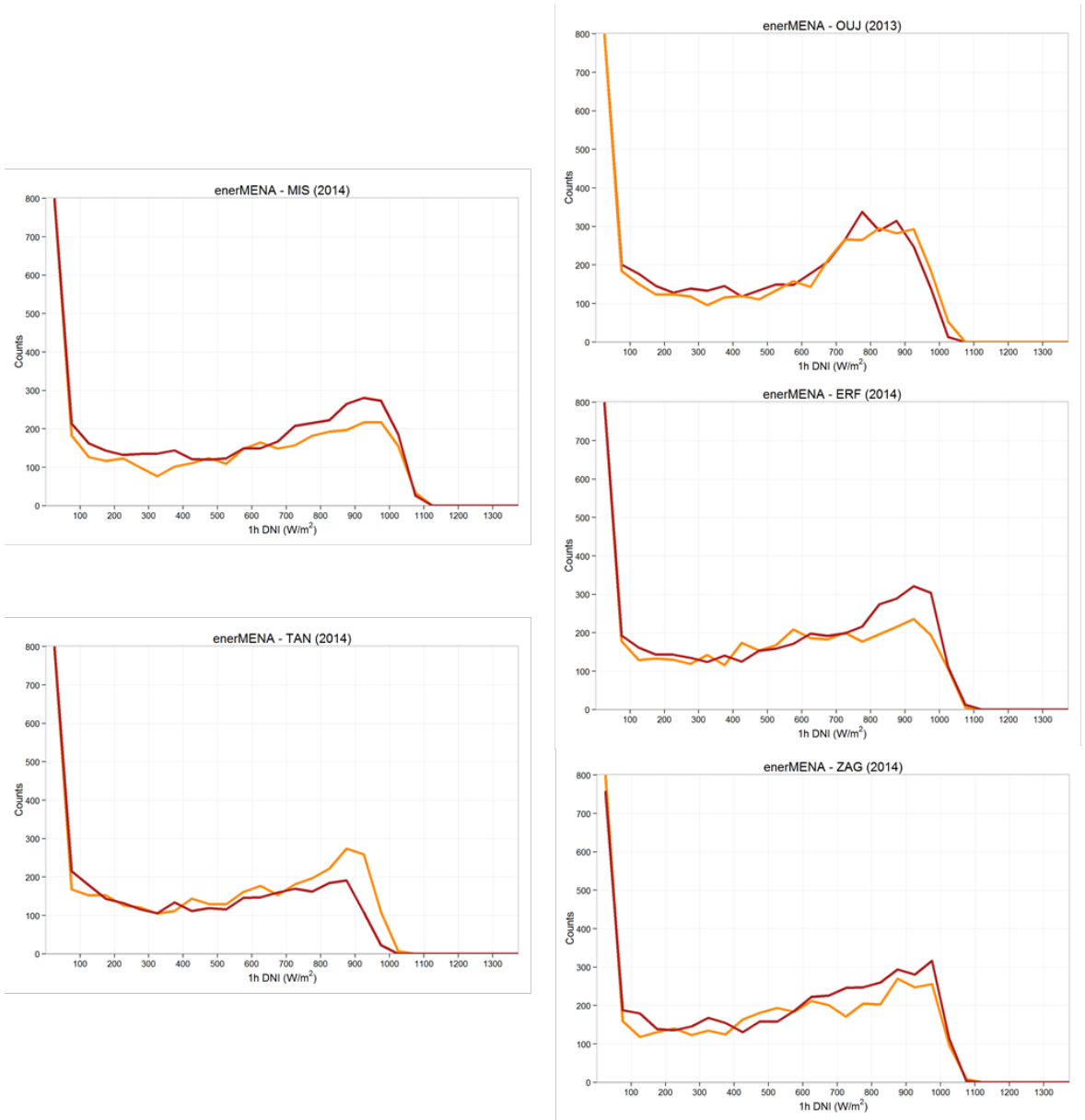

Figure 2.39 Ground based (red) and CAMS-based (orange) hourly DNI values at EnerMENA stations Oujda, Missour, Erfoud, Tan-Tan and Zagora. The placement of the plots reflects the geographical position relative to each other.

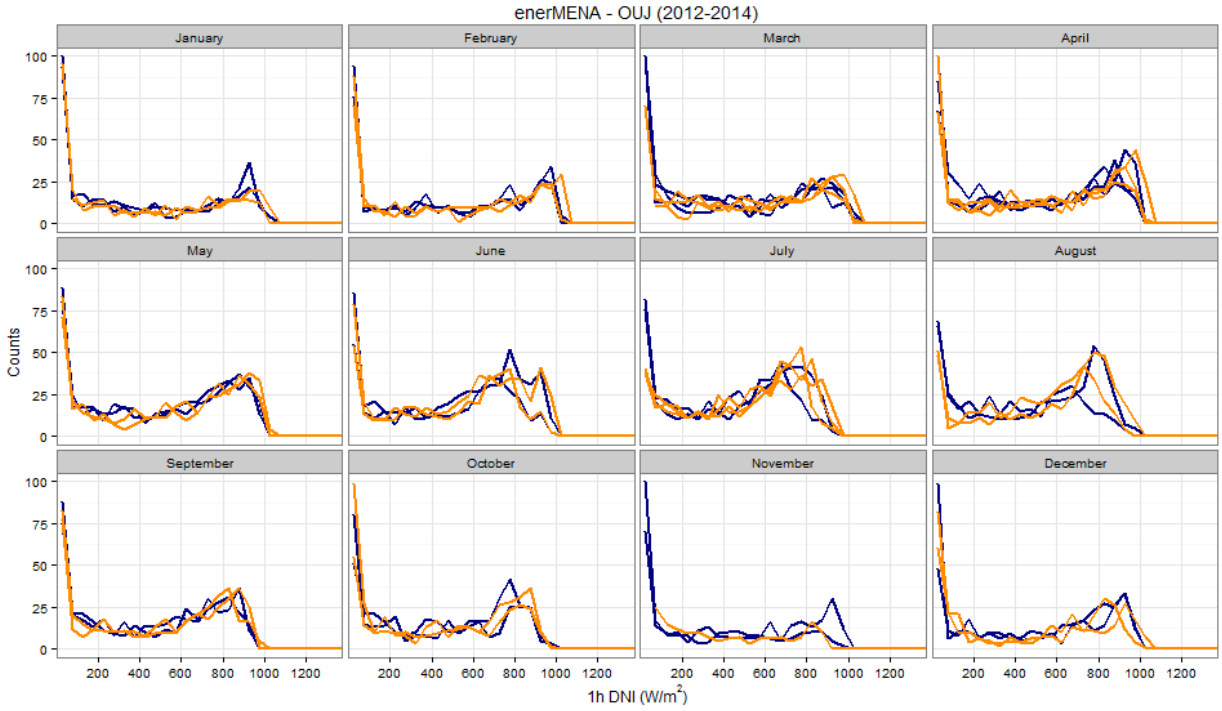

Figure 2.40 Ground based (blue) and CAMS-based (orange) hourly DNI values at EnerMENA station Oujda and split in monthly frequency histograms.

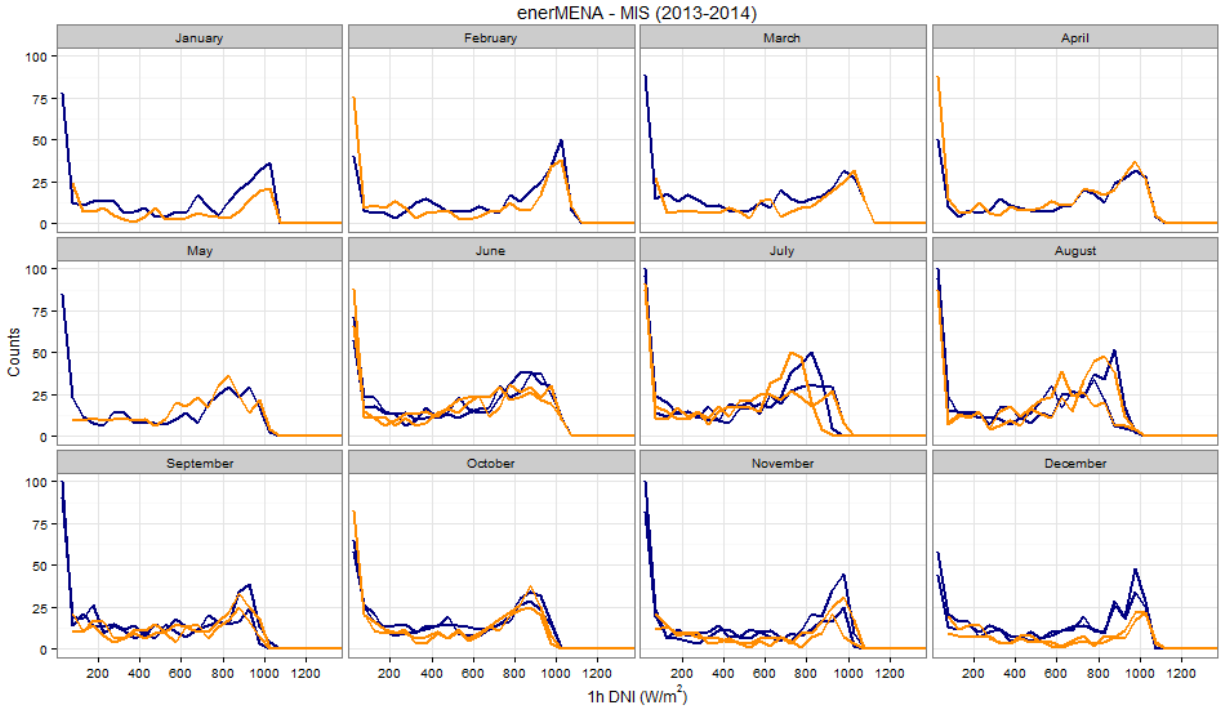

Figure 2.41 Ground based (blue) and CAMS-based (orange) hourly DNI values at EnerMENA station Missour and split in monthly frequency histograms.

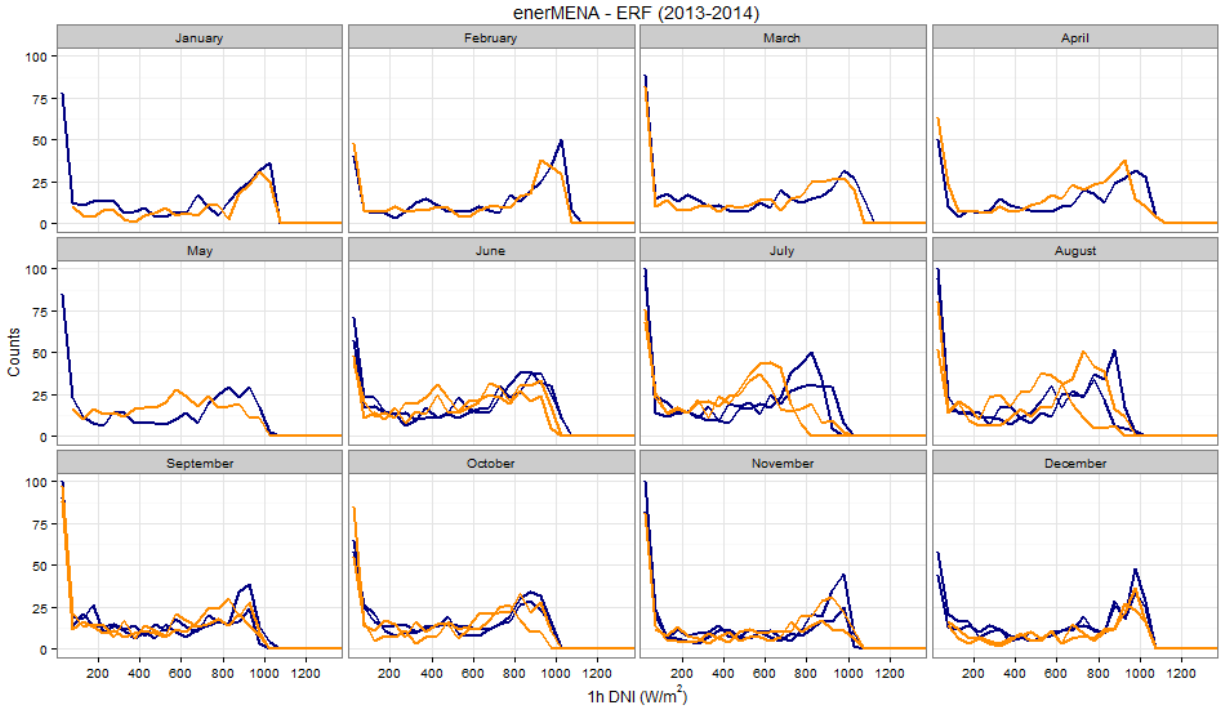

Figure 2.42 Ground based (blue) and CAMS-based (orange)hourly DNI values at EnerMENA station Erfoud and split in monthly frequency histograms.

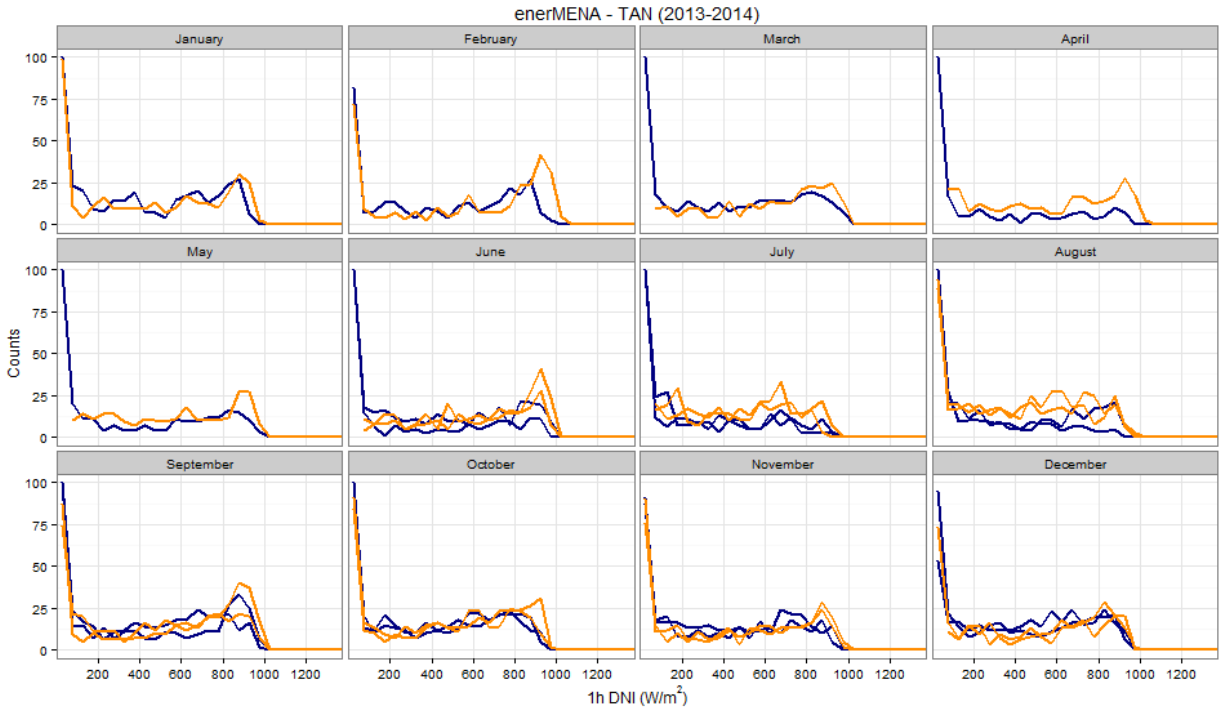

Figure 2.43 Ground based (blue) and CAMS-based (orange) hourly DNI values at EnerMENA station Tan-Tan and split in monthly frequency histograms.

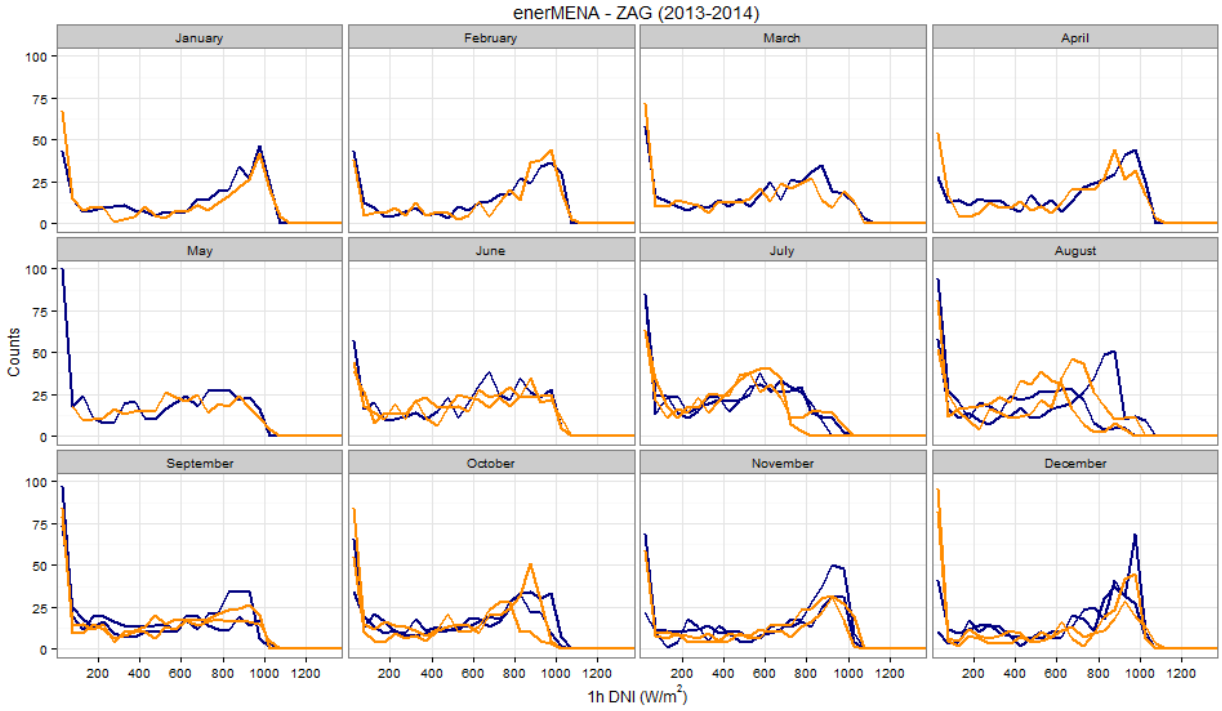

Figure 2.44 Ground based (blue) and CAMS-based (orange) hourly DNI values at EnerMENA station Zagora and split in monthly frequency histograms.

In the annual histograms, Missour, Erfoud, and to a lesser extent also Zagora, are underestimated in the CAMS satellite observations. Please note, that from other projects we know about an underestimation of DNI especially in the morning hours in winter months at these stations. This is due to a cloud retrieval error over cold, bright desert surfaces already being identified. Nevertheless, the current database still has this effect. This effect can clearly been seen in November to January in Missour, to a lesser extent in Erfoud, and from September to January in Zagora.

Second main differences are found in June to August. Please note that June to August are the months with the most intense dust loads in Morocco (Fig. 2.44 a and 2.44 b). CAMS is known to overestimate Saharan dust in Tamanrasset, Algeria, and one can assume that this also applies to Morocco. This results in an underestimation of DNI in the months June to August if being close to the Sahara. This can be seen in June to August in Missour, July and August in Erfoud, and July to September in Zagora. Oujda is not affected as it is in the North of Morocco, not affected so heavily by Saharan dust.

Concerning the location of Noor used below, we do not know definitely, but assume that both effects also exist in CAMS data for Noor. So, any relative comparisons of CAMS at e.g. Erfoud vs. CAMS at Noor are still meaningful despite the known difficulties of the current version of CAMS in this region. Both effects are under investigation in CAMS, but will only be improved in the next CAMS version by better cloud retrievals (APOLLO_NG – Next Generation is not showing this effect anymore) and more extensive data assimilation of aerosol observations (MODIS deep blue with new data being available now also over deserts) in the CAMS model.

Tan-Tan on the other hand is always overestimated by CAMS and shows very low DNI in general.

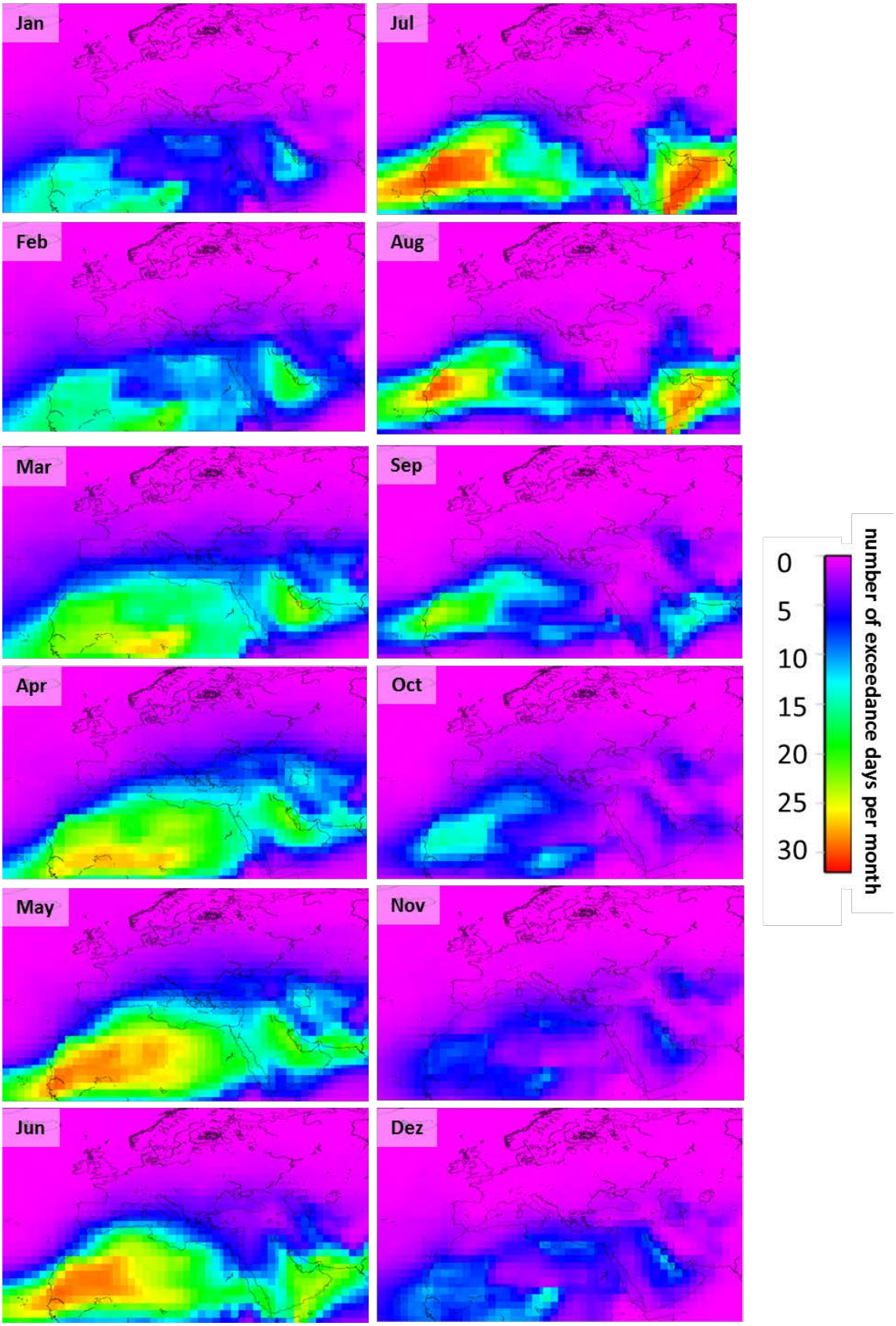

Figure 2.44a: Spatial distribution of more than 30% DNI extinction due to dust AOD (Schroedter-Homscheidt et al., 2016b)

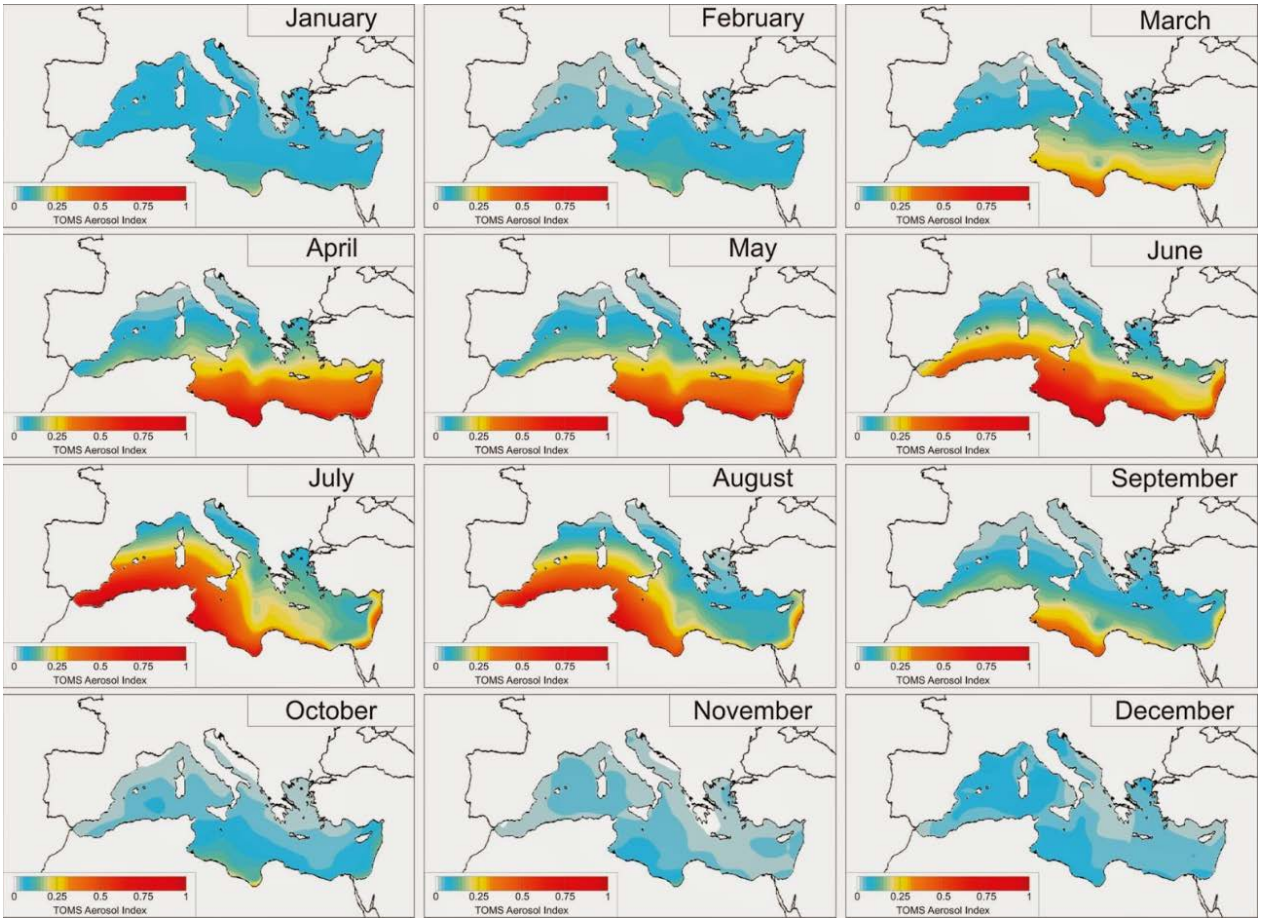

Figure 2.44b: TOMS aerosol index over the Mediterranean Sea (Varga et al., 2014)

Having discussed the difference between ground and satellite-based observations, we now continue to look at long-term satellite observations. They are available for a 10-years period and at any point of interest in Morocco.

In the following histograms we compare results versus the location of Noor (30.994°N, -6.863°E) in the vicinity of various CSP power plant projects. Hourly resolved, satellite-based CAMS DNI is used from 2006 to 2015.

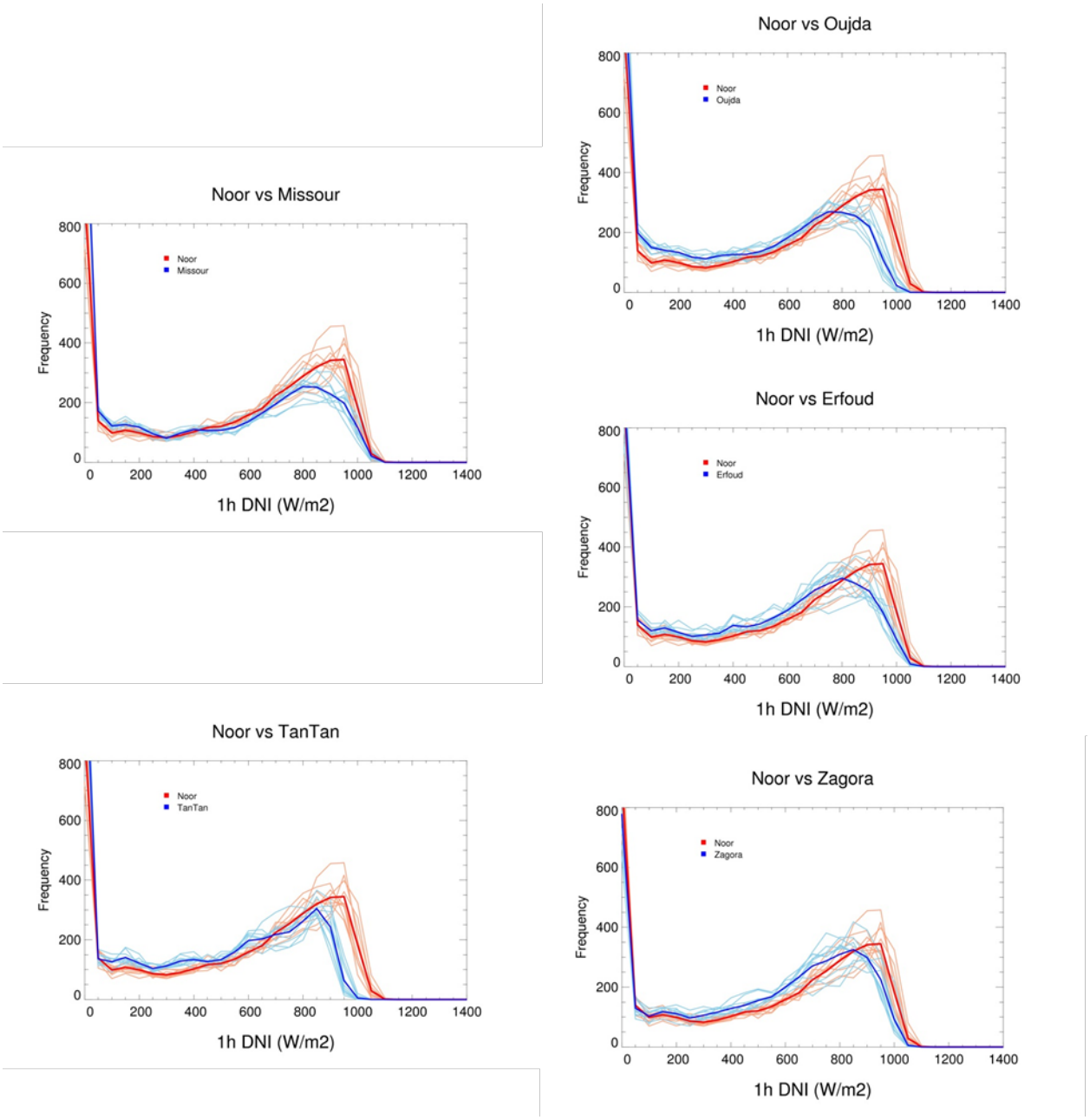

Figure 2.45: CAMS based DNI, frequency distributions of hourly DNI at EnerMENA stations Oujda, Missour, Erfoud, Tan-Tan and Zagora together with the Noor location for 2006-2015. The placement of the plots reflects the geographical position relative to each other.

Zagora station is the station having the closest annual histogram, even if the peak of the histogram is still shifted to smaller DNI values. None of the EnerMENA stations is close to the conditions at the Noor site.

With respect to the monthly histograms, Zagora shows for all months a similar shift towards smaller DNI values, but the overall seasonal pattern is met. The shift is more pronounced in May to September than in the winter months. Erfoud has a DNI peak shifted to smaller DNI values especially in the months April to November. Without discussing the other stations in detail, we still would like to mention, that this consistent shift over the months cannot be found at Oujda, Missour, Erfoud, and Tan-Tan. For the other

EnerMENA stations there are always some months which are very similar to Noor and others which differ very much. Having all months in mind, Zagora seems to be the best choice.

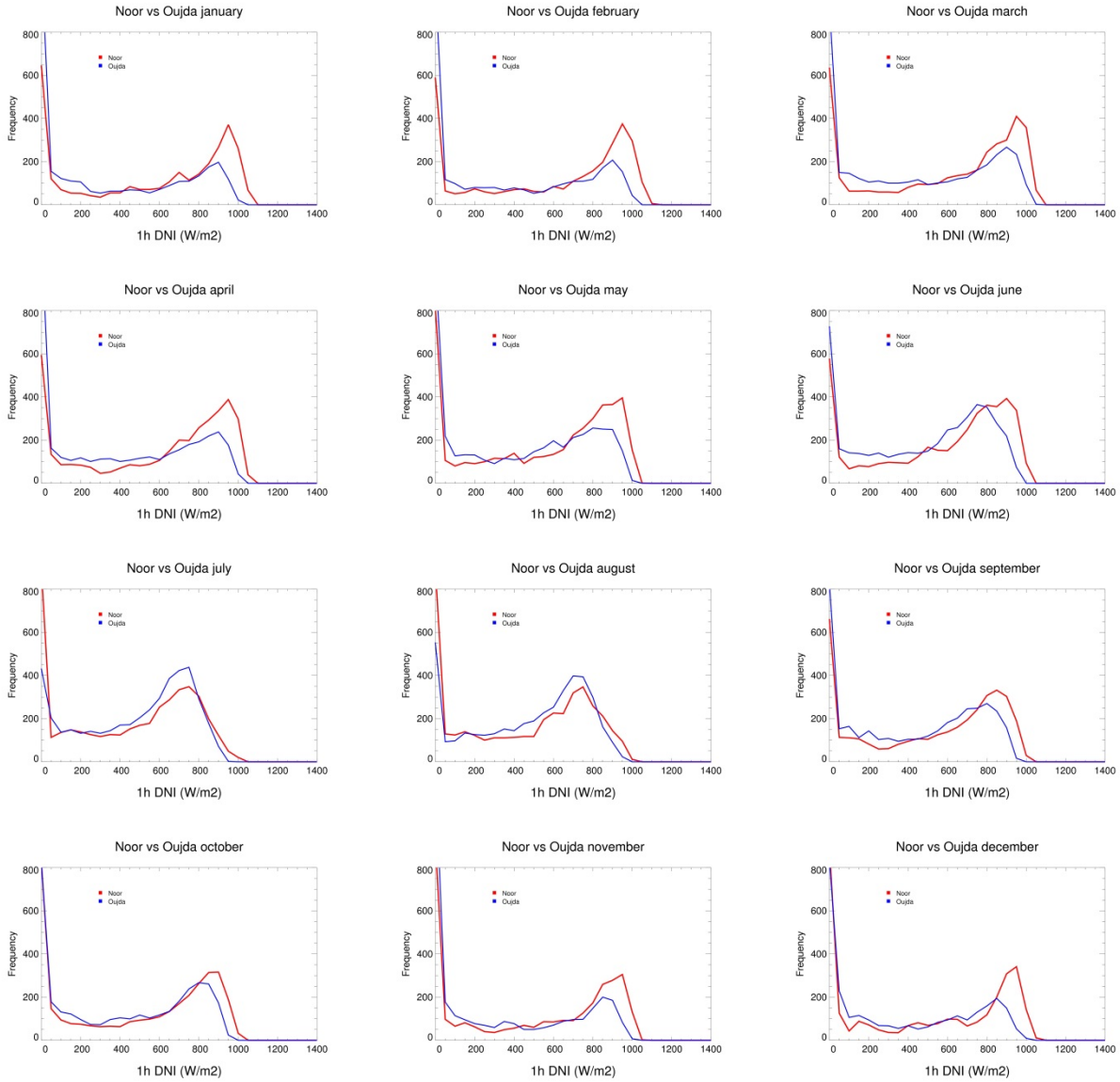

Figure 2.46: CAMS based DNI, frequency distributions of hourly DNI at EnerMENA station Oujda (blue) and Noor (red) for all calendar months, based on data from 2006-2015

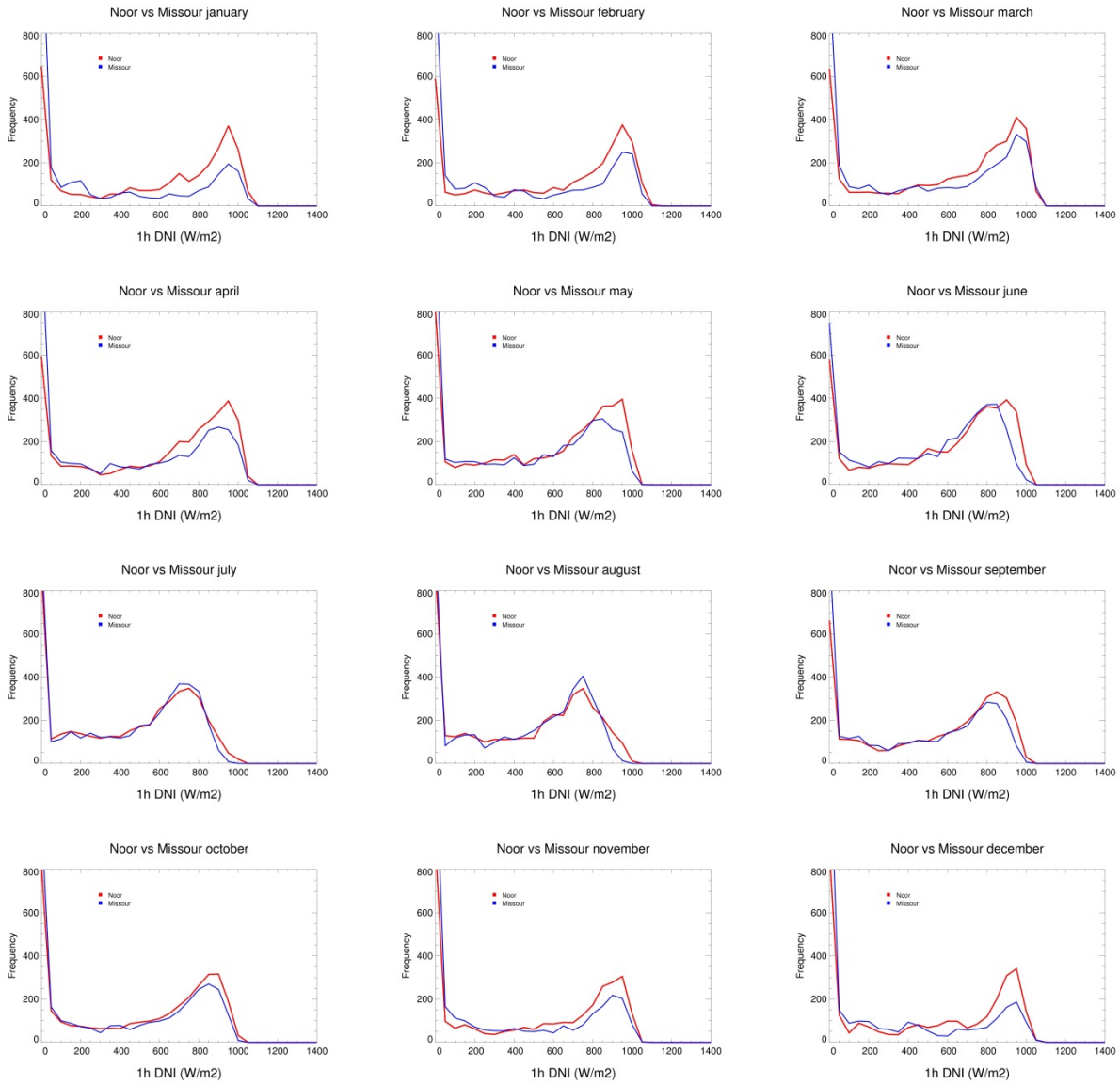

Figure 2.47: CAMS based DNI, frequency distributions of hourly DNI at EnerMENA station Missour (blue) and Noor (red) for all calendar months, based on data from 2006-2015

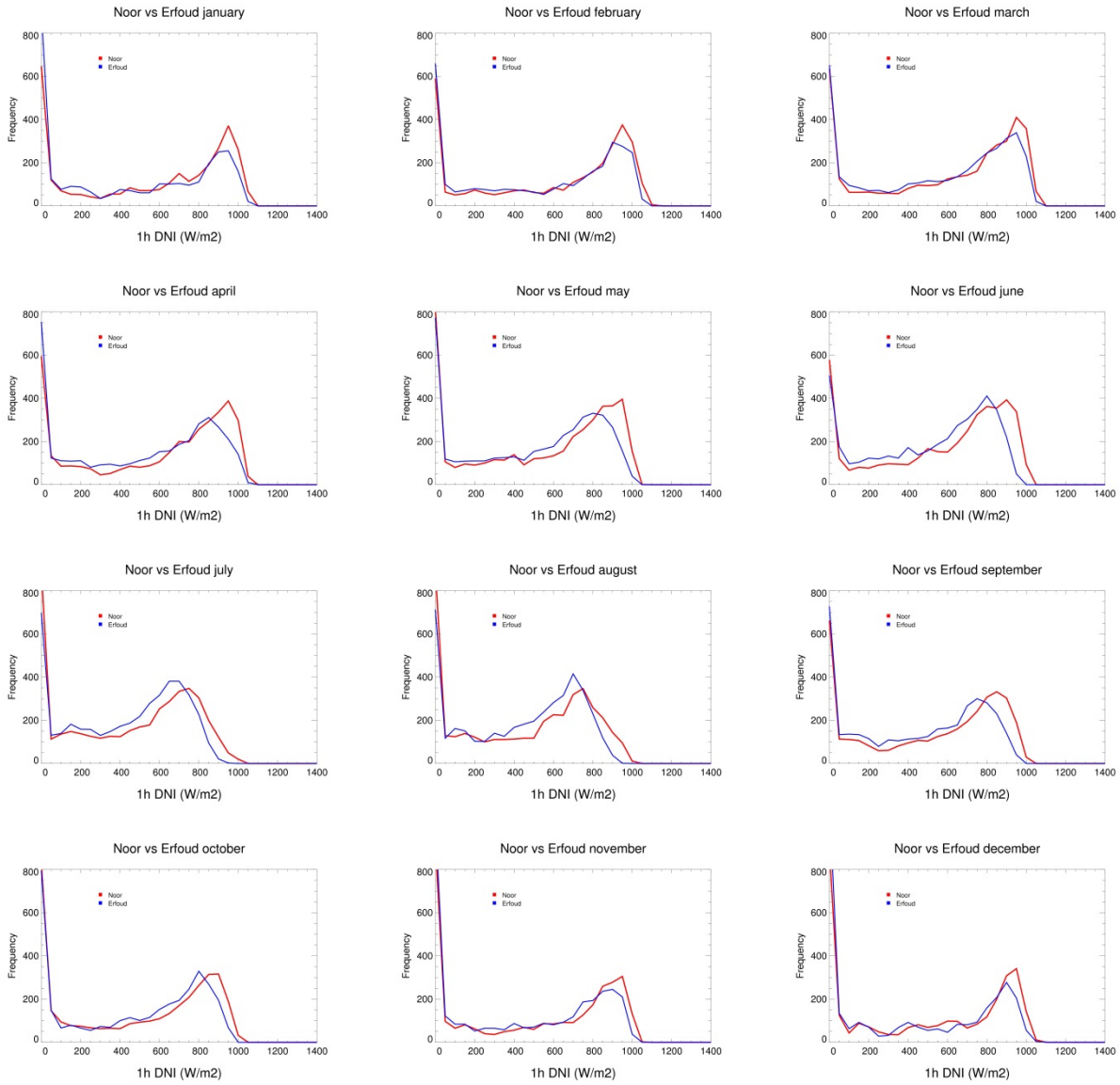

Figure 2.48: CAMS based DNI, frequency distributions of hourly DNI at EnerMENA station Erfoud (blue) and Noor (red) for all calendar months, based on data from 2006-2015

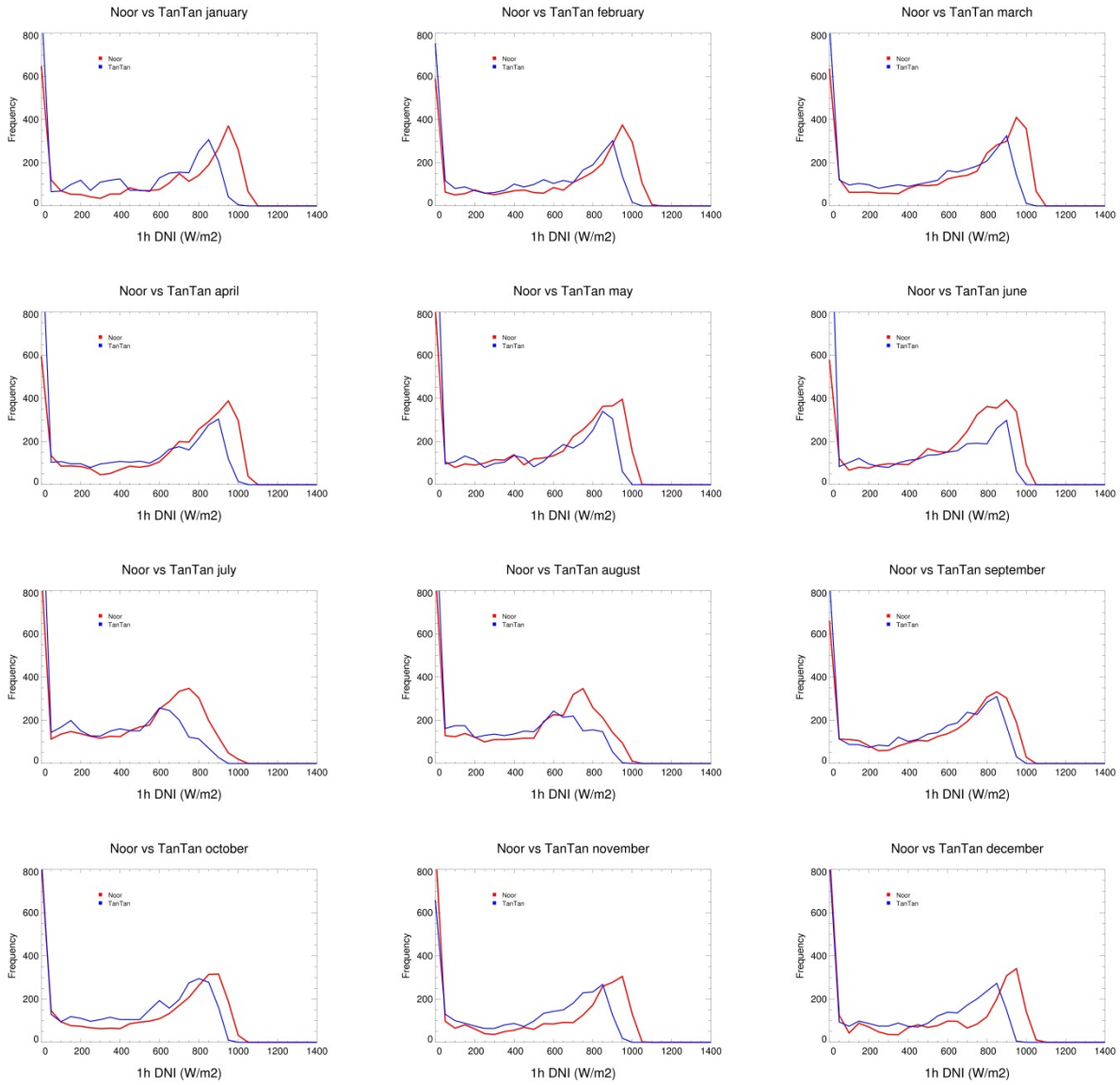

Figure 2.49: CAMS based DNI, frequency distributions of hourly DNI at EnerMENA station Tan-Tan (blue) and Noor (red) for all calendar months, based on data from 2006-2015

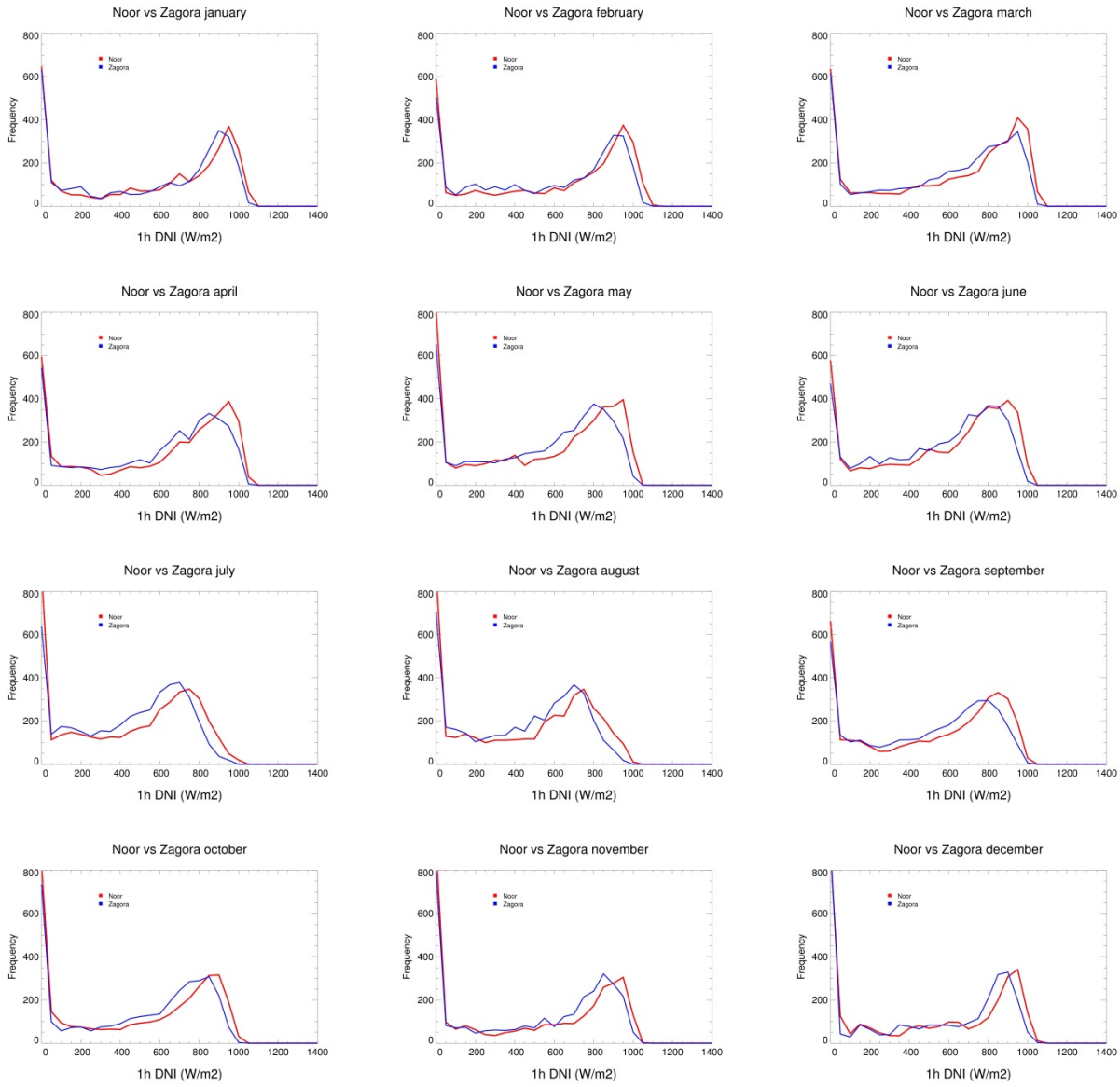

Figure 2.50: CAMS based DNI, frequency distributions of hourly DNI at EnerMENA station Zagora (blue) and Noor (red) for all calendar months, based on data from 2006-2015

2.3.3 Cloud conditions

First of all, we compare the stations by the occurrence of clouds. We take the station Noor as reference and compare the others against it. In Fig. 2.51 we discriminate cloud-free from cloudy cases. Cloud-free, but snow on the ground cases are also given, as this evaluation tool is also used for more PV related studies in more snowy regions. Zagora has 80% of cloud-free cases, while Noor has about 75% and is closer to Erfoud in this parameter. Oujda, Tan-Tan and Missour have only about 60% cloud-free cases.

In Fig. 2.52 the cloudy cases are further split in optically thick cases with low, medium and high cloud top levels (named ‘low water’, ‘medium wat.’, and ‘high wat./mix.’) and optically thin cirrus cases (‘high thin ice’). With respect to DNI the separation in optically thick and thin cloud types is most relevant, for meteorologists the further split into vertical levels is of further interest to assess the situation at a site.

With respect to thin ice clouds, all stations with exception of Tan-Tan are close to the conditions at the Noor site. For optically thick clouds, Tan-Tan has very often low level clouds, while all other clouds are less than at Noor. Low level clouds are also more frequently found for Oujda and Missour, while Erfoud and Zagora have similar conditions as the Noor site.

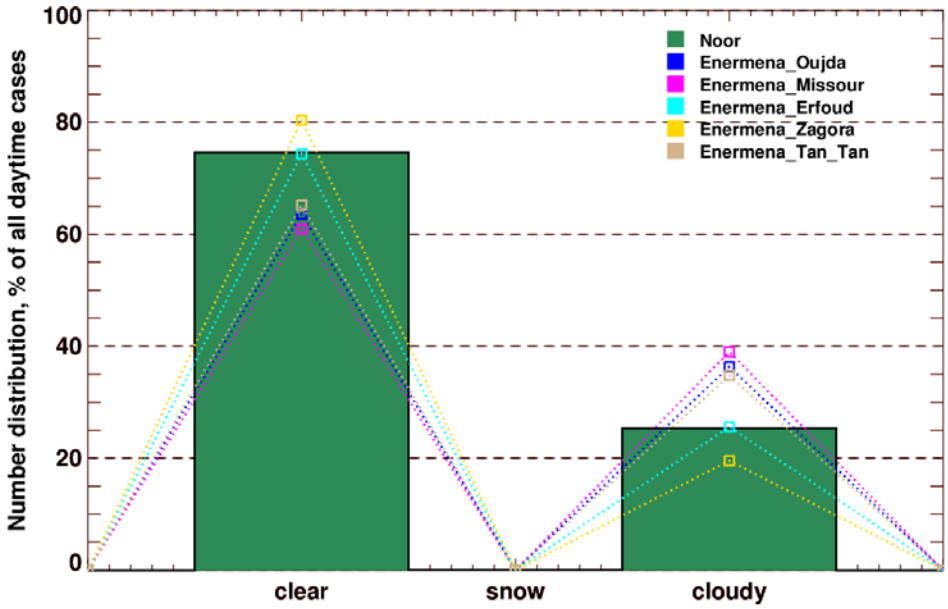

Figure 2.51 Cloud statistics of Noor and 5 EnerMENA stations: cloud mask; frequency of occurrence in percentage of all daytime satellite images; split into cloud-free, cloud-free but snow on surface, and cloudy cases; based on 2004-2015.

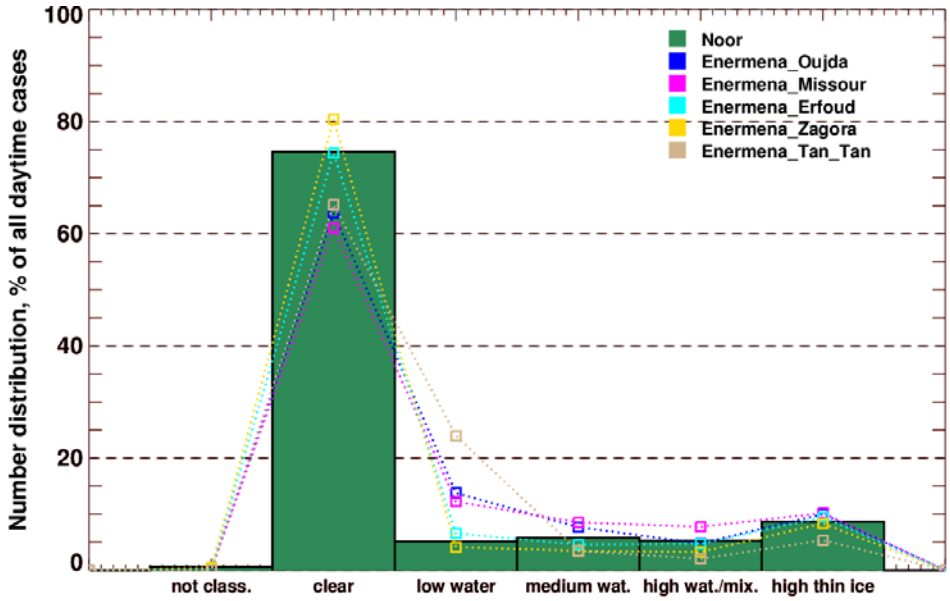

Figure 2.52 Cloud statistics of Noor and 5 EnerMENA stations: cloud type; frequency of occurrence in percentage of all daytime satellite images; split into cloud-free and cloudy cases – cloudy cases are separated in low, medium, high cloud top height clouds being optically thick and optically thin ice cloud cases; based on 2004-2015.

The split of all cases in scattered, broken/overcast, thin ice clouds, clear and snow conditions is done first for each station separately, but split into time of the day and month of the year (Fig. 2.53 to 2.58) and normalized on the number of daytime cases in each bin. Several seasonal and daily cycles can be seen – some of them we discuss as examples before we compare the stations.

Please note that the first and last hours of the day are typically populated with less cases due to shorter days in winter time. But we prefer to give relative values here. If needed, absolute histograms can be provided as well.

Please note: During winter months, the underlying cloud database is detecting cloud situations during morning hours too frequently. The next version of the database will not have this data anymore, but it is not available for statistical evaluation so far. Therefore, the shown maximum cloud cover during morning hours from October to January is not reliable.

Noor has a dedicated seasonal cycle. Months April to September show much more cloudy cases during the afternoon than in the morning. During October to March this feature is not existing in a similar way.

For Oujda, the same behavior of afternoon clouds is found for July to September, but the effect is much smaller. Cloud cover is much higher in February to May compared to June to August, and during November to January the number of cloudy cases around noon is higher than in the afternoon. Please, take the note given above into account and do not worry about the early morning in winter peak.

Missour on the other hand has the afternoon peak in all months and not only during summer. Again, do not take the morning peak in winter months seriously.

Erfoud has a more similar pattern over the months to Noor. During April to October an increase of cloud cases in the afternoon is observed, while in winter and spring months the dependence over time of the day is not visible. Especially the increase of cirrus cases in September to November is similar to the Noor situation.

The same applies for Zagora, which has an afternoon increase of cloud situations during April to October. Nevertheless, the dependency of the time of the day in June to September is not as strong as in Noor.

Finally, Tan-Tan is an example of a complete different seasonal pattern. Here we see a decrease of cloud situations over the time of the day. Thin cirrus clouds occur mostly only in winter months while there are frequent in Noor during August to May.

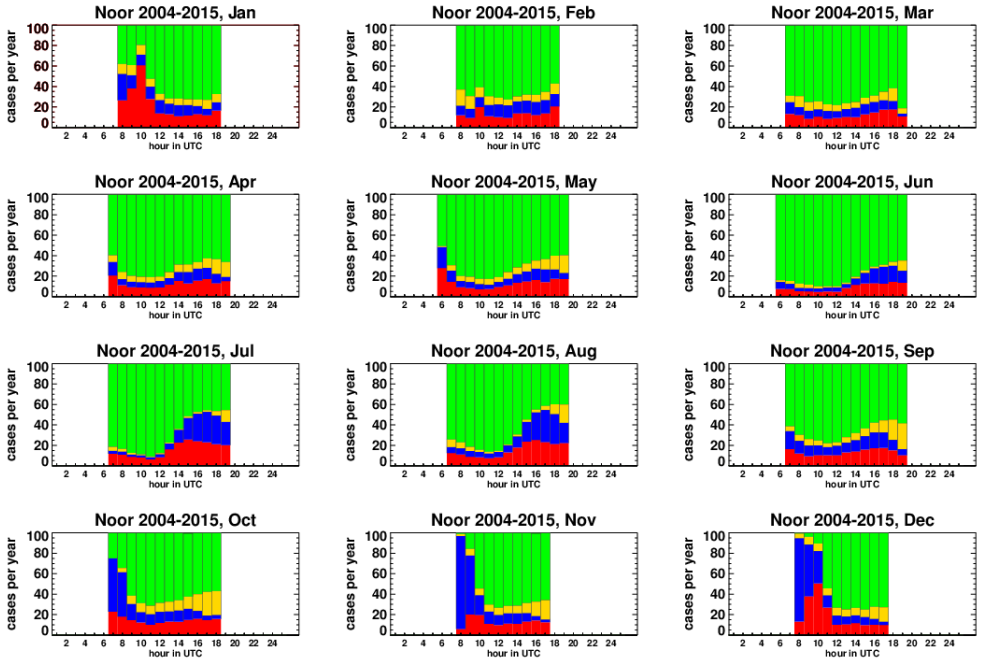

Figure 2.53 Cloud statistics Noor station: cloud area type (red = scattered water/mixed phase; blue = broken/overcast water/mixed phase; yellow = thin ice phase; green = clear; dark green = snow); frequency of occurrence in percentage of all daytime satellite images; split into calendar month and hours of the day; based on 2004-2015. PLEASE NOTE COMMENT ABOUT MORNING HOURS IN WINTER MONTHS MADE ABOVE.

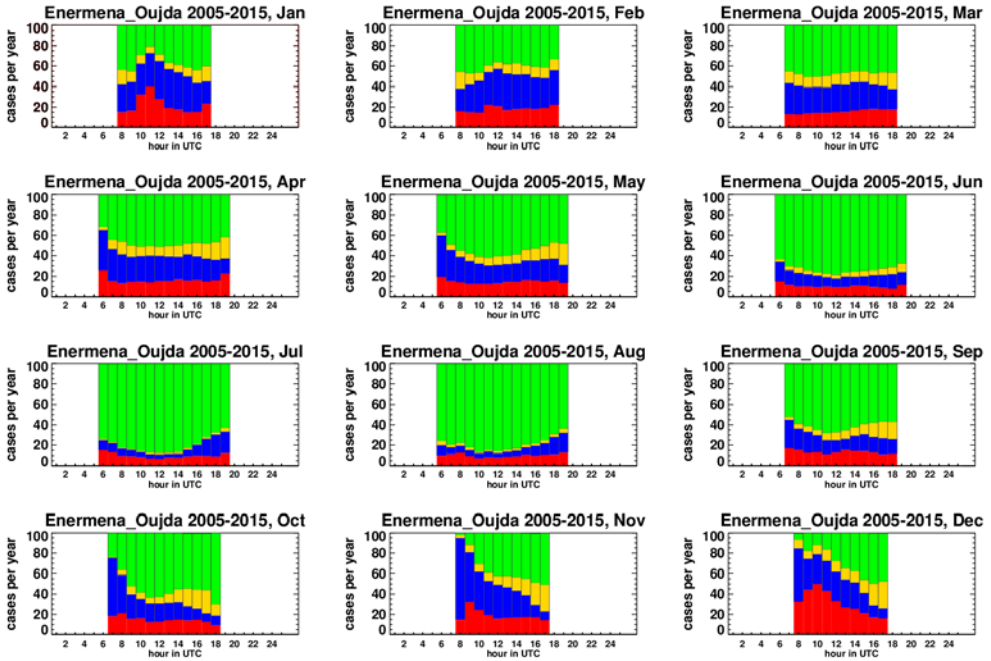

Figure 2.54 Cloud statistics EnerMENA Oujda station: cloud area type (red = scattered water/mixed phase; blue = broken/overcast water/mixed phase; yellow = thin ice phase; green = clear; dark green = snow); frequency of occurrence in percentage of all daytime satellite images; split into calendar month and hours of the day; based on 2004-2015. PLEASE NOTE COMMENT ABOUT MORNING HOURS IN WINTER MONTHS MADE ABOVE.

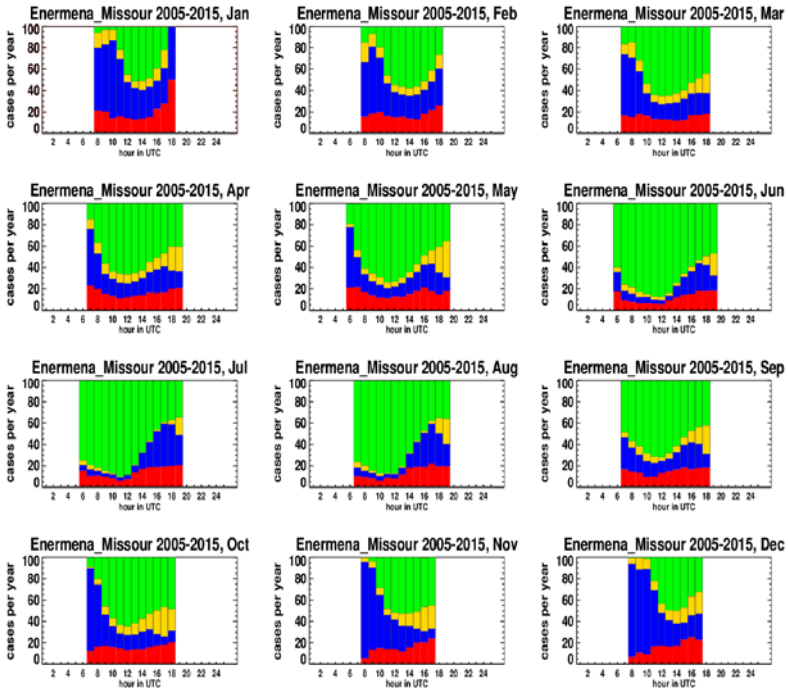

Figure 2.55 Cloud statistics EnerMENA Missour station: cloud area type (red = scattered water/mixed phase; blue = broken/overcast water/mixed phase; yellow = thin ice phase; green = clear; dark green = snow); frequency of occurrence in percentage of all daytime satellite images; split into calendar month and hours of the day; based on 2004-2015. PLEASE NOTE COMMENT ABOUT MORNING HOURS IN WINTER MONTHS MADE ABOVE.

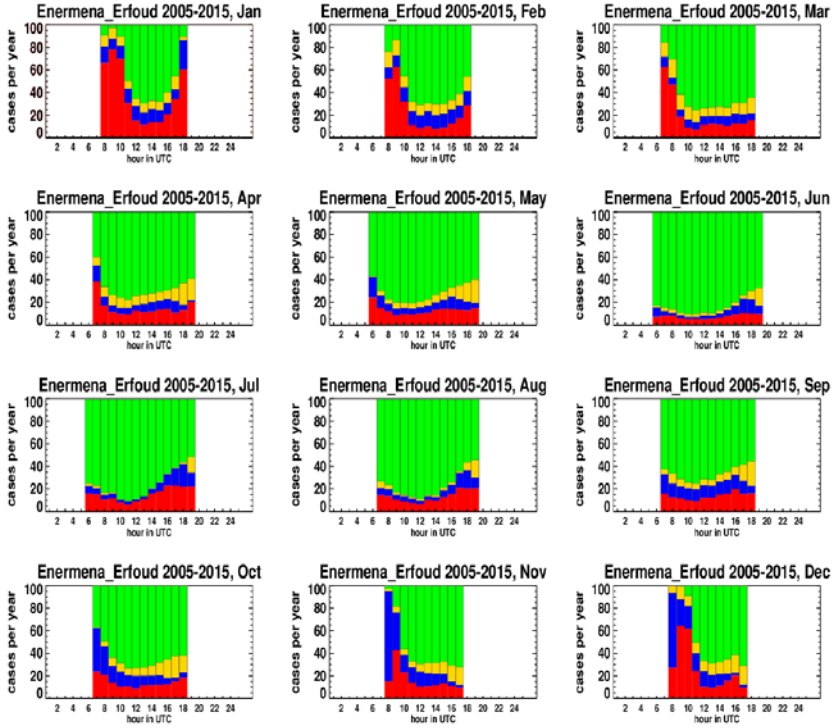

Figure 2.56 Cloud statistics EnerMENA Erfoud station: cloud area type (red = scattered water/mixed phase; blue = broken/overcast water/mixed phase; yellow = thin ice phase; green = clear; dark green = snow); frequency of occurrence in percentage of all daytime satellite images; split into calendar month and hours of the day; based on 2004-2015. PLEASE NOTE COMMENT ABOUT MORNING HOURS IN WINTER MONTHS MADE ABOVE.

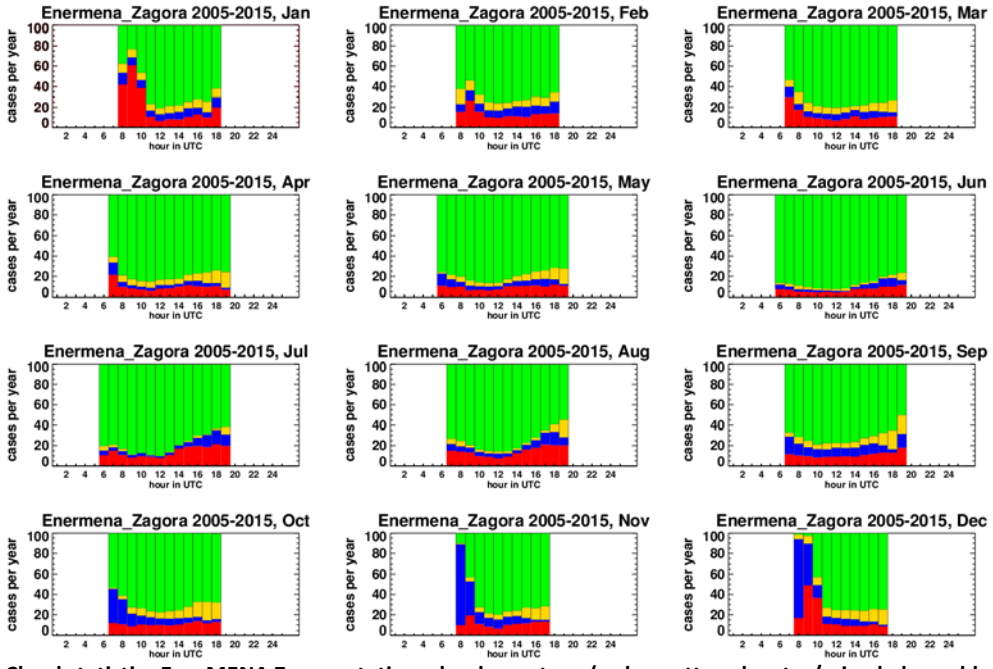

Figure 2.57 Cloud statistics EnerMENA Zagora station: cloud area type (red = scattered water/mixed phase; blue = broken/overcast water/mixed phase; yellow = thin ice phase; green = clear; dark green = snow); frequency of occurrence in percentage of all daytime satellite images; split into calendar month and hours of the day; based on 2004-2015. PLEASE NOTE COMMENT ABOUT MORNING HOURS IN WINTER MONTHS MADE ABOVE.

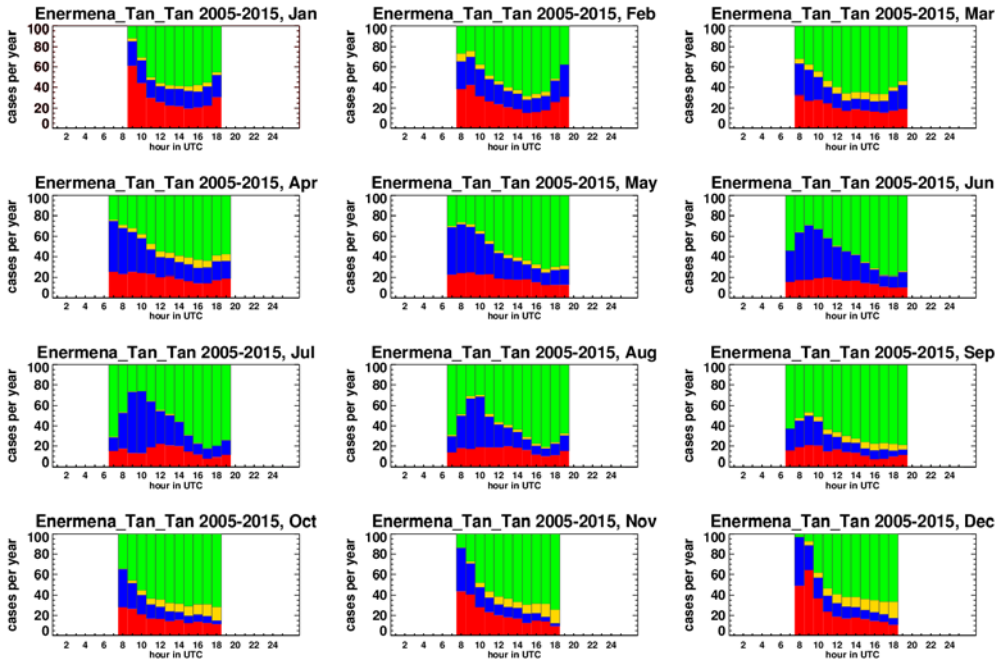

Figure 2.58 Cloud statistics EnerMENA Tan Tan station: cloud area type (red = scattered water/mixed phase; blue = broken/overcast water/mixed phase; yellow = thin ice phase; green = clear; dark green = snow); frequency of occurrence in percentage of all daytime satellite images; split into calendar month and hours of the day; based on 2004-2015. PLEASE NOTE COMMENT ABOUT MORNING HOURS IN WINTER MONTHS MADE ABOVE.

Having discussed some seasonal and daily cycles which are different at the 6 stations, we now combine the monthly and hourly plots of all stations (Fig 2.59 and 2.60).

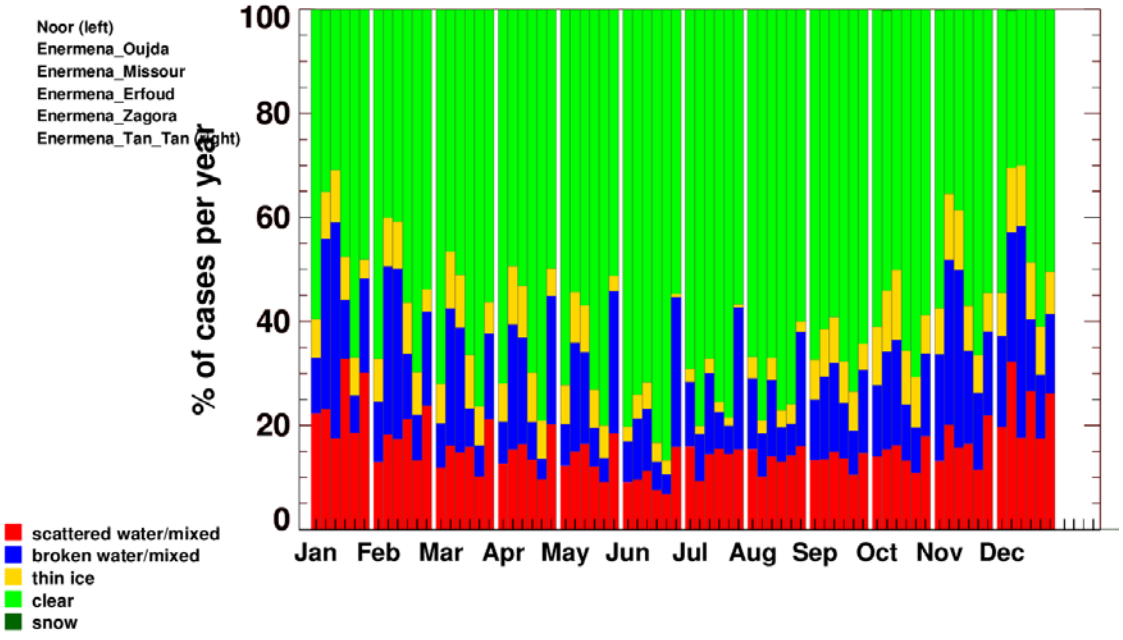

Figure 2.59 Cloud statistics of Noor and 5 EnerMENA stations: cloud area type; relative frequency of occurrence over months; split into scattered, broken/overcast, thin ice, clear and snow cases; based on 2004-2015.

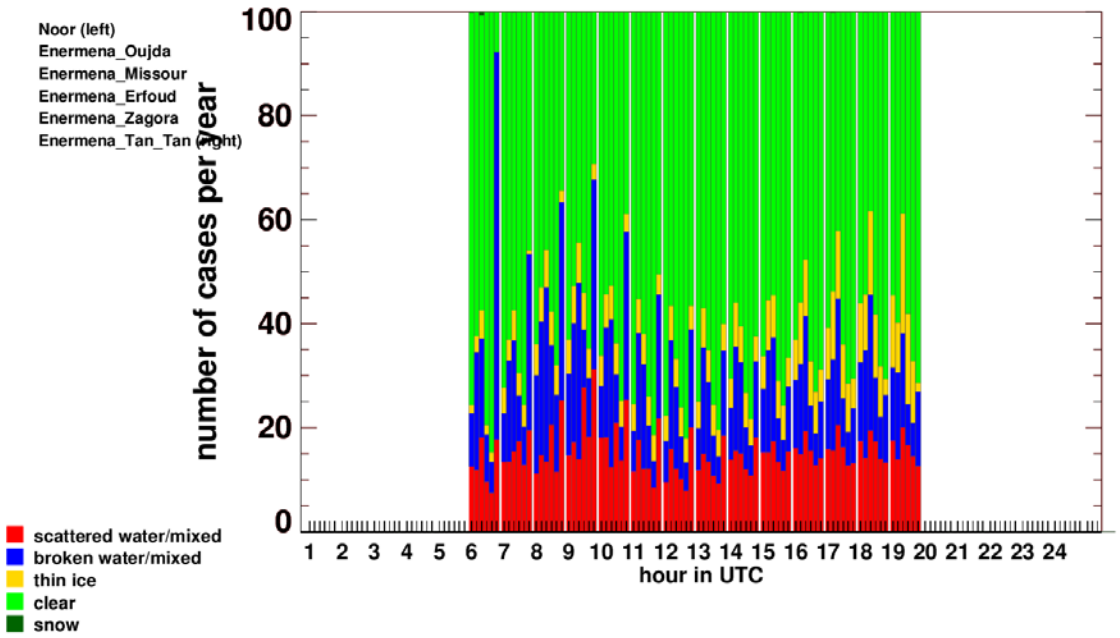

Figure 2.60 Cloud statistics of Noor and 5 EnerMENA stations: cloud area type; relative frequency of occurrence over hours of the day; split into scattered, broken/overcast, thin ice, clear and snow cases; based on 2004-2015.

And finally, the duration of cloud periods inside a day is evaluated. We separate in optically thick (DNI < 200 W/m2) and optically thin (DNI reduced) cases. Based on these numbers none of the stations is very close to Noor in all characteristics. The values being closest to the Noor site are marked in green, the station with the best agreement is Erfoud. Zagora shows good agreement with respect to the 90 and 98% percentiles, but not with respect to the short-term cloud duration.

Table 12: Length of cloud periods occurring in a day – optically thick clouds

Station	% of cloud< periods <= 15 min duration	% of cloudy periods <=1 hour duration	90% of cloud periods are <= X hours	98% of cloud periods are <= X hours
Noor	**28.55**	**58.44**	**4.0**	**8.5**
Oujda	27.92	57.11	6.0	10.25
Missour	24.94	52.42	4.75	9.0
Erfoud	30.5	60.8	3.5	8.75
Zagora	32.60	64.92	3.0	8.0
Tan Tan	31.31	61.33	4.75	9.75

Table 13: Length of cloud periods occurring in a day – optically thin clouds

Station	% of cloud< periods <= 15 min duration	% of cloudy periods <=1 hour duration	90% of cloud periods are <= X hours	98% of cloud periods are <= X hours
Noor	**31.58**	**66.73**	**3.25**	**7.75**
Oujda	28.91	60.51	4.25	9.0
Missour	27.65	61.66	4.0	9.0
Erfoud	31.14	67.7	3.5	8.75
Zagora	34.79	71.70	2.75	7.0
Tan Tan	27.91	63.78	3.75	8.0

Please note: Due to the cloud overestimation in winter time in morning hours, the numbers of 90 and 98% percentiles are too large, but the relative agreement to each other is still valid information.

2.3.4 DNI variability conditions

DNI variability classes are derived based on MSG cloud parameters as described in section 1.3. Histograms of their frequency in 2005-2015 cases are given (Fig 2.61). Noor is characterized by a large number of no or small variation and cloud-free sky (class 1 and 2) or by no variation and cloudy sky (class 8). Class 2 is represented but significantly less than class 1 and as often as class 8. Class 2 is characterized by high DNI and small amplitude variability. Very variable conditions (classes 4 and 6) and medium variable conditions (classes 3, 5, and 7) are less frequent. This is confirmed by the 2nd best fitting class (Fig. 2.29) where classes 2 and 7 are most frequent.

With respect to the variability classes Zagora is not very similar. It has many more class 1 and less variable class 2 to 7 conditions. Also, the low DNI and low variability class 8 is less frequent.

Erfoud has very similar occurrence of classes 5 and 8 and is among the most closest 3 for classes 1, 3, 4, 6,7. Oujda and Missour are also more similar than Zagora and finally, Tan-Tan shows completely different characteristics.

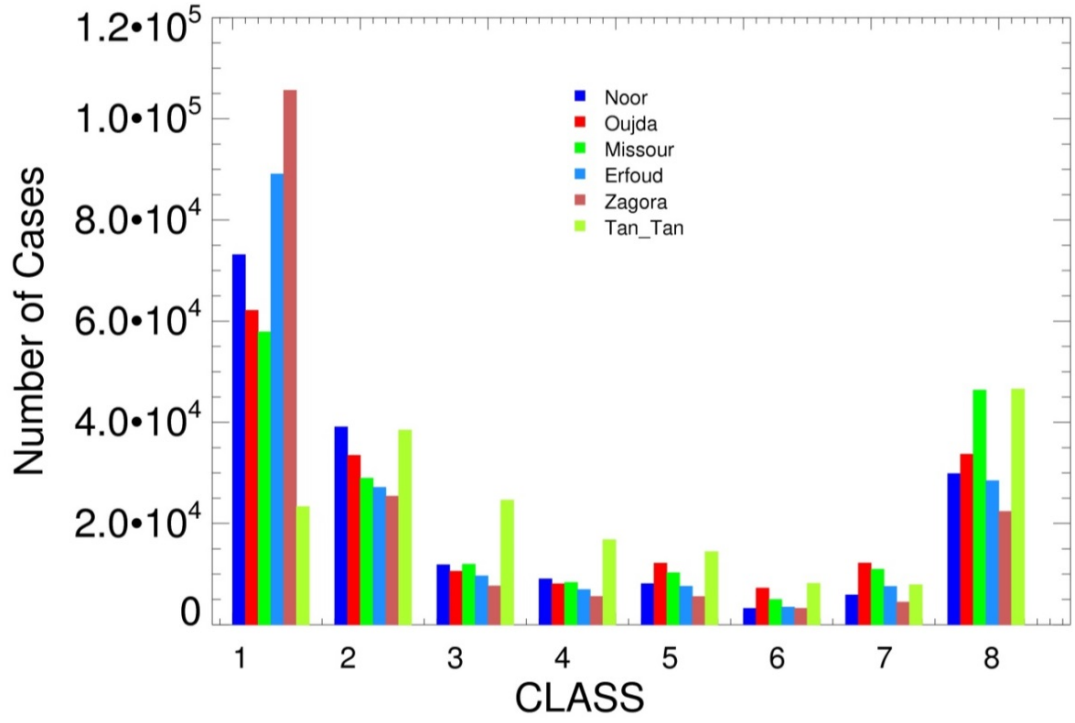

Figure 2.61 DNI variability class statistics of Noor and 5 EnerMENA stations based on 2004-2015.

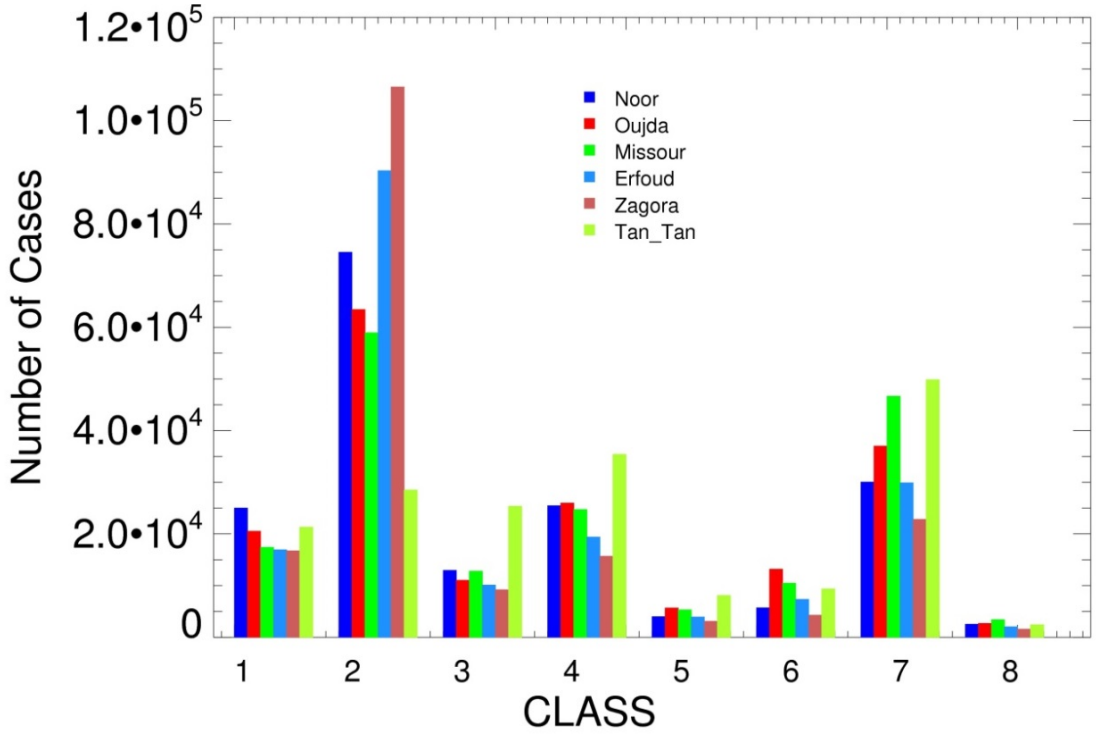

Figure 2.62 DNI variability class statistics of Noor and 5 EnerMENA stations based on 2004-2015. The 2nd best fitting class is shown.

2.3.5 Aerosol conditions

For Morocco, only AERONET stations Saada (31.626N, 8.156 W) and Oujda have sufficient long data records to provide an assessment. As seen on the Iberian Peninsula, the monthly distribution of strong AOD events between 0.5 and 1.0 and above 1.0 does not follow the general mean AOD seasonality.

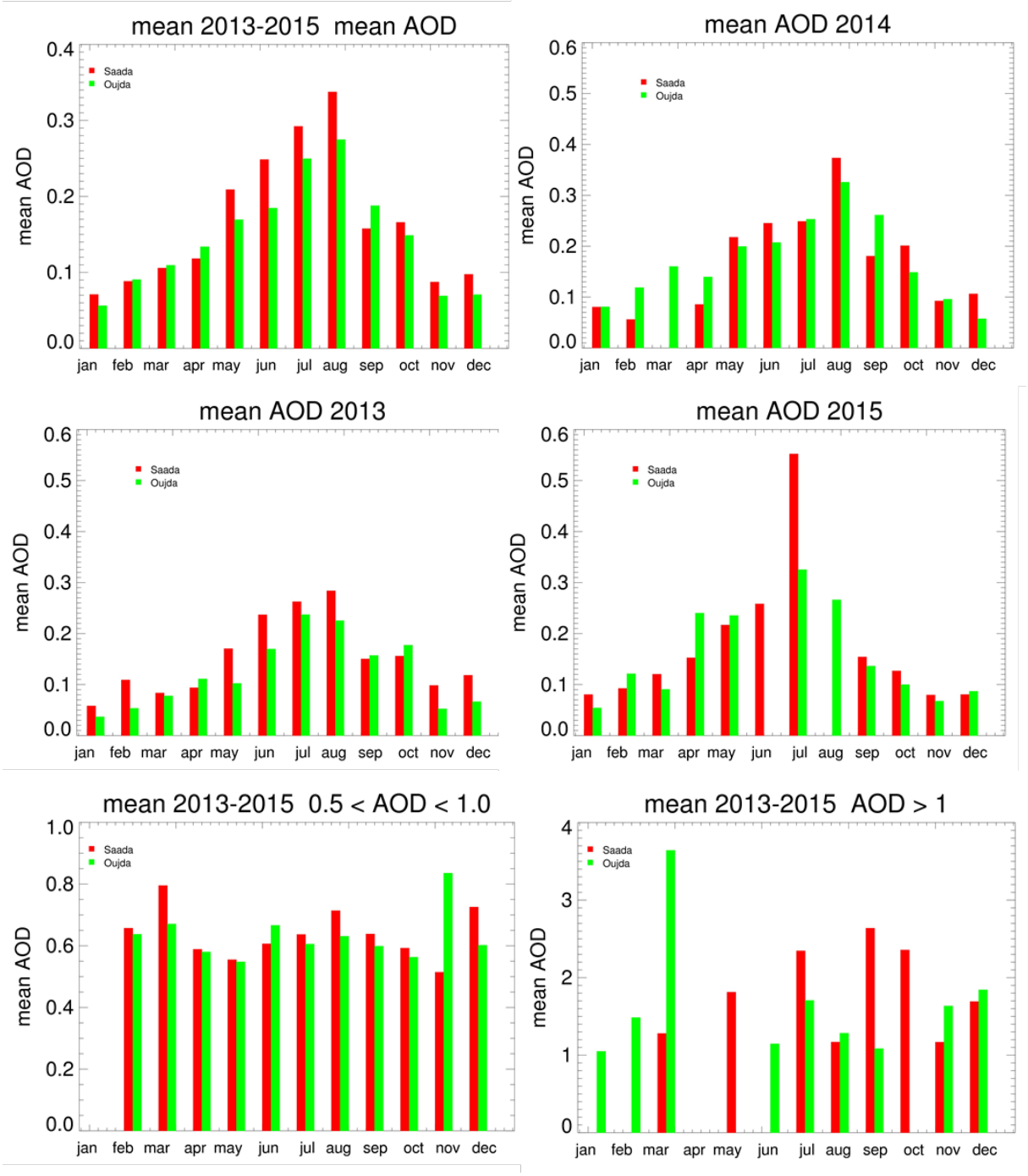

Fig 2.63: AERONET based mean aerosol optical depth (AOD) as found at stations Saada and Oujda. Average over 2013-2015 (upper left) and the individual years. In the lowest row, only AOD values between 0.5 and 1.0 (left) and AOD greater 1.0 (right) are evaluated.

2.3.6 Available meteo forecasts

Table 14: Available NWP datasets

Available deterministic models	ECMWF/ IFS	AROME/ HARMONIE (RUC3 from 2016 onwards; no Zagora)	ECMWF/ IFS + post-processing	AROME/ HARMONIE + post-processing; no Zagora	AROME/ HARMONIE RUC1 no Zagora
Available probabilistic models	ECMWF EPS	gSREPS	ECMWF EPS + post-processing	gSREPS + Post processing	

Legend: Green = available, red = not available, orange = available if effort or upcoming verification results allows

blue = available in EnerMena stations (**with exception of Zagora**)

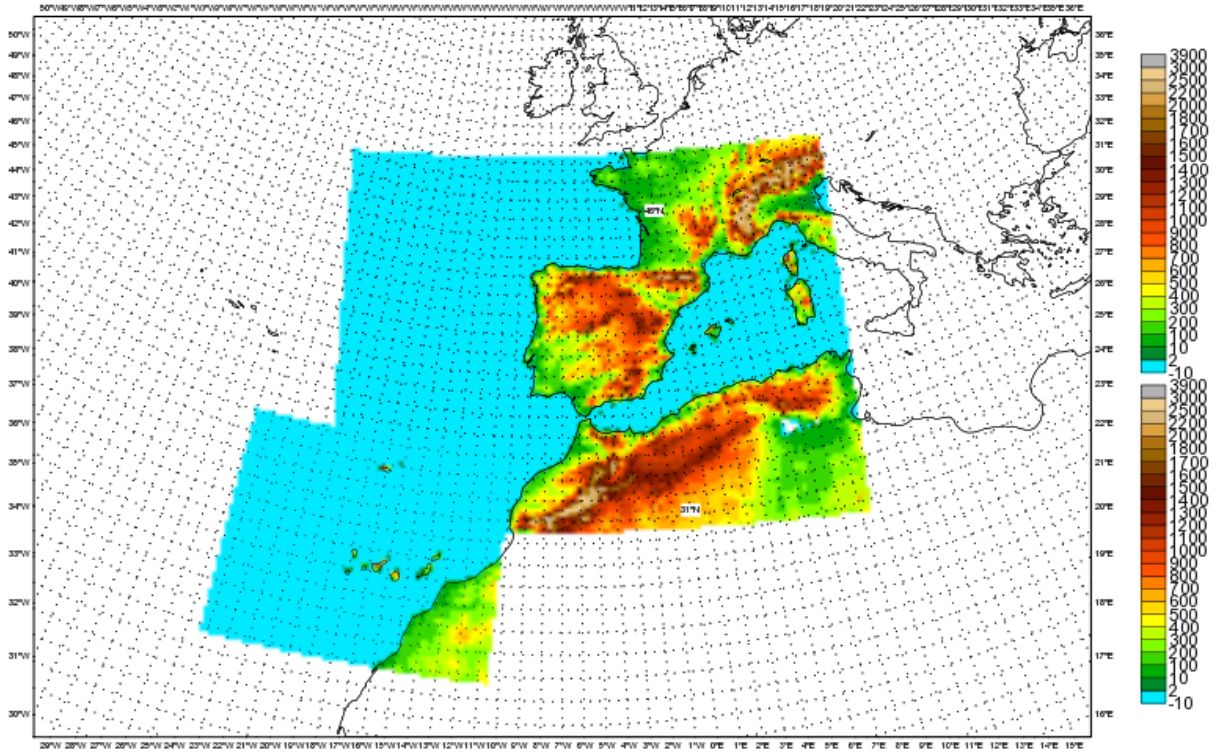

Figure 2.64: AEMET AROME/HARMONIE forecast region

2.4 Chile

2.4.1 Available ground observations

Measured solar irradiance data by the Ministry of Energy of Chile (available online)

The Ministry of Energy of Chile together with the Deutsche Gesellschaft für Internationale Zusammenarbeit (GIZ) is operating a network of wind and solar radiation measuring stations in northern Chile. The objective of this measurement campaign is to better understand the characteristics of these resources in northern Chile. It is not intended in this measurement campaign to obtain quality data that meets the highest standards, but reliable, consistent and comparable data. In this network there are 10 stations, detailed in the following table and shown in the following map:

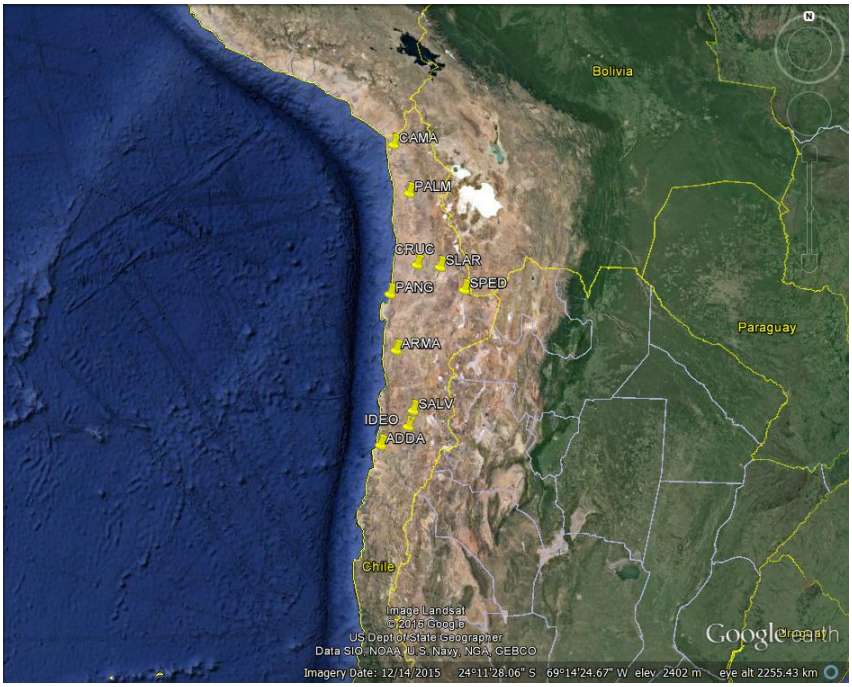

Figure 2.65 Location of GIZ stations in Chile. Based on GoogleMaps as background.

Table 15: Station information Chile

Station (code)	Start	end	latitude	longitude	Elevation (m)
Inca de Oro (IDEO)	2010-03-26	2013-04-10	26.75°S	69.91°W	1541
Pampa Camarones (CAMA)	2010-01-27	2013-04-08	18.86°S	70.22°W	795
Aerodromo Salvador (SALV)	2010-08-09	2013-02-21	26.31°S	69.75°W	1617
Armazones (ARMA)	2010-10-30	2013-05-04	24.63°S	70.24°W	2581
Crucero (CRUC)	2009-08-28	2013-05-02	22.27°S	69.57°W	1176
Salar (Chuquicamata) (SLAR)	2010-05-20	2013-01-01	22.34°S	68.88°W	2407
Punta Angamos (PANG)	2010-05-16	2013-05-04	23.07°S	70.39°W	24.07

Pozo Almonte (PALM)	2008-08-01	2013-05-02	20.26°S	69.78°W	1024
Aeropuerto Copiapo (ADDA)	2013-02-23	2013-05-05	27.26°S	70.78°W	210
San Pedro de Atacama (SPED)	2009-05-15	2013-05-06	22.98°S	68.16°W	2390

These stations measures GHI, and tracked global and diffuse solar irradiances. The calculation of DNI by these quantities has led to acceptable DNI daily profiles in summer months (figure 2.66, left) but unrealistic DNI daily profiles in winter months (figure 2.66, right).

Consequently, quality tests applied (detailed in Annex B) are reduced to

- Control of the data recording time
- Visual inspection of solar radiation components (in measured GHI and calculated DNI).
- Quality control tests of the BSRN: Physically Possible and Extremely Rare tests (in measured GHI and calculated DNI).

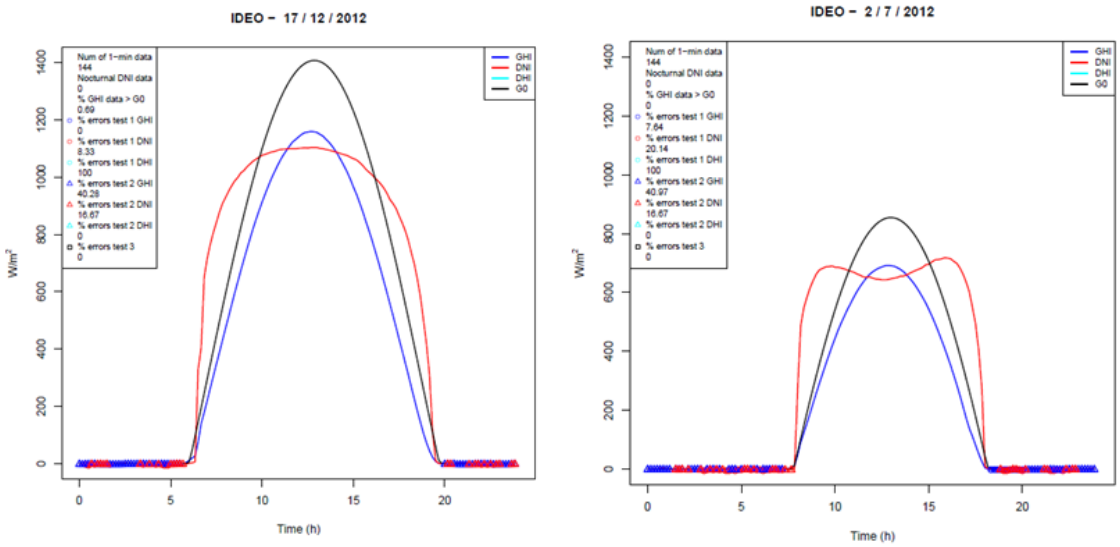

Figure 2.66 Location of GIZ stations in Chile. Based on GoogleMaps as background.

Below are detailed the main characteristic of these stations, their data availability and quality:

1. Inca de Oro (IDEO)

This station measures GHI and tracked global and diffuse solar irradiance with the following instruments:

Instrument	Model	Variables
Pyranometer	Kipp & Zonen (CMP11)	Tracked diffuse irradiance
Pyranometer	Kipp & Zonen (CMP11)	Tracked global irradiance
Pyranometer	Kipp & Zonen (CMP11)	GHI

In IDEO station, data are available from 2010-03-26 to 2013-04-10, with a gap between 2012-02-26 to 2012-06-30. Daily evaluation of QC tests can be made available on request.

GHI measurements show a low number of QC errors, and also good visually performance (except for several days between October and November 2011, where a non-realistic GHI dynamics are found at the beginning of the day). DNI calculated values show also a low number of QC errors, but a good visually performance only in summer months.

2. Pampa Camarones (CAMA)

This station measures GHI and both tracked global and diffuse solar irradiance with the following instruments:

Instrument	Model	Variables
Pyranometer	Kipp & Zonen (CMP11)	Tracked diffuse irradiance
Pyranometer	Kipp & Zonen (CMP11)	Tracked global irradiance
Pyranometer	Kipp & Zonen (CMP11)	GHI

In CAMA station, data are available from 2010-01-27 to 2013-04-08. Daily evaluation of QC tests can be made available on request.

GHI measurements show a low number of QC errors, and also good visually performance (except for spare days in 2012, where a non-realistic GHI dynamics are found at the beginning of the day). DNI calculated values show also a low number of QC errors, but a good visually performance only in summer months.

The rest of the stations show a similar behavior to the observed in these stations. Therefore, we do not investigate this instrument network any further.

Measured solar irradiance data by PUC-FONDEF (not available online)

A research project financed through FONDEF (El Fondo de Fomento al Desarrollo Científico y Tecnológico, run within the Ministerio de educación, Chile) has deployed a network of 13 ground stations starting in January 2010. 4 of these stations are designed and operated under BSRN standards, being the remaining 9 of three different rotating shadow band radiometer configurations. This network has the objective of supplying data that satisfies international standards and criteria for design, operation and maintenance. The name, type, and start date of operation for the stations are shown in the following table (the map shows the approximate location of the ground stations of this network).

Station	Type	Start date
Arica	RSBR	01/08/2011
Pozo Almonte	RSBR	04/04/2012
Patache	RSBR	16/01/2013
Sur Viejo	RSBR	07/07/2011
Crucero	RSBR	16/01/2012
Coya Sur	RSBR	05/07/2011
San Pedro	Sun Tracker	03/12/2010*
El Tesoro	RSBR	01/01/2009
Diego de Almagro	RSBR	02/08/2011
Santiago	Sun Tracker	22/12/2010
Curico	Sun Tracker	01/06/2012
Talca	Sun Tracker	09/08/2012
Marimaura	RSBR	12/07/2012

** Operation finished 04/07/2011.*

Figure 2.67 Location of FONDEF stations in Chile (Escobar et al., 2015).

The Type of stations is detailed below:

- *Sun Tracker* stations

  Although these stations are not part of BSRN, their operation follows its main guidelines. They are composed of sun trackers, sun sensors for accurate positioning, pyranometers, heating and ventilation units, pyrgeometers, pyrheliometers, UV meters, and also temperature, atmospheric pressure, relative humidity, wind speed and direction sensors, all connected to data loggers, with power supply from the grid.

- *RSBR* stations

  Their basic configuration includes photoelectric radiometers, a motor controller and rotating shadow band, temperature, atmospheric pressure, relative humidity, wind speed and direction sensors, all connected to data loggers, with power supply from a small-scale PV system. A second configuration lacks all meteorological sensors, for use in locations that already have a meteorological. A third configuration is similar to the first one, with the addition of a thermopile pyranometer for a redundant measurement of global horizontal radiation, which is used at sites where radiation conditions are particularly interesting and where local personnel is readily available for maintenance and cleaning of the thermopile pyranometer.

Some remarks on the solar resource of Chile are drawn below (Fig. 2.68):

- Crucero, with a yearly DNI measured in 2012 of 3389 kW h/m2 is one of the top solar resource worldwide sites. Several regions of northern Chile share these high DNI values. In Crucero, there are a large number of days with high DNI during most of the day, with only a few low-DNI days occurring during altiplanic winter and seasonal winter.
- Alto Patache, is located on the edge of the region that rises from sea level up to 1000 m in less than 2 km from the coastal line (note that even if it is close to Crucero, is not located in the intermediate depression of Chile). Its yearly DNI is 1908 kW h/m2. Its climate is very similar to that shared by the major cities in northern Chile and thus useful to gain insight on the potential for solar energy supply to the residential and commercial sectors that concentrate most of the population. Northern coastal climate is characterized by clear skies from December to April, with presence of cloud cover which led to variability with decreased DNI the rest of the year.
- The solar resource variability in Santiago and Curico is higher than in Crucero, as they belong to a Mediterranean climate (characterized by occurrences of cloudy and clear days throughout the year with strong summer/winter seasonality). In winter, cloud covers are more common, days are shorter, and radiation levels are greatly reduced. The yearly totals are 1911 kW h/m2 for DNI in Santiago, and 1952 kW h/m2 for DNI in Curico.

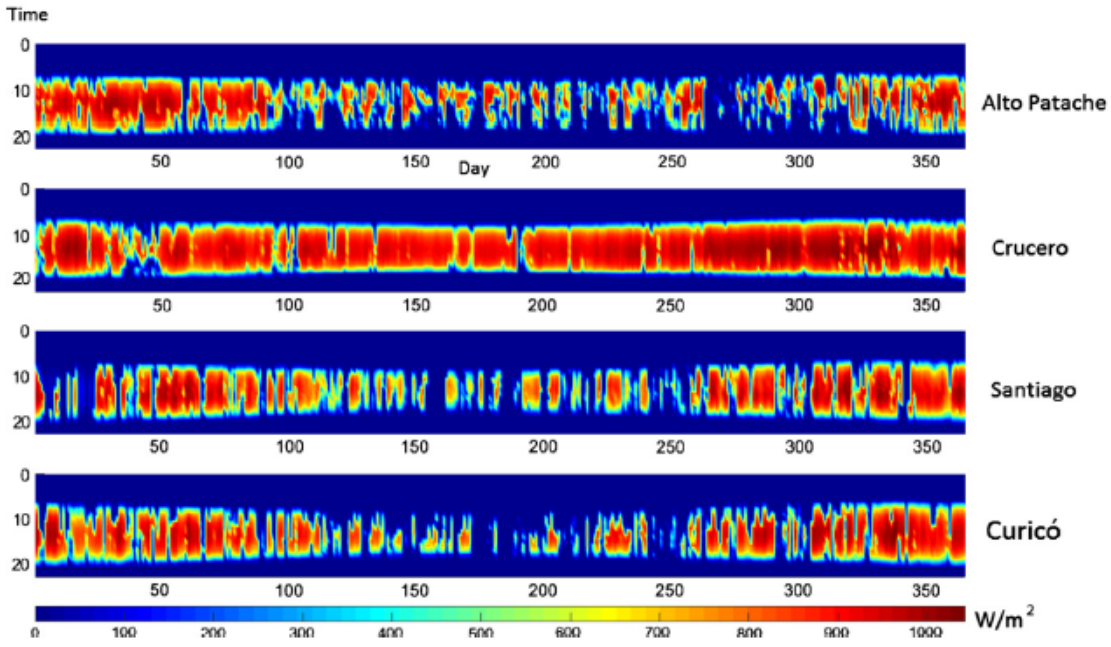

Figure 2.68 DNI daily totals from January to December 2012 at four different locations (Escobar et al., 2015)

Finally, it is interesting to note that even as the maximum distance between Crucero and Santiago is slightly less than 1600 km, in clear days the DNI has very similar profiles and maximum levels that are only slightly reduced by the effects of latitude and altitude. Thus, yearly total in Patache for DNI is closer to Santiago than to Crucero. This, even as Crucero and Patache are closely located, they show how the coastal and desert climates of northern Chile have very different solar resource availability.

2.4.2 Ground based irradiances

The FONDEF network has only recently be found by the PreFlexMS team after realizing the difficulties with the network operated by the Ministry of Energy of Chile. The complete ground data need to be ordered in the FONDEF network and will be analysed only later.

2.4.3 Cloud conditions

Due to missing satellite capabilities we have no information about typical cloud conditions in Chile as available for the other countries.

2.4.4 DNI variability conditions

Due to missing satellite capabilities we have no information about typical DNI variability conditions in Chile as available for the other countries.

2.4.5 Aerosol conditions

For Chile, only AERONET stations Arica (18.472S, 70.313 W) and Santiago_Beauchef (33.457S, 70.662 W) have sufficient long data records to provide an assessment. Different to the Iberian Peninsula, the monthly distribution of AOD in Chile shows less seasonality. Nevertheless, the distribution of strong AOD events between 0.5 and 1.0 and above 1.0 does not follow the general mean AOD pattern.

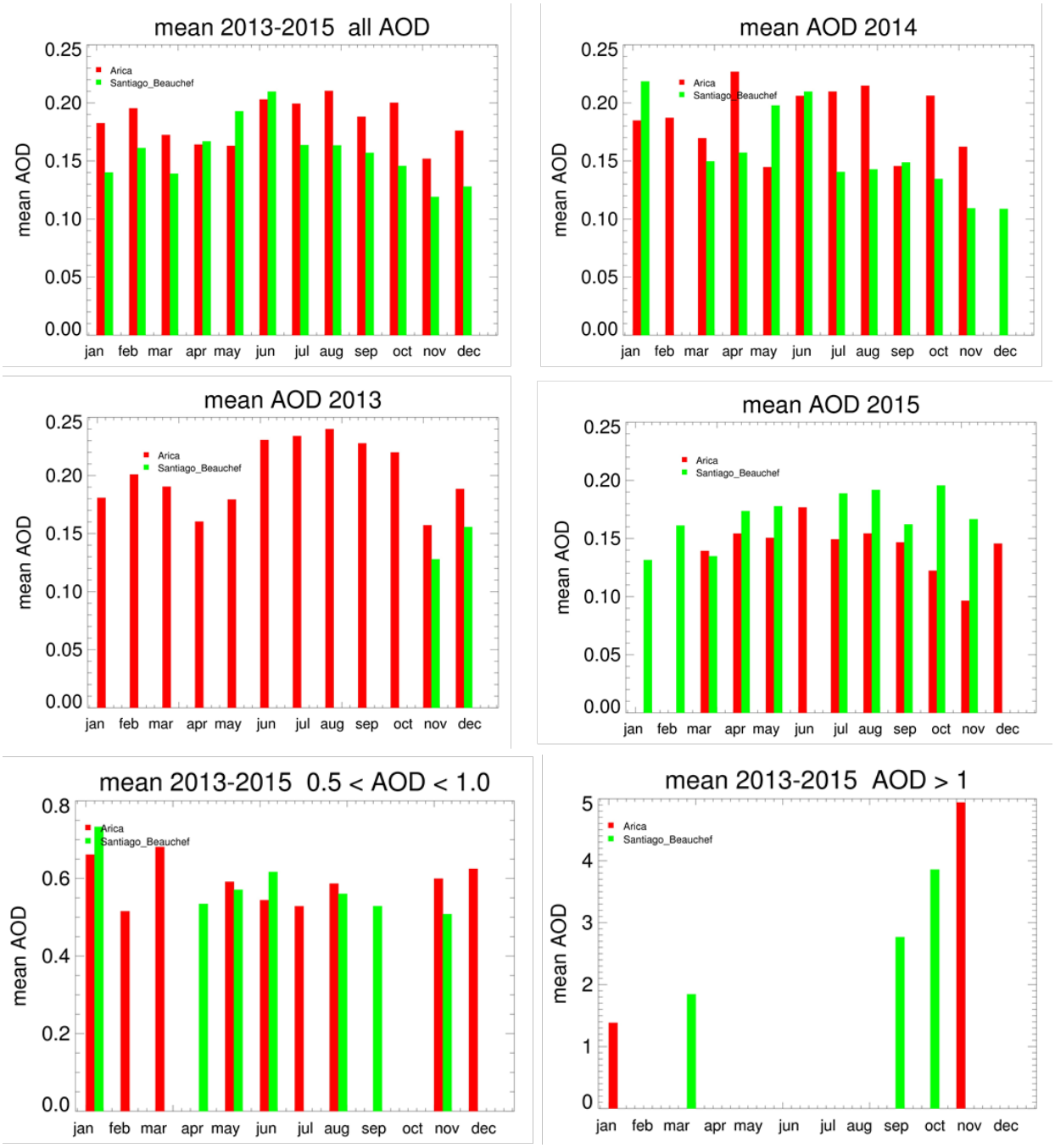

Fig 2.76: AERONET based mean aerosol optical depth (AOD) as found at stations Arica and Santiago Beauchef. Average over 2013-2015 (upper left) and the individual years. In the lowest row, only AOD values between 0.5 and 1.0 (left) and AOD greater 1.0 (right) are evaluated.

2.4.6 Available meteo forecasts

Table 16: Available NWP datasets

Available deterministic models	ECMWF/ IFS	AROME/ HARMONIE (RUC3 from 2016 onwards)	ECMWF/ IFS + post-processing	AROME/ HARMONIE + post-processing	AROME/ HARMONIE RUC1
Available probabilistic models	ECMWF EPS	gSREPS	ECMWF EPS + post-processing	gSREPS + post-processing	

Legend: Green = available, red = not available, orange = available if effort or upcomings verification results allows

2.5 Saudi Arabia

2.5.1 Available ground observations

For Saudi-Arabia a number of stations is available, but they only provide data until 2002 or 2003.

Table 17: Station information Saudi Arabia

Name	Latitude (+N)	Longitude (+E)	Elevation (m)	Period	Pyrheliometer	Temporal resolution	Network	Comments
Solar Village	24.91	46.41	650	1998-08-01 to 2002-12-12	Eppley NIP		BSRN	Data available in BSRN website
Abha	18.23	42.66	2039	1998-01-01 to 2003-01-31	Eppley NIP		NREL & KACST	Data available in rredc.nrel website
Al-Ahsa	25.30	49.48	178	1998-01-01 to 2003-01-31	Eppley NIP		NREL & KACST	Data available in rredc.nrel website
Gizan	16.90	42.58	7	1998-01-01 to 2003-01-31	Eppley NIP		NREL & KACST	Data available in rredc.nrel website
Qassim	26.31	43.77	647	1998-01-01 to 2003-01-	Eppley NIP		NREL & KACST	Data available in rredc.nrel website

				31				
Jeddah	21.68	39.15	4	1998-01-01 to 2003-01-31	Eppley NIP		NREL & KACST	Data available in rredc.nrel website
Al-Madinah	24.55	39.70	626	1998-01-01 to 2003-01-31	Eppley NIP		NREL & KACST	Data available in rredc.nrel website
Al-Qaisumah	28.32	46.13	358	1998-01-01 to 2003-01-31	Eppley NIP		NREL & KACST	Data available in rredc.nrel website
Sharurah	17.47	47.11	725	1998-01-01 to 2003-01-31	Eppley NIP		NREL & KACST	Data available in rredc.nrel website
Al-Jouf	29.79	40.10	669	1998-01-01 to 2003-01-31	Eppley NIP		NREL & KACST	Data available in rredc.nrel website
Solar Village	24.91	46.41	650	1998-01-01 to 2003-01-31	Eppley NIP		NREL & KACST	Data available in rredc.nrel website
Tabouk	28.38	36.61	768	1998-01-01 to 2003-01-31	Eppley NIP		NREL & KACST	Data available in rredc.nrel website
Wadi Al-Dawaser	20.44	44.68	70	1998-01-01 to 2003-01-31	Eppley NIP		NREL & KACST	Data available in rredc.nrel website

Due to the station data availability before 2003, the ECMWF forecasts are only available in a model version which is not valid anymore. Schroedter-Homscheidt et al. (2016a) has shown, that the results in biases have dramatically changed in 2003. Therefore, making an assessment of pre-2003 forecasts is not representative anymore. The following figures 2.77 to 2.79 are taken from this paper. Before October 2003, the ECMWF had strong negative biases and RMSE was also much larger than for more recent years. Station names used in these plots are given in Tab. 18.

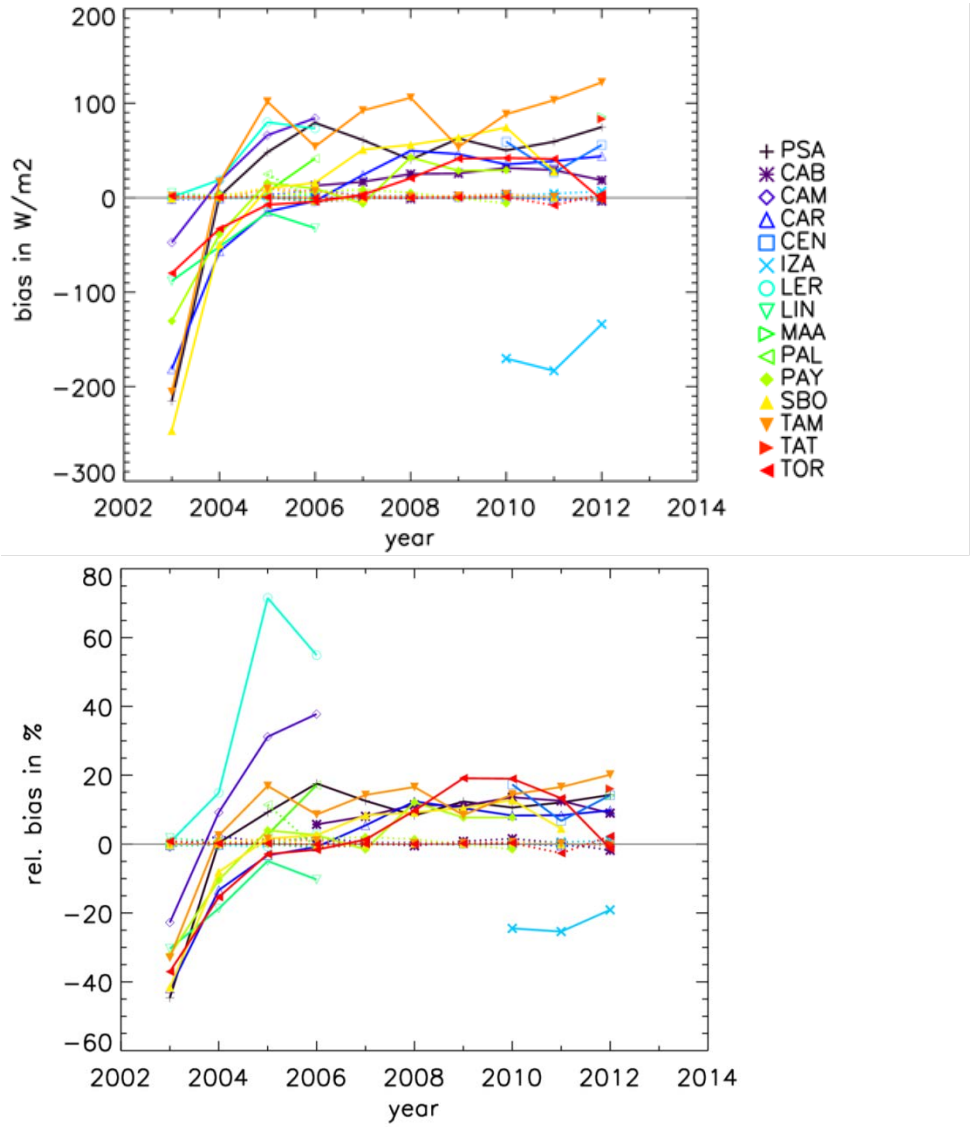

Figure 2.77. Day ahead hourly DNI forecast verification – annual absolute and relative bias of ECMWF/IFS (line) together with two-day persistence (dotted). This is Fig. 4 from Schroedter-Homscheidt et al. (2016a).

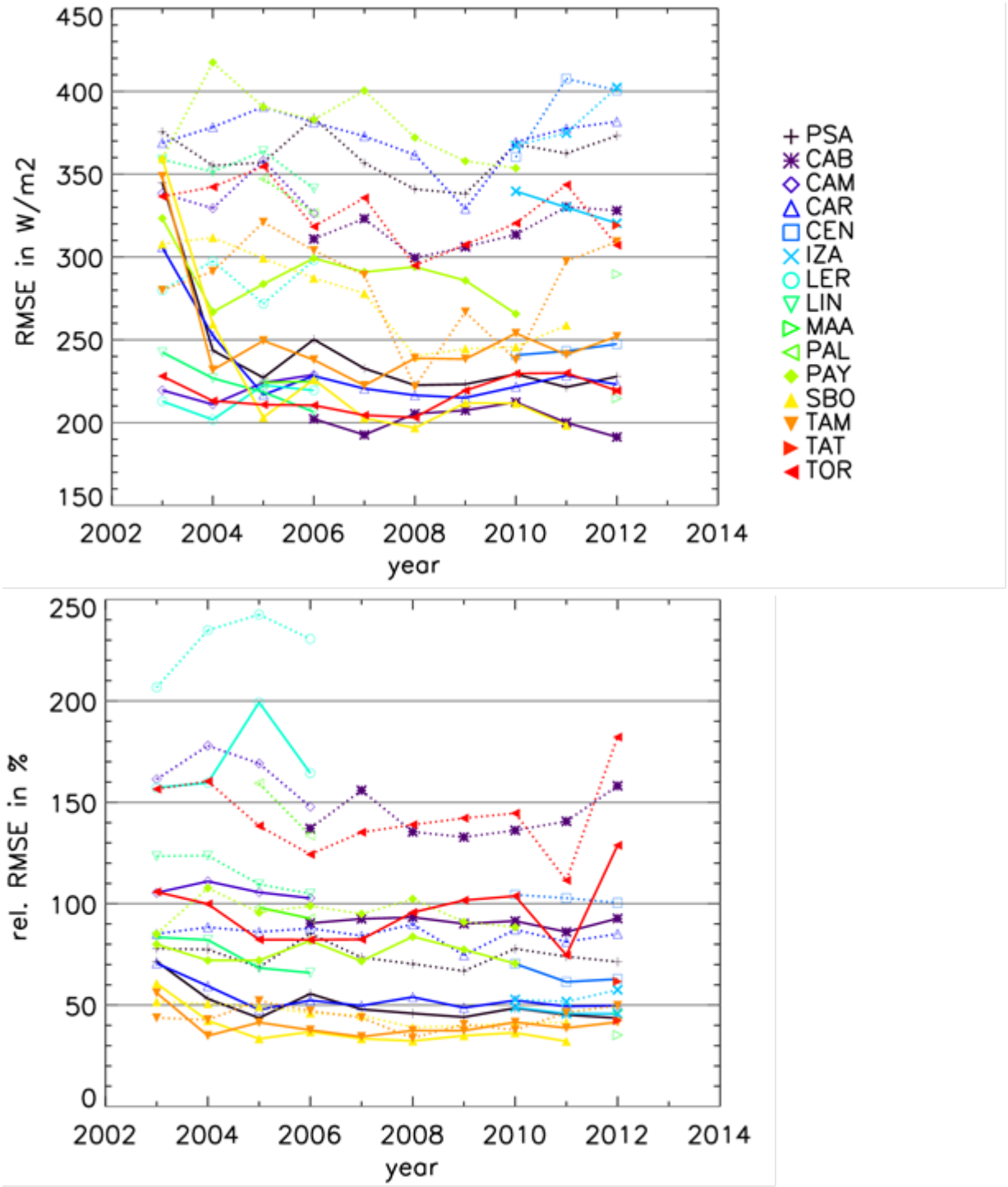

Figure 2.78. Day ahead hourly DNI forecast verification – annual absolute and relative RMSE of ECMWF/IFS (line) together with two-day persistence (dotted). This is Fig. 5 from Schroedter-Homscheidt et al. (2016a).

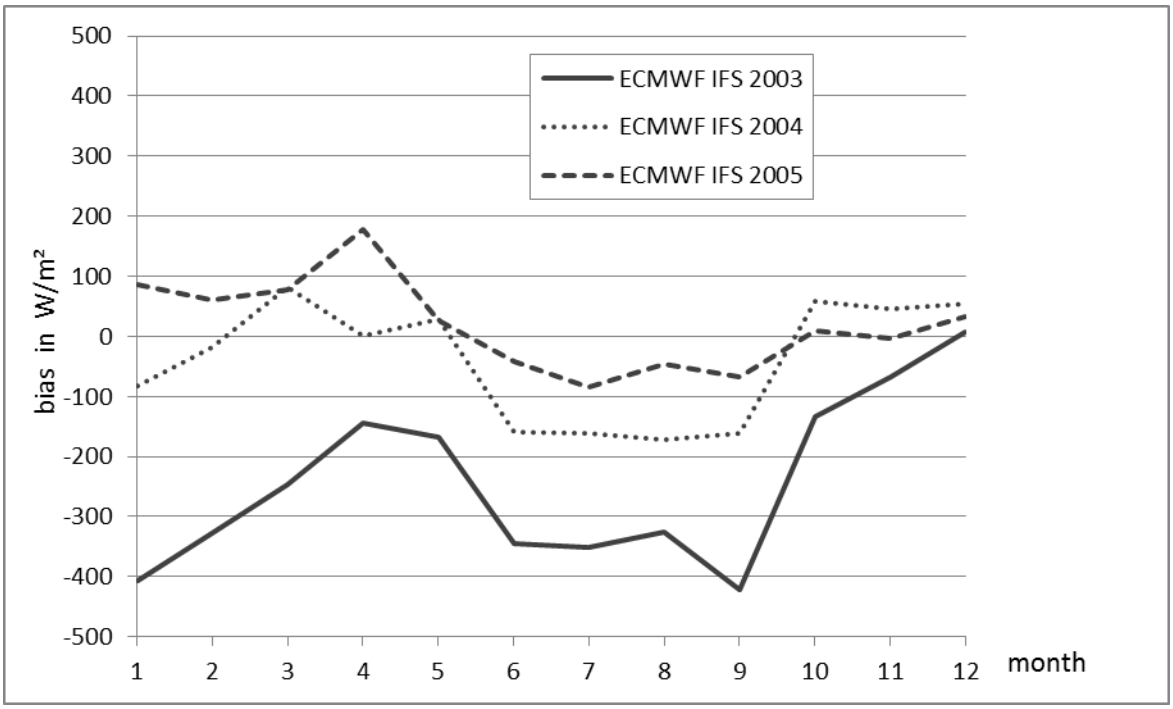

Figure 2.79. Day ahead hourly DNI forecast verification – monthly resolved absolute bias of ECMWF/IFS for the station SBO (IL) for 2003, 2004, and 2005. This is Fig. 6 from Schroedter-Homscheidt et al. (2016a).

Table 18. Details of ground stations used in in Schroedter-Homscheidt et al. (2016a)

Name	Code	Lat. (°)	Lon (°)	Elev (m)
DLR/PSA	PSA (E)	37.091	-2.358	492
Cabauw (BSRN)	CAB (NL)	51.971	4.927	0
Camborne (BSRN)	CAM (UK)	50.217	-5.317	88
Carpentras (BSRN)	CAR (F)	44.083	5.059	100
Cener (BSRN)	CEN (E)	42.816	-1.601	471
Izana (BSRN)	IZA (E)	28.309	-16.499	2373
Lerwick (BSRN)	LER (UK)	60.133	-1.183	84
Lindenberg (BSRN)	LIN (D)	52.210	14.122	125
Maan (EnerMena)	MAA (JO)	30.172	35.8183	1012
Palaiseau (BSRN)	PAL (F)	48.713	2.208	156
Payerne (BSRN)	PAY (CH)	46.815	6.944	491
Sede Boquer (BSRN)	SBO (IL)	30.905	34.782	500
Tamanrasset (BSRN)	TAM (DZ)	22.780	5.510	1385
Tataouine (EnerMENA)	TAT (TN)	32.9741	10.4851	210
Toravere (BSRN)	TOR (EE)	58.254	26.462	70

2.5.2 Irradiances

As we already have discussed that there are no representative forecasts available for the observation period, we do not perform any further evaluation of these locations.

2.5.3 Cloud conditions

As we already have discussed that there are no representative forecasts available for the observation period, we do not perform any further evaluation of these locations.

2.5.4 DNI variability conditions

As we already have discussed that there are no representative forecasts available for the observation period, we do not perform any further evaluation of these locations.

2.5.5 Aerosol conditions

As we already have discussed that there are no representative forecasts available for the observation period, we do not perform any further evaluation of these locations.

2.5.6 Available meteo forecasts during ground observation period

Table 19: Available NWP datasets

Available deterministic models	ECMWF/ IFS	AROME/ HARMONIE (RUC3 from 2016 onwards)	ECMWF/ IFS + post-processing	AROME/ HARMONIE + post-processing	AROME/ HARMONIE RUC1
Available probabilistic models	ECMWF EPS	gSREPS	ECMWF EPS + post-processing	gSREPS + post-processing	

Legend: Green = available, red = not available, orange = available if effort or upcoming verification results allows

3. Suggested validation sites

3.1 Rationale

The site Évora is pre-selected in PreFlexMS as the demonstration site. A detailed description of Évora versus other stations (Badajoz and PSA) on the Iberian Peninsula has been given in chapter 1.

In order to widen the geographical scope of knowledge on DNI forecasting, a number of stations is selected for the further validation work within WP4 (Task 4.4 Comparing forecasts) and in the interaction task between WP3 (dispatch optimizer) and WP4. The stations selected in this chapter will serve as 'virtual demo sites' in PreFlexMS.

The countries have been selected based on the PreFlexMS market analysis outcomes and GE priorities.

We want to find 3 stations separate to Évora as additional validation sites in

- Different climate conditions
- Different meteo forecast availability conditions

Please note: This is not only a question on different meteorological conditions. The selection process also should reflect the reality of different forecast options being available for real power plants. Therefore, having not all PreFlexMS forecasts available is not a show-stopper – it is even a good argument for a site, as in reality the user of the PreFlexMS technology wants to know how this performs in conditions with less advanced forecast capabilities in real life.

3.2 Availability of observations

Suitable stations are found based on:

1st criterion: They should have ground observations. This allows both the development of post-processing for forecasts as also the forecast verification.

2nd criterion: Ground observations should be available 2004 or later to cover the nowadays ECMWF forecast capabilities.

3rd criterion: They should provide extended site auditing information based on DNI, cloud and aerosol conditions. Such information is only available in the Meteosat Second Generation field of view, so, Europe, Africa, Middle East and parts of Brazil.

Table 20: Quick-look on stations with respect to the availability criteria

Country	Available observations	Observations after 2004	Extended site audit possible
Portugal	yes	yes	yes
Spain	yes	yes	yes
South Africa	yes	yes	yes
India	no	no	no
Morocco	yes	yes	yes
Chile	yes, but to be checked further	yes	no
Saudi Arabia	yes	no	yes

Based on these options, stations from South Africa, Morocco, and Chile are suggested.

3.3 NWP availability

In the following table we summarize the available NWP forecasts for all countries.

Table 21: Available NWP datasets

Iberian Peninsula	Deter-ministic	ECMWF/ IFS	AROME/ HARMONIE (RUC3 since 2016)	ECMWF/ IFS +PP	AROME/ HARMONIE + PP	AROME/ HARMONIE RUC1
	Proba-bilistic	ECMWF EPS	gSREPS	ECMWF EPS + PP	gSREPS + PP	
South Africa	Deter-ministic	ECMWF/ IFS	AROME/ HARMONIE (RUC3 since 2016)	ECMWF/ IFS + PP	AROME/ HARMONIE + PP	AROME/ HARMONIE RUC1
	Proba-bilistic	ECMWF EPS	gSREPS	ECMWF EPS + PP	gSREPS + PP	
India	Deter-ministic	ECMWF/ IFS	AROME/ HARMONIE (RUC3 since 2016)	ECMWF/ IFS +PP	AROME/ HARMONIE + PP	AROME/ HARMONIE RUC1
	Proba-bilistic	ECMWF EPS	gSREPS	ECMWF EPS + PP	gSREPS + PP	
Morocco	Deter-ministic	ECMWF/ IFS	AROME/ HARMONIE (RUC3 since 2016, no Zagora)	ECMWF/ IFS + PP	AROME/ HARMONIE + PP; no Zagora	AROME/ HARMONIE RUC1; no Zagora
	Proba-bilistic	ECMWF EPS	gSREPS	ECMWF EPS + PP	gSREPS + PP	
Chile	Deter-ministic	ECMWF/ IFS	AROME/ HARMONIE (RUC3 since 2016)	ECMWF/ IFS + PP	AROME/ HARMONIE + PP	AROME/ HARMONIE RUC1
	Proba-bilistic	ECMWF EPS	gSREPS	ECMWF EPS + PP	gSREPS + PP	
Saudi Arabia	Deter-ministic	ECMWF/ IFS	AROME/ HARMONIE (RUC3 since 2016)	ECMWF/ IFS + PP	AROME/ HARMONIE + PP	AROME/ HARMONIE RUC1
	Proba-bilistic	ECMWF EPS	gSREPS	ECMWF EPS + PP	gSREPS + PP	

Legend: Green = available, red = not available, orange = available if effort or upcoming verification results allows; blue = available in EnerMena stations (**with exception of Zagora**), PP = post-processing

3.4 Research questions

Based on the NWP data availability the following questions can and should be addressed by the dispatch optimizer developers and the meteorological forecast assessment team for the different countries:

Influence of the storage on error cancelling?

- In case of a power plant with storage, a low MAE is helpful, but over a number of hours the storage allows absolute errors to cancel out over a certain period. Does this occur in practice? If yes, the assessment of meteorological forecasts should take this into account into their metrics. (applicable in Évora, MA, ZA, CL)

Influence of aerosol forecasts?

- Having the dependency of CSP from only strong AOD events in mind, the evaluation of aerosol affected NWP forecast should be done for all cases as well as being concentrated on the strong AOD event cases only. An evaluation with respect to aerosols to all situations only may result in misleading outcomes.
  Based on the available AERONET observations, WP4 developers can perform evaluations for all cases, but also should restrict their evaluation with respect to aerosols to a number of relevant cases as being observed by AERONET. Results should be given for 'all AOD', 'AOD in 0.5 to 1.0' and 'AOD > 1.0' cases separately. (applicable in Évora)

Is higher spatial and temporal resolution of value?

- Does AROME/HARMONIE perform better than ECMWF/IFS? (applicable in Évora, MA)
- Does gSREPS perform better than ECMWF/EPS? (applicable in Évora)

Is a higher update frequency of value?

- Does AROME/HARMONIE RUC1 perform better than AROME/HARMONIE? (applicable in Évora, MA)

Is post-processing worth the effort?

- Does ECMWF/IFS + Post-Processing perform better than ECMWF/IFS only? (applicable in Évora, ZA, MA, CL)
- Does AROME/HARMONIE + Post-Processing perform better than AROME/HARMONIE only? (applicable in Évora, MA)
- Does ECMWF/EPS + Post-Processing perform better than ECMWF/EPS? (applicable in Évora, ZA, MA, CL)
- Does gSREPS + Post-Processing perform better than gSREPS? (applicable in Évora)

Is higher spatial and temporal resolution + post-processing of value?

- Does AROME/HARMONIE + Post-Processing perform better than ECMWF/IFS? (applicable in Évora, MA)

Is a probabilistic forecast of value?

- Does ECMWF/EPS perform better than ECMWF/IFS? (applicable in Évora, ZA, MA, CL)
- Does gSREPS perform better than AROME/HARMONIE? (applicable in Évora)

Which NWP approaches should be finally used?

- For tests in the demonstration phase (WP7) only one or two NWP approaches per station will be used. The dispatch optimization (WP3) and meteorological forecast assessment (WP4) need to make this recommendation as prerequisite for the virtual demo site testing in WP7.

3.5 Virtual demo site recommendation

Finally, we have to select a station in South Africa, Morocco, and Chile based on the analysis made in chapter 2.

South Africa

- Based on ground data quality control all stations are suitable.
- Stations RVD, VAN, SUT, GRT, UFS, and UPR have sufficiently long data records and are located in regions of interest for CSP.
- Comparing long-term satellite observations versus Upington, SUT and GRT are excluded and RVD and VAN have the highest similarity in monthly patterns.
- Stations RVD and VAN show a good agreement of CAMS satellite-based with the ground-based DNI observations.
- With respect to cloud/cloud-free statistics, RVD and VAN are most similar to Upington.
- With respect to the occurrence of optically thin cirrus clouds with highly variable and non-zero DNI values, VAN is similar to Upington.
- Both RVD and VAN show a very different cloud pattern over time of the year and over time of the day than Upington. With respect to these cloud patterns, the station UFS is more similar, but UFS shows generally higher DNI values than Upington and at UFS CAMS strongly overestimates DNI compared to the ground observations.
- With respect to the duration of optically thick clouds, the station RVD and UFS are more similar to Upington than the others.
- With respect to the duration of optically thin clouds, the station VAN and UFS are more similar to Upington than the others.
- With respect to DNI variability in the 1-min range, the stations RVD, VAN and SUT show the smallest amount of variable conditions, but still more such conditions than in Upington.
- We do not have any spatial observations of aerosol conditions.

Finally, we reduced the number of stations under evaluation to two: RVD and VAN. **Setting priority on the duration and availability of ground observations and the availability of consistent CAMS long-term observations we suggest using station VAN (Vanrhynsdorp) further. This allows validating forecasts for 2013-2016 against ground observations and for 2004 to 2016 against satellite observations.**

Morocco

- Based on ground data quality control all stations are suitable.
- Comparing satellite-based CAMS to ground based DNI, the best fitting station is Oujda. Missour, Erfoud and Zagora are affected by both missing aerosols and a winter morning cloud retrieval error in the current CAMS version.
- Annual DNI histograms are all different from Noor, but Zagora is closest compared to other EnerMENA stations. Erfoud is second closest, but has less DNI values above 800 W/m² and more between 600 and 800 W/m². We know that the closer to the Saharan desert, the more dust aerosols are overestimated in CAMS and the less DNI values above 800 W/m² will be in the CAMS dataset.
- Monthly DNI histograms from Zagora are shifted to smaller DNI values, but the overall pattern is similar while the other EnerMENA stations have a larger variability in the differences to the Noor histograms.
- With respect to cloud/cloud-free ratio, Erfoud is more similar and Zagora is next.
- With respect to thin cirrus clouds, all stations besides Tan-Tan are suitable.
- With respect to optically thick clouds, Erfoud and Zagora have similar conditions.
- With respect to seasonal and diurnal cycles, Erfoud and Zagora are similar.
- With respect to cloud duration, Erfoud is closest to Noor and Zagora the 2nd best choice.
- DNI variability in Erfoud is closest to Noor.
- Zagora is not included in the AROME/HARMONIE region.

Overall, we suggest to use Erfoud, despite its larger deviation in the annual DNI histograms than Zagora. It is the 2nd best choice with respect to DNI and has more similar cloud patterns. Also, it is part of the AROME/HARMONIE domain providing a 2nd evaluation of this model suite.

Chile

- Based on ground data quality control we cannot yet decide which station is suitable.
- Based on GE priorities, a station close to the Atacama desert is of interest.

San Pedro de Atacama or Crucero are possibilities, but the ground data needs to be checked first.

4. References

Brooks, M.J., du Clou, S., van Niekerk, J.L., Gauche, P., Leonard, C., Mouzouris, M.J., Meyer, A.J., van der Westhuizen, N., van Dyk, E.E. and Vorster, F. 2015. "SAURAN: A new resource for solar radiometric data in Southern Africa". Journal of Energy in Southern Africa, 26, 2-10

Carvalho, L. M., and Silva Dias, M. A. (1998). An application of fractal box dimension to the recognition of mesoscale cloud patterns in infrared satellite images. Journal of Applied Meteorology, 37(10), 1265-1282.

Escobar, R.A., C. Cortés, A. Pino, M. Salgado, E. Bueno Pereira, F. Ramos Martins, J. Boland, J. Miguel Cardemil, 2015. Estimating the potential for solar energy utilization in Chile by satellite-derived data and ground station measurements, Solar Energy, 121, 139-151.

Gilgen, H., Ohmura, A., 1999. The global energy balance archive. Bull. Am. Meteorol. Soc. 80, 831–850.

Geuder, N., N. Janotte, S. Wilbert, 2009: Precise Measurements of Solar Beam Irradiance through Improved Sensor Calibration, Proceedings of SolarPACES, Berlin, Germany http://solarpaces2009.org.

Kriebel, K.T., R.W. Saunders and G. Gesell, 1989: Optical Properties of Clouds Derived from Fully Cloudy AVHRR Pixels. Beiträge zur Physik der Atmosphäre, Vol. 62, No. 3, pp. 165-171, August 1989

Kriebel K. T., Gesell G., Kästner M., Mannstein H., The cloud analysis tool APOLLO: Improvements and Validation, Int. J. Rem. Sens., 24, 2389-2408, 2003

Long, C.N., E.G. Dutton, 2012: BSRN Global Network recommended QC tests, V2.0, document accessible via
http://www.bsrn.awi.de/fileadmin/user_upload/Home/Publications/BSRN_recommended_QC_tests_V2.pdf.

Ohmura, A., E.G. Dutton, B. Forgan, C. Fröhlich, H. Gilgen, H. Hegner, A. Heimo, G. König-Langlo, B. McArthur, G. Müller, R. Philipona, R., Pinker, C.H. Whitlock, K. Dehne, 1998: Baseline Surface Radiation Network (BSRN/WCRP): New Precision Radiometry for Climate Research. - B. Am. Meteorol. Soc. 79, 2115-2136.

Qu, Z., Oumbe, A., Blanc, P., Espinar, B., Gesell, G., Gschwind, B., Klüser, L., Lefevre, M., Saboret, L., Schroedter-Homscheidt, M., Wald, L., 2016. Fast radiative transfer parameterisation for assessing the surface solar irradiance: the Heliosat-4 method. Meteorol. Z. (in press).

Saunders, R.W. and K.T. Kriebel, 1988: An improved method for detecting clear sky and cloudy radiances from AVHRR data. International Journal of Remote Sensing, 9, 123-150

Saunders, R.W., 1988: Cloud top temperature/height: A high resolution imagery product from AVHRR data, Meteorological Magazine, Vol 117, pp 211-221

Schroedter-Homscheidt, M., Oumbe, A., Hoyer-Klick, C., 2010, Aerosol load and dust event mapping based on chemical transport modeling, SolarPaces conference proceedings

Schroedter-Homscheidt, M., A. Benedetti, N. Killius (2016a) Verification of ECMWF and ECMWF/MACC's global and direct irradiance forecasts with respect to solar electricity production forecasts, Metzet, in press

Schroedter-Homscheidt, M., L. Klüser, M. Kosmale, M. Lefèvre, A. Oumbe (2016b) Dust-based irradiance extinction - a climatology of extinction threshold exceedance days for solar energy planning purposes, Solar Energy, under review

Varga, Gy., Újvári, G., Kovács, J. (2014). Spatiotemporal patterns of Saharan dust outbreaks in the Mediterranean Basin. Aeolian Research 15, 151–160.

5. Annex A– NWP forecasts

This table originates from D3.1. We add it here for an easier reading.

Table 22: Available NWP datasets

Task	Product	Horizon [h]	Temp.-Resolution [min]	Spat. Res.	Run started at .. [UTC]
4.3.1 Det	AROME/HARMONIE* (will get an update for 3-hourly runs)	48	>=15	2.5 km	0,6,12,18 0,3,6,…21
4.3.1 Det	ECMWF	240	>=60 (available 180)	0.16°	0,12
4.3.1 Det	AROME/HARMONIE/Stat. Post-Proc				
4.3.1 Det	ECMWF/Stat. Post-Proc				
4.3.1 Det	AROME/HARMONIE RUC 1*	48	>=15	2.5 km	0,1,2,3,4,..23
4.3.2 Prob	ECMWF, EPS	360	180	0.25°	0,12
4.3.2 Prob	gSREPS	36/48	60	2.5km	0,6,12,18
4.3.2 Prob	ECMWF, EPS/Stat. PostProc				
4.3.2 Prob	gSREPS/Stat. Post Proc				

6. Annex B – Ground observation quality control

The final objective of this task is to dispose of high quality ground measured DNI series. Quality analysis procedures established by the BSRN for measured solar radiation data have been applied (Ohmura et al., 1998). Quality control methodology includes the following procedures:

Control of the data recording time. For each of the days with available data, there is be a check of the correct timestamp corresponding to the measured data.

Visual inspection of solar radiation components (GHI, DNI and DHI). Before a comprehensive numerical check, the recorded values are visually analyzed day by day to classify them as valid or invalid. This checking allows detecting possible problems that are not detected by means of a numerical method.

Quality control tests of the BSRN. In order to evaluate the quality of solar irradiation data measured at station, these data will be checked according with the following recommendations of BSRN:

- "Physically Possible" test, intended to detect extremely large errors in the measurements and the large random errors introduced during data handling. This check is to ensure that solar irradiances measured are below the physical limits. Table 23 shows the physical limits pointed out in the BSRN recommendations.

Table 23. Physical limits for the components of solar radiation

Component	Minimum	Maximum
GHI	0	$I_{SC}\ \varepsilon 1.5(\cos\theta_z)^{1.2}+100\ W/m^2$
DHI	0	$I_{SC}\ \varepsilon 0.95(\cos\theta_z)^{1.2}+50\ W/m^2$
DNI	0	$I_{SC}\ \varepsilon$

I_{SC} *Solar Constant (1367 Wm^{-2}), ε eccentricity, Θ_z solar zenith angle*

- "Extremely Rare" test, used to evaluate whether the measurements are within the limits known as extremely rare. Table 24 shows the extremely rare limits proposed in the BSRN recommendations.

Table 24. Extremely rare limits for the components of solar radiation

Component	Minimum	Maximum
GHI	-2 W/m^2	$I_{SC}\varepsilon 1.2(cos\theta_z)^{1.2}+50W/m^2$
DHI	-2 W/m^2	$I_{SC}\varepsilon 0.75(cos\theta_z)^{1.2}+30W/m^2$
DNI	-2 W/m2	$I_{SC}\varepsilon 0.95(cos\theta_z)^{0.2}+10W/m^2$

- "Across Quantities" test, based on empirical relations of the different quantities measured. The fail in this check could indicate that any component has not been measured properly or that the solar tracker has not worked correctly indicating misalignment of the pyrheliometer. Table 25 shows the limits for checking the fulfillment of this test.

Table 25. Conditions for the Across Quantities test

Parameter	Condition	Limit
$\frac{GHI}{DHI + DNI\cos\theta_z}$	$\theta_z < 75^o$, $DHI + DNI\cos\theta_z > 50\,W/m^2$	1 ± 8%
$\frac{GHI}{DHI + DNI\cos\theta_z}$	$75^o < \theta_z < 93^o$, $DHI + DNI\cos\theta_z > 50\,W/m^2$	1 ± 15%
$\frac{DHI}{GHI}$	$\theta_z < 75^o$, $GHI > 50\,W/m^2$	< 1.05
$\frac{DHI}{GHI}$	$75^o < \theta_z < 93^o$, $GHI > 50\,W/m^2$	< 1.10

References:

Ohmura, A., Gilgen, H., Hegner, H., Müller, G., Wild, M., Dutton, E. G., et al. (1998). Baseline Surface Radiation Network (BSRN/WCRP): New precision radiometry for climate research. Bulletin of the American Meteorological Society, 79(10), 2115-2136